People's Democratic Republic of Algeria
Ministry of Higher Education and Scientific Research

Kasdi Merbah University - OUARGLA

Faculty of Mathematics and Material Sciences

Department of Physics

Doctoral thesis in 3rd Cycle

Orrder number : .....

Serial number : .....

Specialty: Physics

Option: Materials Physics

Presented by :

Miss BOUCHAALA Afaf

Titled

Elaboration of New Nanomaterials for Spintronic Applications

Publicly supported on : 17/01/2024

Before the jury composed of :

Mr. BENTOUILA Omar	Professor	Chairman	University of Ouargla
Mr. BENHAMIDA Soufiane	MCA	Examiner	University of Ouargla
Mr. SOUIGAT Abdelkader	MCA	Examiner	Postgraduate School for Teachers - Ouargla
Mrs. BENKRIMA Yamina	MCA	Examiner	Postgraduate School for Teachers – Ouargla
Mr. BENMEBROUK Lazhar	Professor	Supervisor	University of Ouargla
Mr. MOHAMMADI Lazhar	Professor	Co-supervisor	University of Ouargla

Academic year : 2023-2024

DEDICATION

I thank God Almighty first and foremost for the great grace that he has bestowed upon me

To those who are not matched by anyone in the universe, to whom God has commanded us to honor them, to those who have made a great deal, and have given what cannot be returned, to you these words, my dear mother and father, i dedicate this research to you, you have been my best supporter throughout my academic career.

To my brothers and sisters

To all of my friends

To everyone who taught me a letter

To everyone who supported me, even with a smile

To all of you I dedicate this research.

BOUCHAALA Afaf.

Acknowledgments

Praise be to God, lord of the worlds, and prayers and peace be upon the prophet of mercy and the seal of the prophets and messengers, Muhammad, may God bless him and grant him peace, his family and all his companions.

Thanks first and last to God Almighty for granting me the grace to complete this humble work, and in accordance with what he, may God bless him and grant him peace, said "whoever does not thank people does not thank God'' i extend my thanks to ***Mr. BENMEBROUK Lazhar*** professor of higher education at the University of Kasdi-Merbah Ouargla for his suggestion and supervision of the doctoral thesis and for his assistance.

I extend my sincere thanks to ***Mr. MOHAMMADI Lazhar*** professor of higher education at Kasdi Merbah University, Ouargla, for being an assistant professor in this work.

I also extend my thanks to ***Mr. BENTOUILA Omar*** Professor of higher education at the University of Ouargla for agreeing to chair the discussion committee.

Thanks and appreciation go to the members of the discussion committee: ***Mr. BENHAMIDA Soufiane*** lecturer class "A" at the University of Ouargla, ***Mr. SOUIGAT Abdelkader*** lecturer class "A" at the postgraduate school for teachers – Ouargla, ***Mrs. BENKRIMA Yamina*** lecturer class "A" at the postgraduate school for teachers – Ouargla, on their acceptance to participate in the discussion committee.

I also extend my sincere thanks to the Laboratory **LRPPS** (**L**aboratory of **R**adiation and **P**lasma and **S**urface **P**hysics) at the University of Ouargla, which i am honored to join throughout the duration of the completion of this research, and to all the professors responsible for it for their efforts.

I also do not forget to thank Professor ***Mr. HENNI Abdellah*** in particular for all the information he provided us and for his constructive cooperation. I also extend my sincere thanks to the **CRAPC (R**esearch **C**enter for **P**hysical-**C**hemical **A**nalysis) at the University of Ouargla for the measurements they made for us during the completion of this work.

I extend my deepest thanks to the **CRAPC (R**esearch **C**enter for **P**hysical-**C**hemical **A**nalysis) at the University of Laghouat, especially those with whom i worked to carry out the measurements, as well as those who provided me with scientific and technical assistance.

I also extend my sincere thanks, appreciation and gratitude to my friends and colleagues: **Aicha FAKROUN, Hadjira MOKADMI, Maroua BRELLA, Hamza BERREHAL, and Nedjmi SAIDAT** for their support of me throughout the completion of this research.

Terminology

English	French	العربية
Thin films	Couches minces	الطبقات الرقيقة
Semiconductors	Semi-conducteurs	أنصاف النواقل
Conductor band	Bande conducteur	عصابة النقل
Valence band	Bande valence	عصابة التكافؤ
Deposition	Déposition	الترسيب
Band gap energy	Gap énergétique	فجوة عصابة الطاقة
Crystalline lattice	Réseau cristallin	الشبكة البلورية
Stress	Stress	الاجهاد
Dislocations	Dislocation	الانخلاعات
Strain	Déformation	التشوه
Growth	Croissance	نمو
Diffraction	Diffraction	حيود
The precursors	Les précurseurs	السلائف
Spintronic	Spintronic	الالكترونيات الدورانية
Nanomaterials	Nanomatériaux	المواد النانوية
Hydrothermal method	Méthode hydrothermale	الطريقة الحرارية المائية
Stretch vibration	Vibrations d'étirement	اهتزاز التمدد
Asymmetric Vibration	Vibrations asymétriques	اهتزاز تمدد غير متناظر
Symmetric Vibration	Vibrations symétriques	اهتزاز تمدد متناظر
Bending Vibration	Vibrations de flexion	اهتزاز الانحناء

Contents

List of figures……... I

List of tables…….…….... VI

General Introduction ……..... 1

References Bibliographies……..... 5

Chapter I:* *Generalities about nanotechnology and methods for synthesizing nanomaterials

I.1. Introduction……..… 9

I.2. Nano Technology …… 9

I.3. Historical stages of the development of nanotechnology……. 10

I.4. The concept of Nano……..... 12

I.5. Properties of nanotechnology……. 13

I.6. Nanoscience and nanotechnology……..... 14

I.7. Principles of nanotechnology…….. 14

I.8. The importance of nanotechnology……..... 15

I.9. Methods of synthesis of nanomaterials……..... 15

I.9.1. Nanomaterials……..... 15

I.9.2. Classification of nanomaterials…….... 16

I.9.2.1. Zero-dimensional nanomaterials…..... 16

I.9.2.2. One-dimensional nanomaterials…..... 17

I.9.2.3. Two-dimensional nanomaterials……..... 17

I.9.2.4. Three -dimensional nanomaterials……..... 18

I.10. Properties of nanomaterials……..... 19

I.10.1. Mechanical properties…..... 19

Contents

I.10.2. Chemical properties……..... 22
I.10.3. Physical properties……..... 22
I.10.4. Magnetic properties……..... 23
I.10.5. Electrical properties……..... 23
I.10.6. Optical properties…..... 23
I.11. Preparation of nanomaterials…….... 24
I.11.1. Preparation by physical methods…..... 25
I.11.1.1. Ablation method using laser beams (laser ablation method)..... 25
I.11.1.2. Physical vapor deposition (PVD) method……..... 26
I.11.2. Preparation by chemical methods……..... 27
I.11.2.1. Sol-gel Method……..... 27
I.11.2.2. Hydrothermal Method……..... 28
I.11.3. Preparation by mechanical methods……..... 28
I.11.3.1. Ball milling method……..... 28
I.11.3.2. Mechanical structure method……..... 29
I.12. Nanotechnology applications……..... 29
I.13. Conclusion……..... 31
References Bibliographies……..... 32

Chapter II: Basics of electronic spin technology and its applications

II.1. Introduction..... 40
II.2. The Spin..... 40
II.2.1. Electron discovery..... 40
II.2.2. The internal angular momentum of an electron..... 41
II.3. Self-Spin..... 41
II.4. The scientific and technical perspective of self-winding..... 41
II.5. Definition of electronic spin..... 43
II.6. Basic principles of spintronics..... 43
II.6.1. Spin electronics and magnetism..... 43

Contents

II.6.2. The direction of the electronic spin is preserved..... 44

II.6.3. Spread of electrons according to spin..... 44

II.6.4. Electron spin accumulation..... 45

II.7. Electron spin phenomena 45

II.7.1. Great magnetic resistance..... 45

II.7.1.1. Cross stream perpendicular to the plane of layers (CPP)..... 46

II.7.1.2. Current parallelism to layer level (CIP)..... 47

II.7.2.Transition Zone……..... 48

II.7.3.Tunnel magnetic resistance TMR..... 49

II.7.4. Spin electron transfer through nanotubes and nanowires..... 50

II.8. Electro-spin applications..... 51

II.9. Conclusion..... 54

References Bibliographies……..... 55

Chapter III:* *Laboratory synthesis of nanomaterials and analysis methods

III.1. Introduction..... 59

III.2. Preparation of thin films (MgO-SiO_2) from natural resources..... 60

III.2.1. Preparing the raw material..... 60

III.2.2. Chemical preparation of the solution..... 61

III.2.3. Preparing the substrates..... 62

III.3. Preparation of MgO-SiO_2 films by hydrothermal technique..... 63

III.4. Measurements to study the properties of thin layers..... 63

III.4.1. Measuring the thickness of films..... 63

III.5. Techniques for studying structural properties..... 64

III.5.1. Diffraction X-ray technology (DRX)..... 64

III.5.2. Scanning electron microscopy (SEM)..... 67

III.5.3. Fourier transform infrared absorption (FTIR) spectroscopy..... 69

III.5.4. Optical measurements..... 71

III.6. Conclusion..... 74

Contents

References Bibliographies……..... 75

***Chapter IV:* Analysis of the Properties of New Composite Nanomaterials**

IV.1.Introduction……..... 79

IV.2.Structural properties of ($MgO-SiO_2$) thin films……..... 79

IV.2.1.Determine compositional parameters……..... 87

IV.2.2. Determine the crystal lattice constants……..... 87

IV.2.3. Average grain size……..... 88

IV.2.4. Number of crystals and dislocation density……..... 91

IV.2.5. Crystal distortion……..... 94

IV.3. Morphological properties of thin layers ($MgO-SiO_2$)……..... 96

IV.4. Properties of compositional analysis of thin layers ($MgO-SiO_2$)……..... 99

IV.5. Molecular structure properties of thin layers ($MgO-SiO_2$)……..... 102

IV.6. Optical properties of thin layers……..... 108

IV.6.1. Optical transmittance……..... 108

IV.6.2. Optical absorption……..... 111

IV.6.3. Absorption coefficient……..... 113

IV.6.4. Energy Separation……..... 115

IV.7. Conclusion……..... 121

References Bibliographies……..... 122

General conclusion……..... 128

List of figures by chapter

Chapter I

Figure I.1 : A diagram showing a horizontal row of 13 hydrogen atoms, each 0.75 nanometers in diameter..... 12

Figure I.2 : Illustration of a carbon tube and nanofibers..... 17

Figure I.3 : Representative image of a nanoparticle..... 18

Figure I.4 : Stress-strain curves..... 21

Figure I.5 : Absorbance curves for nanoparticles of different sizes..... 24

Figure I.6 : Laser ablation method..... 26

Figure I.7 : How to prepare nanoparticles using sol-gel technology..... 27

Chapter II

Figure II.1 : Stern-Gerlach experiment..... 42

Figure II.2 : Electronic spin (Up=+1/2, Dn=-1/2)..... 43

Figure II.3 : A diagram of the electron spin that determines the direction of the magnetic lines and poles formed..... 44

Figure II.4 : A diagram showing the path of electrons in a CPP configuration and the terms AP and P corresponding to parallel and anti-parallel magnetization..... 46

Figure II.5 : A diagram showing the path of electrons in a CIP configuration and the terms AP and P corresponding to parallel and anti-parallel magnetization..... 47

Figure II.6 : Schematic diagram showing the spin accumulation region in the case of the Fe/Cr layer. 48

Figure II.7 : A diagram showing a magnetic tunnel intersection in parallel and antithetical states..... 49

List of figures by chapter

Figure II.8 : A diagram showing the alignment of planes at the magnetic contact point..... 51

Figure II.9 : Magnetic resistance random access memory (RAM-M)..... 53

Chapter III

Figure III.1 : Steps for experimental work..... 59

Figure III.2 : Stages of rock sample preparation..... 60

Figure III.3 : Chemical materials for preparing the solution, (a) Sodium bicarbonate ($CHNaO_3$), (b) Copper (Cu), (c) Potassium chromium oxide (K_2CrO_4), (d) Rock material (e) The prepared solution..... 62

Figure III.4 : Schematic diagram of X-ray diffraction on crystal planes in Bragg conditions... 65

Figure III.5 : A diagram showing the diffraction of X-rays..... 66

Figure III.6 : Used X-ray diffraction machine (DRX)..... 67

Figure III.7 : Schematic of a scanning electron microscope (SEM)..... 68

Figure III.8 : Used scanning electron microscope (SEM)..... 69

Figure III.9 : Types of bending vibrations..... 70

Figure III.10 : Infrared spectrometer used..... 71

Figure III.11 : Illustration of the ultraviolet-visible spectroscopy model (UV-VIS) and the device used..... 72

Chapter IV

Figure IV.1 : The primary cell of magnesium oxide……..... 80

Figure IV.2 : Crystal structure of quartz……..... 81

Figure IV.3 : X-ray diffraction (XRD) schemes for prepared membranes as a function of deposition temperature and in the presence of two external magnetic fields so that they have the same direction……..... 83

List of figures by chapter

Figure IV.4 : X-ray diffraction (XRD) schemes for prepared membranes as a function of deposition temperature and in the presence of two external magnetic fields so that the external magnetic field has the opposite direction to that of the other field……..... 83

Figure IV.5 : Lattice constants (a_0, c_0) as a function of changing the deposition temperature and in different coordinates: (a) in the presence of two external magnetic fields so that they have the same direction, (b) in the presence of two external magnetic fields so that the external magnetic field has a direction opposite to the direction of the other field…..... 88

Figure IV.6 : The relationship between FWHM and grain size rate as a function of different deposition temperatures and in the presence of two external magnetic fields that have the same direction……..... 90

Figure IV.7 : The relationship between FWHM and grain size rate as a function of different deposition temperatures and in the presence of two external magnetic fields, such that the external magnetic field has a direction opposite to the direction of the other field……..... 90

Figure IV.8 : Changes in the density of dislocations and the number of crystals as a function of the granular size rate in the presence of two external magnetic fields that have the same direction……..... 92

Figure IV.9 : Changes in the density of dislocations and the number of crystals as a function of the granular size rate in the presence of two external magnetic fields, such that the external magnetic field has a direction opposite to the direction of the other field……..... 93

Figure IV.10 : Crystals distortion as a function of changing the deposition temperature and in different coordinates: (a) in the presence of two external magnetic fields so that they have the same direction, (b) in the presence of two external magnetic fields, such that the external magnetic field has a direction opposite to the direction of the other field……..... 94

Figure IV.11 : SEM images of the layers prepared at different sedimentation temperatures and in the presence of two external magnetic fields so that they have the same orientation…….....…..... 97

Figure IV.12 : SEM images of the films prepared at different sedimentation temperatures and in the presence of two external magnetic fields so that the exterior magnetic field has an opposite orientation to the direction of the other field……..... 98

Figure IV.13 : EDX spectra of films prepared at different deposition temperatures and in the presence of two external magnetic fields with the same orientation ((a): T=150 °C, (b): T= 200 °C, (c): T=300 °C)…….... 100

Figure IV.14 : EDX spectra of films prepared at different deposition temperatures and in the presence of two external magnetic fields such that the external magnetic field has an opposite direction to that of the other field ((a): T=150 °C, (b): T= 200 °C, (c): T=300°C)……..... 101

Figure IV.15 : The infrared absorption spectrums of prepared membranes change at different deposition temperatures and in the presence of two external magnetic fields so that they have the same direction……..... 103

Figure IV.16 : The infrared absorption spectrums of prepared membranes change at different deposition temperatures and in the presence of two external magnetic fields such that the external magnetic field has an opposite direction to that of the other field……..... 104

Figure IV.17 : The main vibrations of the SiO_2 molecule……..... 107

Figure IV.18 : Change of transmittance spectrum as a function of wavelength for films prepared at different deposition temperatures in the presence of two external magnetic fields with the same direction…..... 109

Figure IV.19 : Change of transmittance spectrum as a function of wavelength for films prepared at different deposition temperatures in the presence of two external magnetic fields such that the external magnetic field has an opposite direction to that of the other field……..... 110

Figure IV.20 : The changing spectrum of optical absorption of prepared membranes appears at different deposition temperatures in the presence of two external magnetic fields so that they have the same direction……..... 112

Figure IV.21 : The changing spectrum of optical absorption of prepared membranes appears at different deposition temperatures in the presence of two external magnetic fields such that the external magnetic field has an opposite direction to that of the other field……..... 112

List of figures by chapter

Figure IV.22 : Change of absorption coefficient as a function of photon energy for films prepared at different deposition temperatures and in the presence of two external magnetic fields so that they have the same direction……..... 114

Figure IV.23 : Change of absorption coefficient as a function of photon energy for films prepared at different deposition temperatures and in the existence of two exterior magnetic fields so that the external magnetic field has a direction opposite to the direction of the other field.....…..... 114

Figure IV.24 : Energy gap for indirect transmission permitted at different deposition temperatures and in the existence of two exterior magnetic fields so that they have the same direction……..... 116

Figure IV.25 : Energy gap for indirect transmission permitted at different deposition temperatures and in the existence of two exterior magnetic fields so that the exterior magnetic field has an opposite orientation to the orientation of the other field…….....……... 117

Figure IV.26 : The energy gap for the indirect prohibited transition at different deposition temperatures and in the presence of two external magnetic fields that have the same direction.....…..... 118

Figure IV.27 : The energy gap for the indirect prohibited transition at different deposition temperatures and in the existence of two exterior magnetic fields so that the exterior magnetic field has an opposite orientation to the orientation of the other field……..... 119

Figure IV.28 : The relationship between the allowed indirect transition energy gap and different deposition temperatures and at different coordinates: (a) in the existence of two exterior magnetic fields so that they have the same direction, (b) in the existence of two exterior magnetic fields so that the external magnetic field has a direction opposite to the direction of the other field……..... 119

List of tables

Chapter I

Table I.1 : Multiples of metric units..... 13

Chapter III

Table III.1 : Properties of materials needed for the chemical preparation of the solution..... 61

Chapter IV

Table IV.1 : X-ray diffraction results for films prepared at different deposition temperatures in the presence of two external magnetic fields with the same direction……... 85

Table IV.2 : X-ray diffraction results for films prepared at different deposition temperatures in the presence of two external magnetic fields, where the external magnetic field has an opposite direction to the direction of the other field……. 86

Table IV.3 : it represents the crystal lattice constants, granular average size, density of dislocations, number of crystals and the crystal distortion of films prepared at different deposition temperatures in the presence of two external magnetic fields so that they have the same direction……..... 95

Table IV.4 : it represents the crystal lattice constants, granular average size, density of dislocations, number of crystals and the crystal distortion of films prepared at different deposition temperatures in the presence of two external magnetic fields, such that the external magnetic field has a direction opposite to the direction of the other field…….. 95

Table IV.5 : represents the atomic and mass ratios of the chemical elements of the layers prepared at different sedimentation temperatures in the presence of two external magnetic fields so that they have the same direction……..... 100

Table IV.6 : represents the atomic and mass ratios of the chemical elements of the membranes prepared at different deposition temperatures in the existence of two exterior magnetic fields, so that the exterior magnetic field has an opposite orientation to the direction of the other field.. 101

Table IV.7 : Molecular structure of the prepared films metals and their corresponding vibrations at different deposition temperatures and different magnetic field strengths were determined using FTIR……. 106

List of tables

Table IV.8 : Thickness and transmittance values obtained at different temperatures…..... 111

Table IV.9 : The energy gap values of the two indirect transitions allowed and forbidden by the change of sedimentation temperatures…….. 120

General introduction

General introduction

Technological development from the seventeenth century to the present has contributed to a revolution and radical transformations in all aspects of life, although man has revolutionized the field of information, communications, steam engines, the textile industry, computers, and electronic inventions such as micrometer chips and others, but he still seeks to develop the physical world and its components in smaller dimensions, technological development today is linked to the ability to manufacture electronic devices with the smallest size and highest efficiency, and finally, a new technological revolution, known as the nanotechnology revolution exploded, this is achieved by producing systems and devices based on materials at the atomic and molecular levels by controlling shape and size at nanoscales and discovering the concept of the quantum confined atom, thus being able to describe the particles of the material next to each other and develop the pattern of arranging new atoms with the sites of crystal networks, which led to the development of new types of materials with physical, biological and chemical features and properties distinct from similar traditional materials without changing their chemical composition, therefore, today, global laboratories are racing to produce new nanomaterials at a tremendous pace, and many discoveries and numerous studies have been made of nanomaterials and their chemical, physical and structural properties, including shape, size and surface area, and crystal structure, chemical composition, and surface morphology, and because this is the latter offers increasing innovations and procedures for many applications, such as biosensors, transistor manufacturing, and drug delivery, food packaging etc. Methods for manufacturing nanomaterials varied depending on their dimensions and relied on many new technologies with the required and unique properties, and among the new species we find the thin layers, in this category, it was required to determine the conditions for the growth mechanism of nanoparticles from precursors, whether they are metals extracted from natural or industrial resources, and temperature, and the concentration of the middle, and the method of preparation, and it is considered the thin layers of nano-semiconductor materials are suitable for various applications, such as electronic and optical ones, for example, energy fields, solar cells, information storage, sensors, flat screens and touch screens, and semiconductors play an important role in the technological progress of nanoscience, they are considered materials with electrical conductivity due to the flow of electrons and the movements of holes, compared to

conductive materials in which current flows due to electrons only, however, the semiconductor material is not only considered a crystalline solid, it also belongs to amorphous and liquid materials as well, and metal oxides are considered one of the classes that belong to nano-semiconductor materials, and thermal and chemical stability, and promises to be used in a variety of practical and scientific applications for their association in many fields such as chemistry, physics, materials science, etc, therefore, this opens new horizons for technology and science[1-5].

Semiconductor materials with electrical conductivity have received the attention of many researchers due to their diverse uses in industrial applications, therefore, researchers are seeking to find energy-saving alternatives to traditional metal oxide semiconductor devices. Over the past 25 years this field has evolved rapidly down to magnetic electronics and spintronics, and it includes the field of magnetic electronics on determine the effects of magnetic resistance based on metals, in this case this property can be exploited in magnetic field sensors such as magnetic hard drives of reading and writing heads, also, combining the degrees of freedom of spin of an electron and its charge in the same material will allow the direct implementation of spintronic devices with new functions, and enhanced to control, read and store information, although the use of magnetic materials is not new for uses in memory and information storage, as is evident today from magnetic tapes and hard drives, however, spin electronic devices will generate faster memory technologies, in particular magnetic random access memory (MRAM), which is characterized by high reading power and endurance and low switching power compared to current memory devices, from another angle, “spintronics” is known as an abbreviation for SPIN TRAnsport ElectroNICS[6][7], and in pursuit of achieving the desired technological development, this term has been used in the phenomena of spin-polarized transport of metals, oxide materials, and semiconductors, and a huge research effort has been focused in recent years on the so-called diluted magnetic semiconductors[8], anisotropy of properties in metal/metal magnetic oxides has been an interesting topic in the field of spintronics due to its importance for applications[9], interestingly, strong room temperature ferromagnetic semiconductors were reported in MgO nanoscale powders, an artificially important material[10], MgO is considered one of the best magnetic metal oxide materials, the magnetic properties of these films have been extensively studied by Pacchioni[11] and Noguera and co-workers [12], indicating the appearance of magnetic movements of low-coordination O atoms on the surface. Well-defined procedures

for preparing high-quality SiO_2-MgO surfaces are also important in a number of surface physics and materials science cases, because the properties of membranes are sensitive to their structure[13], MgO thin films were prepared using a variety of techniques including electron beam evaporation[14], chemical vapor deposition[15-17], spray pyrolysis[18], atomic layer deposition[19], radio frequency magnetron sputtering[20], and the sol-gel process[21-23], MgO membranes were also prepared using the addition of SiO_2 by evaporation method with the electron beam [24], it was also proposed to prepare MgO films to replace SiO_2 using spray pyrolysis technology [25], however, the study related to the case of MgO-SiO_2 has not been reported yet and needs further study. The hydrothermal method appears to have several degrees of freedom to be used to prepare MgO-SiO_2 due to simple synthesis process and convenient operation, in addition, substrate solution is subject to hydrothermal treatment suitable for forming stable crystalline phase membranes on substrate, the membranes obtained are highly purified and have good homogeneity [26].

With the availability of rocks and sand in very huge quantities in the regions of southern Algeria, and Ouargla is a sample of them, it made us look at it as a natural, local and it's free source of many minerals and oxides, given that minerals are the structural unit of rocks, this is based on the average chemical analysis of it, and also considering that oxide is a basic chemical unit that makes up all the chemical compounds of rocks present on the surface of the earth's crust [27], in addition, we have previously studied the chemical composition of a rock sample from the Ouargla region using X-ray diffraction (DRX), infrared absorption (FT-IR) and X-ray fluorescence spectroscopy (XRF), most of its ingredients have been identified, perhaps the most important of which is Si and Mg magnesium, which is the most important primary material for modern electronic and applied industries[28], despite the large and available quantities of this natural resource, it has not been valued and only a small number of studies have been conducted on it in terms of its physical properties or composition, especially related to the Ouargla region, rather, it has been limited to its use in the field of agriculture and construction.

Therefore, in this study, we will seek to exploit the natural resources from rocks for use in the preparation and deposition of thin, nanofilms prepared by the hydrothermal method and with specific properties that allow for spintronic applications in the future, because they contains chemical elements that can be exploited in microelectronic applications and are not polluting to the environment, and study the effect of both the deposition temperature and the magnetic field applied to reach good structural and optical properties and collect low cost of these membranes.

We divided this thesis into four chapters. In its first chapter, "**Generalities about nanotechnology and methods for synthesizing nanomaterials**", we collected all the information about nanotechnology, starting with its origin, origin, properties, and methods for synthesizing nanomaterials, to conclude in the end by presenting the most important applications of nanotechnology.

As for the second chapter, "**Basics of electronic spin technology and its applications**", we defined electronic spin, starting with the internal angular momentum of the electron and the various basics of electronic spin, all the way to its applications.

In the third chapter, "**Laboratory synthesis of nanomaterials and analysis methods**", we will take care of experimental work to prepare various samples as well as diagnostic methods.

In the last chapter, "**Analysis of the Properties of New Composite Nanomaterials**", we will present the experimental results obtained, discuss them, and provide an accurate scientific explanation for them.

At the end of this thesis, we will mention the most important results obtained in a **general conclusion**, while presenting future prospects for how to exploit them practically, and on the basis of which other applied research can be carried out.

References

[1] Rajput, Namita, "Methods of preparation of nanoparticles-a review", international Journal of Advances in Engineering & Technology, 7, 6, 2015.

[2] Ghulam Nabi Dar, Metal Oxide Nanostructures and Their Applications, A thesis Submitted to the Department of Materials Science, School of Natural Sciences, University of Patras, in partial fulfilment of the requirements for the degree of Doctor of Philosophy, 2015.

[3] Gatoo, Manzoor Ahmad, et al. "Physicochemical properties of nanomaterials: implication in associated toxic manifestations", BioMed research international, 2014.

[4] أ.د. محمود محمد سليم صالح، تقنية النانو وعصر علمي جديد، المملكة العربية السعودية، 2015.

[5] أ.د.محمد شريف الاسكندري، تكنولوجيا النانو من أجل غد أفضل، عالم المعرفة الكويت، 2010.

[6] Joseph T. Finley, Spintronics Using Low Magnetization Materials, Submitted to the Department of Electrical Engineering and Computer Science in partial fulfillment of the requirements for the degree of Doctor of Philosophy, University of California Berkeley, 2020

[7] Zabel, Hartmut, "Progress in spintronics," Superlattices and microstructures, 46, 4, 541-553, 2009.

[8] C. Martínez-Boubeta, J. I. Beltrán, Ll. Balcells, Z. Konstantinović, S. Valencia, D. Schmitz, J. Arbiol, S. Estrade, J. Cornil, and B. Martínez, Ferromagnetism in transparent thin films of MgO, PHYSICAL REVIEW B 82, (2010)

[9] Sato, P. Chureemart, F. Matsukura, R. W. Chantrell, H. Ohno, and R. F. L. Evans, Temperature-dependent properties of CoFeB/MgO thin films: Experiments versus simulations, PHYSICAL REVIEW B 98, (2018).

[10] Mukes Kapilashrami, Jun Xu1, K V Rao, Lyuba Belova, Elin Carlegrim and Mats Fahlman, "Experimental evidence for ferromagnetism at room temperature in MgO thin film," J. Phys. Condens. MATTER, (2010).

[11] Anna Maria Ferrari and Gianfranco Pacchioni, Electronic Structure of F and V Centers on the MgO Surface, J. Phys. Chem,99, 17010-17018, (1995).

[12] J. Goniakowski, C. Noguera, "Characteristics of pd deposition on the mgo(111) surface", Phys. Rev. B - Condens. Matter Mater. Phys., vol. 60, no. 23, pp. 16120–16128, (1999).

[13] Moses Ezhil Raj, M. Jayachandran, C. Sanjeeviraja, Fabrication techniques and material properties of dielectric MgO thin films—A status review, CIRP Journal of Manufacturing Science and Technology 2, 92–113, (2010).

[14] H. Kurt, K. Oguz, T. Niizeki, and J. M. D. Coey, Giant tunneling magnetoresistance with electron beam evaporated MgO barrier and CoFeB electrodes, JOURNAL OF APPLIED PHYSICS 107, 083920, (2010).

[15] W. B. Wang, Y. Yang, A. Yanguas-Gil, N. N. Chang, G. S. Girolami, and J. R. Abelson, "Highly conformal magnesium oxide thin films by low-temperature chemical vapor deposition from Mg(H3BNMe2BH3) 2 and water," Applied Physics Letters, vol. 102, no. 10. (2013).

[16] J. H. Boo, S. B. Lee, K. S. Yu, W. Koh, and Y. Kim, "Growth of magnesium oxide thin films using single molecular precursors by metal-organic chemical vapor deposition," Thin Solid Films, vol. 341, no. 1. pp. 63–67, (1999).

[17] yutaka TAKESHIMA, Kosuke SHIRATSUYU, Hiroshi TAKAGI and Kunisaburo TOMONO, Preparation of Lead Magnesium Niobate Titanate Thin Films, Jpn. J. Appl. Phys. Vol.34, pp 5083-5085, (1995).

[18] J. M. Bian, X. M. Li, T. L. Chen, X. D. Gao, and W. D. Yu, "Preparation of high quality MgO thin films by ultrasonic spray pyrolysis," Applied Surface Science, vol. 228, no. 1–4. pp. 297–301, (2004).

[19] B. B. Burton, D. N. Goldstein, and S. M. George, Atomic Layer Deposition of MgO Using Bis (ethylcyclopentadienyl) magnesium and H2O, J. Phys. Chem. C, 113, 1939–1946, (2009).

[20] Lou Yongle(**娄永**乐) , Zhang Yuming (张玉明), Xu Daqing (**徐大**庆), Guo Hui (**郭**辉), Zhang Yimen (张义门) , and Li Yuchen(**李妤**), Influence of oxygen content on the crystallinity of MgO layers in magnetic tunnel junctions, Journal of Semiconductors, Vol. 35, No. 8, August (2014).

[21] Hyungsoo Choi and Soontaik Hwang, Sol-gel-derived magnesium oxide precursor for thin-film fabrication, J. Mater. Res., Vol. 15, No. 4, Apr (2000).

[22] S. Chakrabarti, D. Ganguli, and S. Chaudhuri, "Preparation of hydroxide-free magnesium oxide films by an alkoxide-free sol-gel technique," Materials Letters, vol. 57, no. 29. pp. 4483–4492, 2003.

[23] S.K. Shukla, G.K. Parashar, A.P. Mishra, Puneet Misra, B.C. Yadav, R.K. Shukla, L.M. Bali,G.C.Dubey,"Nano_like_magnesium_oxide_films_and_its, Sensors and Actuators B 98 5–11, (2004).

[24] I.A. Kariper, F. Meydaneri Tezel, Synthesis and characterization of magnesium oxide / silver oxide electrode for supercapacitors by simple Sol-Gel process, Journal of Energy Storage, 32, 1-8, 2020.

[25] Fatma Meydaneri Tezel, Ugur Veli, I. Afs¸in Kariper, Synthesis of MgO thin films: How heat treatment affects their structural, electro-optical, and surface properties, Materials Today Communications, 33, 1-10, 2022.

[26] İ.A. Kariper, F. Meydaneri Tezel, UV region supercapacitor: Bi-doped natural MgO rock salt thin film, Ceramics International, 45, 1-6, 2019.

[27] د. محمد عز الدين حلمي، علم المعادن، مكتبة الأنجلو المصرية، 2002.

[28] S. Amin, M. Amin, Thermoplastic elastomeric (TPE) materials and their use in outdoor electrical insulation, Rev.Adv.Mater.Sci.29, March 2011, page 15-30.

Chapter I

Generalities about nanotechnology and methods for synthesizing nanomaterial

Chapter I : Generalities about nanotechnology and methods for synthesizing nanomaterials

I.1.Introduction

Nanotechnology is considered one of the latest scientific technologies that must be known and followed up on its development. It is generally known as a technology that focuses on understanding and controlling materials with dimensions ranging from approximately 1 to 100 nanometers. It has been shown that the unique phenomena and properties of materials at the nanoscale allow for new and diverse applications such as chemical catalysis. Sustainable energy, medicine, consumer products and electronics according to final requirements, which means more efficiency and optimal use of resources, and it is expected that this technology will generate a series of industrial revolutions over the next two decades. In this chapter, we will try to shed light on generalities about nanotechnology and its concept, as well as the history of its development. We will also mention the characteristics of nanotechnology, its importance, and the principles that distinguish it. We will also discuss methods for preparing nanomaterials, their types and properties, and concluding with the applications of nanotechnology in various fields.

I.2. Nano Technology

Technology is defined as a system of processes that proceed according to specific standards, and uses all available capabilities, whether material or immaterial, in an effective manner to accomplish the desired work, with a high degree of mastery and efficiency for the sake of sophistication and progress. It is a word of Greek origin derived from two words (Techne), which means Technical skill and (Logos) means study, meaning that the word technology means organizing technical skill. As for nanotechnology, it is the technology that has the ability to work at the molecular level. It includes research and technical developments at the atomic and molecular levels in a length range of about 1-100 nano. Meter, to provide a basic understanding of materials at the nanoscale and as they create large structures with fundamentally new molecular organization, they manufacture and use structures that have unique properties due to

their small size. More specifically, the word nanotechnology refers to the technology of building and assembling matter from a single atom[1-3].

I.3. Historical stages of the development of nanotechnology

Despite the modernity of nanotechnology, it was used in ancient civilizations without them realizing its nature or name. Craftsmen used it in the seventeenth century to make swords known for their sturdiness and flexibility, which were equipped with blades of steel called “wotz.” It was also used in the Greek civilization and the Chinese civilization in the manufacture of glass, and perhaps one of the oldest applications of this technology is the famous Greek cup of the Roman king “Lycurgus”, which used nano particles of gold in its manufacture and then mixed them with glass. The black hair dye that was famous in Rome and Athens two thousand years ago was made with it, by mixing lead oxide paste with lime, and it was used In the manufacture of linen threads to close wounds during the Middle Ages in Europe[4- 7].

In the modern era, nanotechnology has undergone several developments, which we summarize as follows:

- In 1959: In his classic lecture before the American Physical Society at the California Institute under the title (There is a plenty of room at the bottom), the American physicist Richard Feynman wondered what would happen if we were able to arrange atoms one after another. The way we want it ! In it, he described that atomic manipulation was inevitable and suggested that it would eventually be possible to manipulate atoms and molecules to create the nanoscale. Feynman generalized this observation toward manipulating and controlling objects on an ever smaller scale, and this type of activity is also abundant. For new inventions [8-11].
- In 1974: The Japanese scientist Norio Taniguchi was the first to use the term "nanotechnology" at the International Conference on Industrial Production in Tokyo in order to describe the ultra-precise processing of materials with nanometer precision and the creation of nano-sized mechanisms. He also stated in his paper "Basic Concepts of Nanotechnology" that nanotechnology consists mainly from the processing of separation, combination and deformation of materials by a single atom or molecule [12][11][5].
- In 1981: Researchers Gerd Binnig and Henrik Rohrer of IBM invented the scanning tunneling microscope, which was the first instrument that could generate real images of

surfaces with atomic resolution and manipulate atoms. This discovery opened an important new field of nanotechnology [12][13].

- In 1986: Eric Derexler of the Massachusetts Institute of Technology used ideas from Feynman and Taniguchi in his book, "Engines of Creation: The Next Age of Nanotechnology". He proposed an atomic stacking mechanism to produce machines smaller than a beehive. He also presented some potential applications for nanotechnology. Derexler's vision of nanotechnology is often called "molecular nanotechnology" [14][15].
- In 1989: A research team from IBM (International Business Machines) was able to use the fine needle in a scanning tunneling microscope to capture atoms of the inert element xenon and move them with extreme precision to rearrange them one by one on a cold surface of nickel metal[16].
- In 1991: Japanese scientist Sumio Legima discovered carbon nanotubes, which contain at least two layers (multi-walled carbon nanotubes), at NEC Electronic Industries in Japan when he was examining carbon materials from various sources for the purpose of clarifying the growth mechanism of fullerene molecules using a high-resolution electron microscope. It is given this name because it has a tubular structure of carbon atom sheets[17][18].
- In 1992: The Palestinian physicist Munir Nayfeh was able to write the smallest font in history using atoms, by writing the letter P as a symbol for Palestine. It was published in scientific news outlets and major scientific journals, where he was able to rearrange the atoms and control them. He used a scanning tunneling microscope to photograph them magnifying [19].
- In 1993: Scientist Bethune of the American company IBM was able to discover a new class of carbon nanotubes with only one layer. These single-walled tubes are generally narrower than multi-walled tubes with diameters usually in the range of 1-2 nanometers, and tend to be curved rather than straight[17][20].

Through the previous achievements, the door was opened wide for the world to enter the era of nanotechnology, and scientists entered it forcefully through scientific research, and presented a lot of valuable scientific research and amazing inventions, and by transferring them from laboratories and research papers to companies and factories, and starting to manufacture devices

and tools that do not their sizes exceed a few nanometers, as in 2003 AD it was noted that companies around the world in the nanotechnology sectors were active in nanomaterials and nanotechnology [16][21].

I.4. The concept of Nano

The word nano is a prefix (the part with which we start the word) derived from the ancient Greek language "Nanos", which means dwarf, and it means every small thing. In the field of science, nano means one billionth of a thing. For example, "Nanometer", which is abbreviated in Latin letters to nm, is as a unit for measuring the lengths of very small objects that can only be seen under an electron microscope, this unit is used to express the dimensions of diameters and measures of atoms and molecules of materials, compounds, cells, and microscopic particles such as bacteria and viruses. One nanometer is equal to one thousandth of a millionth of a meter. For comparison, one nanometer is equivalent to measuring the length of a row of 13 hydrogen gas atoms, if we imagine that they are placed stacked next to each other, as shown in the **figure (I.1)**[16].

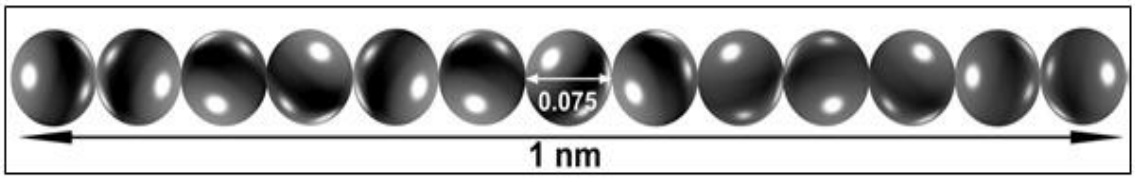

Figure I.1 : A diagram showing a horizontal row of 13 hydrogen atoms, each 0.075 nanometers in diameter[16].

Table (I.1): Multiples of metric units[29].

abbreviation	Prefix	Number
E	exa-	10^{18}
P	peta-	10^{15}
T	tera-	10^{12}
G	giga-	10^{9}
M	mega-	10^{6}
K	kilo-	10^{3}
C	centi-	10^{-2}
m	mili-	10^{-3}
u	micro-	10^{-6}
n	nano-	10^{-9}
P	Pico-	10^{-12}
F	Femto-	10^{-15}
A	atto-	10^{-18}

I.5. Properties of nanotechnology

The focus on the behavior of the atom and the small world created a turning point for thinking about entering a new world of nanotechnology, that is, the reproduction of a group of materials that does not stop at a specific field, instead of traditional methods, in order to solve the problems of the era represented by scarcity of resources and environmental pollution in order to achieve social and economic well-being, as there are many characteristics that distinguish Nanotechnology includes the possibility of controlling individual atoms and rearranging them because the atom is the building unit for all materials and carries the same properties. It can be used to make machines free of defects, as determining the shape, size, distribution and chemical properties of nanomaterials is a vital part of industrial processes, and this is what contributes to New product development achieves product quality, lower cost, and continuous improvement. Modern-day industrialists believe that the techniques used to examine and explore the properties and processes of nanoscale materials, such as AFM, SEM, and building block analysis of nanomaterials, provide a greater understanding of nanomaterials and thus the possibility of controlling size distribution and designing materials. As it was found that nanomaterials have lower elastic properties compared to large-sized materials due to their very high concentration of

defects, and thus the diffusion movement increases and it is expected that they have improved self-diffusion compared to materials that have the same chemical composition. This idea was deduced through measurements self-diffusion in copper nanoparticles [22][23].

I.6. Nanoscience and nanotechnology

During the past decades, there has been a lot of focus on studying the behavior of matter at the atomic scale in most scientific and engineering fields, and one can see the influence of nanotechnology, as this word has gained widespread use in both scientific literature, as this technology constitutes an area of multiple research and development specializations. That depend on knowledge of what is extremely small. Nanoscience means the science that is concerned with studying structures and molecules on the nanometer scale ranging between 1 and 100 nm and determining their unique and interesting chemical and physical properties. Nanoscience aims to design and manufacture new applicable materials, while nanotechnology or nanotechnology (also called sometimes molecular manufacturing) is the design, production and application of structures at the nanoscale. So one studies nanomaterials and their properties and the other uses those materials and properties to create something new or different[22][24][25].

I.7. Principles of nanotechnology

There are many principles that distinguish nanotechnology from the techniques we know, which are the reason why scientists are interested in reaching this nanoscale size. Scientists consider that reaching the precise size leads to changing the properties of materials and thus it is possible to benefit from nanoscale materials, and this in turn threatens a qualitative leap. In various fields, such as the development of electronics science and the production of advanced devices to analyze data accurately, and among the principles of nanotechnology is controlling the arrangement of atoms and the ability to move them, and this leads to the possibility of building any material. It has also become clear that the physical and chemical properties of materials at the nanoscale differ from the properties of the same materials at the natural size. Thus, it is possible to discover useful properties for innovative applications, which encourages the intensification of studies of their physical, chemical, as well as electrical and electronic properties. Controlling atoms leads to the manufacture of defect-free materials with unique

features, devices with high efficiency, cheap cost, lighter, and less energy consumption. This technology is also characterized by the fact that it will transform science fiction into reality[26][27].

I.8. The importance of nanotechnology

Nanotechnology has become at the forefront of the most important fields due to its promising principles for a new scientific revolution in the near future, because it will generate industrial capacity with high efficiency and at the lowest cost. Rather, it will be used in various fields, including electronics, for its ability to increase the capacity of storing information and increasing the size of magnetic tapes, in addition to manufacturing computers rapid quantitative, which led to an increase in scientific research in this field to facilitate difficulties, the most important of which is the possibility of accessing cheap and practical methods to prepare various nanomaterials in a commercial manner, for use in various applications. Another difficulty also lies in how to communicate between the concept of the modern nano world and the macro world currently used in the manufacture of electronic devices. As the size of materials is reduced from the critical value of size, and whenever the size of the material approaches nanometer scales, the material is subject to the laws of quantum mechanics instead of the laws of classical physics and its properties change, such as the electronic structure, conductivity, reactivity, melting point, and mechanical properties of the material, thus giving a new class of The materials, which are called nanomaterials, because their distinct properties suit the needs of advanced technology, and from here it is clear that nanotechnology has a great future in various fields, including medical, military, information, electronic, and others. Nanotechnology has many backgrounds, as it relies on the principles of physics and chemistry, in addition to the disciplines of biology and pharmacy[28][29].

I.9. Methods of synthesis of nanomaterials

I.9. 1. Nanomaterials

Nanomaterials is defined as that distinct class of advanced materials that can be produced, with dimensional scales ranging between 1 nm and 100 nm, or they are those materials that have synthetic components, at least one of their dimensions is in the nanoscale. The small size and scale of these materials has led them to behave differently from traditional large-sized materials

whose dimensions exceed 100 nm, and to have very distinct qualities and characteristics that cannot be found together in traditional materials. Nanomaterials vary in terms of source, such as organic, inorganic, natural, or artificial materials [30][31].

I.9. 2. Classification of nanomaterials

Nanomaterials take many forms, each with a different composition, properties, and uses that are classified according to their dimensions in space. There are zero-dimensional structures, one-dimensional structures, two-dimensional structures, and three-dimensional structures. All nanostructures fall under these classifications, and we mention them as follows:

I.9. 2.1. Zero-dimensional nanomaterials

Zero-dimensional (0D) nanomaterials are defined at the nanoscale and in all three dimensions, and among the zero-dimensional nanomaterials are quantum dots, where the electrons are completely confined in an infinitely deep well within the nanoscale in the quantum dot system and cannot escape from this region. This results in the electrons not moving freely. These nanomaterials are either crystalline or polycrystalline, as well as non-crystalline, and consist of multiple or single chemical elements. According to quantum confinement theory, when an electron moves from the valence band to the transfer band, a pair of electronic holes called an exciton (representing a linked pair of conduction electrons and valence holes) is created in the mass lattice, and the physical separation between the electron and the hole occurs through the Bohr radius of the exciton. It varies depending on the composition of the nanomaterial, especially in semiconductors. In the zero dimensions of nanomaterials, the Bohr exciton radius is the same size as the diameter of the nanocrystal (L), which leads to quantum confinement of the exciton. On the practical side, the strongest quantum confinement will occur when the crystal diameter doubles by two or more times the Bohr radius ($L \leq 2r_b$), at the level of completely zero-dimensional materials. Confinement of both electrons and holes causes an increase in the optical transfer of energy from the valence band to the conduction band, which leads to effectively increase the bandgap[32].

I.9. 2.2. One-dimensional nanomaterials

Nanomaterials are considered one-dimensional (1D) if one of their dimensional scales is less than 100 nm, that is, they have only one nanodimensional dimension. For example, nanotubes, nanofibers, nanowires, nanothreads, in addition to various thin films that are used in packaging Products Depending on their function, one-dimensional nanomaterials can be polycrystalline or monocrystalline, and they can also be amorphous. These materials are not chemically pure or pure, and these materials also appear as materials integrated into another medium or stand alone[32][33].

I.9. 2.3. Two-dimensional nanomaterials

Two-dimensional (2D) materials are sized at the nanoscale and have two dimensions less than 100 nm, for example very thin surface films, disks and platelets. Two-dimensional nanomaterials consist of metal or ceramic. They are made of different chemical compositions. Two-dimensional nanotubes consist of organic materials such as carbon or inorganic materials such as metal oxides. These tubes may be straight, spiral, zigzag, or conical, and nanofibers made of polymers. 2D nanomaterials can be amorphous or crystalline. They are usually deposited on a substrate and incorporated into the surrounding matrix [32][27].

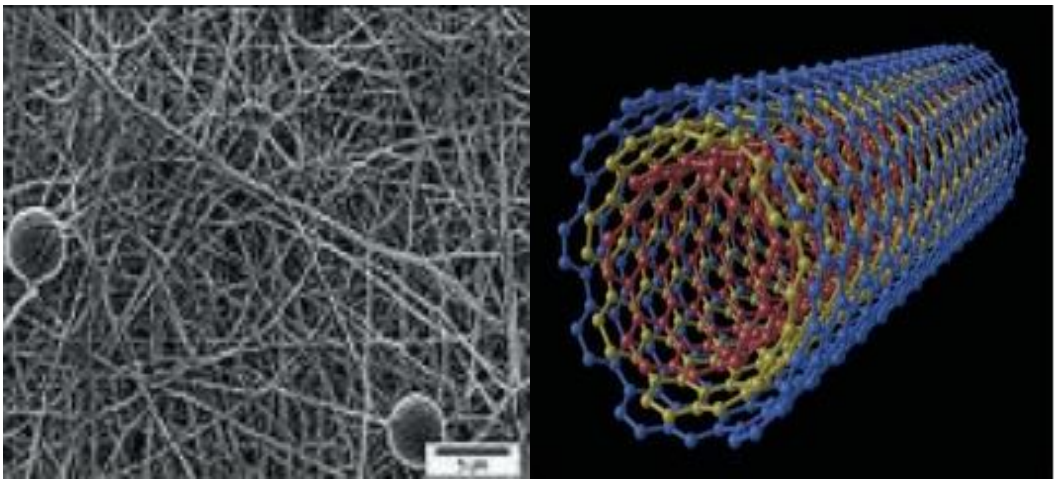

Figure I.2 : Illustration of a carbon tube and nanofibers.

I.9. 2.3. Three -dimensional nanomaterials

Three-dimensional nanomaterials are known because their dimensional measures on the three axes X,Y, Z less than 100nm, the most widely used are solid nanomaterials, which are in the form of nanometer grains and crystals in a specific crystal direction. These materials can be amorphous or crystalline. For example, nanoparticles, which are microscopic atomic or molecular aggregates ranging in number from a few atoms (molecule) to a million atoms, are linked to each other. In three-dimensional nanomaterials, the electrons are completely separated, as it has been shown through research that the smaller dimensions of the nanostructure They lead to a wider separation between energy levels, showing that all electrons move freely in three dimensions. In a semiconductor crystal of materials of larger size it is found that the Bohr exciton radius r_b is much smaller than the total volume (L) of the crystal, that is the exciton is free to migrate through the lattice. The size-dependent electronic properties of quantum dots were studied in the early 1980s by Efros and colleagues, and it was shown that limiting the bandgap would maximize the overall value based on the confinement energy term. According to quantum confinement theory, electrons in the conduction band and holes in the valence band are spatially confined by the barrier potential of surface, and therefore the transition energy of the electronics from the conduction band to the valence band will increase, and this increase in energy effectively leads to an increase in the bandgap[32][29].

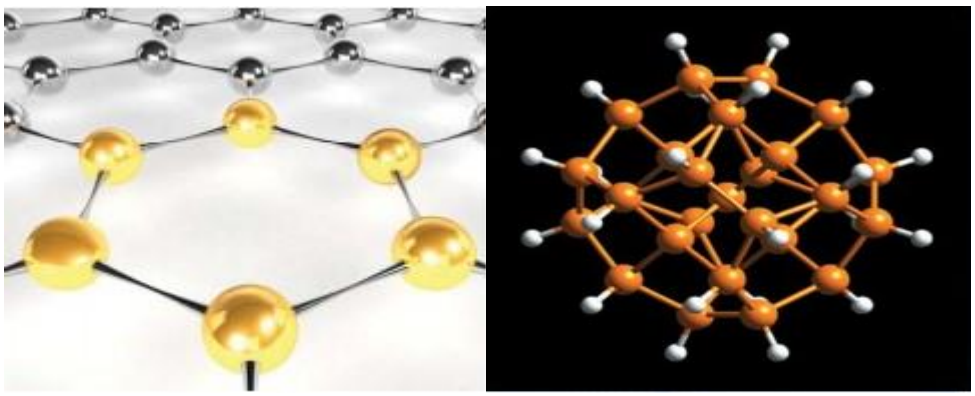

Figure I.3 : Representative image of a nanoparticle.

I.10. Properties of nanomaterials

The properties of materials at the nanometer scale change more unexpectedly than they did above the nanoscale (micro or millimeter dimensions), which gives critical importance to nanomaterials. This is due to the significant change in material properties for the following reasons:

- **The size:** The properties of materials change with their size to the nanometer scale compared to their larger scale, as silicon material at the 3nm scale radiates red, and at a smaller size at the 1nm scale it radiates blue, and at its normal size it is considered an opaque material with no radiation[27].
- **Figure:** On the nanoscale, the shape of the particles plays an important role in determining their properties, and they change as their shape changes, from spherical, tubular, or other shapes. In contrast, the properties of materials do not change at a size larger than the nanoscale, for example a wood board and a wood cube[27].
- **Relative increase of surface area:** Nanomaterials have a larger surface area when compared to the same materials in a larger area, and this makes the materials more chemically active and affects their strength or electrical properties [34].
- **Quantitative effects:** Nanomaterials are not subject to the laws of classical physics due to their small dimensions, which are close to atomic dimensions. Therefore, they are subject to the laws of quantum physics, which is reflected in their properties. Among them are the ability to change color, transparency, great hardness, and great ability to conduct and insulate [34].

We will present below the distinctive mechanical, chemical, physical, magnetic, electrical and optical properties of nanomaterials[32] [16]:

I.10.1. Mechanical properties

Scientists and engineers consider that miniaturizing materials from the traditional scale to the nanoscale has a positive effect on their properties, and leads to improving the hardness values of metallic materials and their alloys, as well as increasing their resistance to the stresses of the various loads imposed on them. An example of this is the minimization of the grains of ceramic materials, which leads to making them more durable, which is a characteristic that is not found in

ordinary ceramic materials. The mechanical behavior of nanoscale copper (Cu) was studied and it was found that there is a very strong metallic behavior, and in return there is a low ductility of 2% compared to traditional standards, as the hardness properties depend greatly on the formation of defects within the material and in the nanosystem has an increasing ability to strengthen defects, and in the near future it looks forward to studies that can reveal principles for manufacturing nanomaterials with mechanical properties that can be controlled in a repeatable manner, as the methods of arranging the atomic and molecular structure of nanoparticles differ compared to traditional materials, and this leads to their difference in Mechanical properties. For example, nanotubes have superior mechanical strength.

- **Stress and pressure:** According to Chaˆtelier's principle when an external force is applied to a substance whether it is a liquid or a powder, it will move along and expand to reduce the force. It will also resist external forces by generating internal forces, and it will also be pressured by external forces according to the following relationship:

$$\boldsymbol{\sigma = F/A_0} \qquad \textbf{(I.1)}$$

As it represents: $\boldsymbol{\sigma}$ Pressure, $\boldsymbol{F}$ applied force, $\boldsymbol{A_0}$ cross-sectional area.

- **Strain:** A solid material changes its length when it is subjected to uniaxial compression or tension, and this is indicated according to the following equation:

$$\boldsymbol{\varepsilon_L = (\Delta L/L_0)} \qquad \textbf{(I.2)}$$

Where represents ΔL the change in length $\Delta L = L - L_0$ and L_0 represents the original length.

- **Elastic equations and Hooke's law:** The modulus of elasticity is defined as the modulus that is proportional to the stress and strain on the material according to Hooke's law and is dimensionless. When a certain pressure is applied to the material, its volume will decrease, which is defined as a relative negative volume, and is explained according to the following equation:

$$\mathbf{\Delta p = -k(\Delta V/V)} \qquad \textbf{(I.3)}$$

Where it represents k the volume modulus, which is the linear portion of the compressive pressure to the relative volume diagram, and its unit is GPa.

The significant change in volume (ΔV/V)relates to its isothermal compression, when the volume decreases as a result of applying external pressure and the mass coefficient, and is explained according to the following equation:

$$\boldsymbol{\beta_T = -\frac{1}{V}\,(\partial V/\partial P)_T} \qquad \textbf{(I.4)}$$

The above equation is simplified as the reciprocal of the compressibility of a liquid or solid substance to the volume coefficient (K) as follows:

$$\boldsymbol{k = {}^{1}/_{\hat{a}_T}} \qquad \textbf{(I.5)}$$

The properties of elastic moduli, or what is known as the properties of compressibility, are an indication of the intrinsic flexibility of the solidification of a liquid or solid material.

- **Strain and stress curves:** External pressure will be applied to the study sample, to test the mechanical properties of the sample material, and then the stress will be recorded in terms of strain. **Figure (I.4)** shows an example of the accompanying stress-strain curve, in addition to the real stress-strain curve in general. Usually, the stress curves differ significantly depending on the materials, as well as the measurement temperature and loading speed on the curves. It was also shown through tensile testing experiments on the same sample that there were different results.

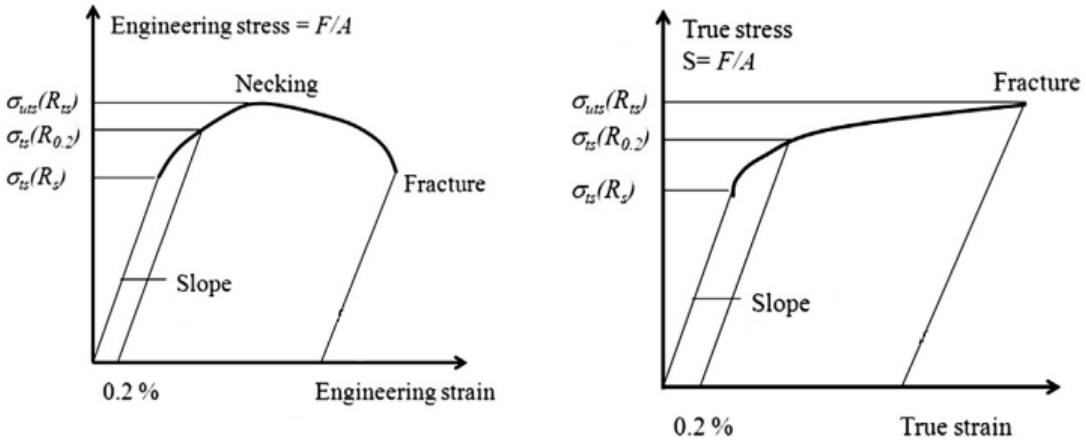

Figure I.4 : Stress-strain curves.

I.10.2. Chemical properties

Changes in size of nanomaterials are an important reason for the increase in chemical activity, which is related to the change in electronic properties. Chemical properties are also partly related to the mechanical properties of liquid or solid materials, by how the electrons are arranged because the ionization energy increases for nanomaterials, which is defined as the energy responsible for removing External electron, this is the result of the closeness of electrons compared to microscopic materials and larger scale materials. Chemical activity is also related to the composition and structure of the electron, and changing the composition or structure changes the degree of catalysis, as nanopowders act as a catalyst and increase the kinetic reaction and enhance the effectiveness of the chemical reaction in combustion. An example of this is gold (Au) nanoparticles that display an improved catalytic reaction and convert them from a noble metal into a reactive catalyst at different scales. It is also possible to benefit from controlling porosity at the nanoscale, and using pore size as a mechanical means to isolate the reactants.

The valence electron, or what is known as the outer electrons of one atom, interacts with the valence shell of the atom adjacent to the solid, which contains several molecules close to each other, but retains their basic electrons. In nanomaterials, a huge number of atoms are present on the faces of their outer surfaces, meaning that they have very high surface area to volume ratios, especially nanoparticles and nanolayers, and as a result both the efficiency of chemical reactions and chemical reactions increases, which always places them at the top of the list of desirable materials for use in various chemical applications, for example newly developed drugs that are characterized by high solubility. Nanoparticles usually exhibit chemistry that distinguishes them from their particle counterparts at the conventional scale, and based on this, a new paradigm for the application of nanomaterials will be opened.

I.10.3. Physical properties

Reducing the dimensions and measurements of material grains to the nanoscale affects the melting temperature, and even affects the physical properties in general. Among the changes to the physical properties of nanomaterials compared to materials of a larger size is an increase in the number of surface atoms, for example when the size of the materials changes to 10nm, 20% of the total atoms will be concentrated on the surface, and when it decreases to a scale less than

1nm, 99% of the total atoms will be concentrated on the surface. These materials contain a huge amount of atoms that are not chemically bonded, which makes them have a strong possibility of bonding with other atoms to reduce kinetic energy, and as a result, high chemical reactions appear. In addition, materials with low masses have a high mobility of electrons, while nanomaterials with quantum size, the band gap energy increases due to the decrease in the nano size.

I.10.4. Magnetic properties

Magnetism arises from electric currents as a result of the rotation of the atom. The intensity and strength of magnetic materials increases as the dimensions of the grains and the surface area become smaller and the presence of atoms on them increases. Therefore, nanomaterials have applications in biotechnology, echo imaging, information storage, and environmental remediation. A study was conducted on iron oxide nanoparticles (Fe_3O_4 NPs) and showed the development of spontaneous magnetization due to the quantum mechanical exchange interaction. These nanoparticles are also highly dynamic from an industrial standpoint, which makes them susceptible to oxidation in the air and loses their magnetic property. To get rid of oxidation, magnetic nanomaterials are mixed using different techniques and to maintain the safety of these particles.

I.10.5. Electrical properties

The small size of materials to the nanoscale and the increase in the surface density of atoms, that is, the increase in the density of the boundary numbers of the grains, reflects positively on their electrical properties. Insulating materials increase their ability to conduct electrical current at the nanoscale, as nanomaterials are subject to the laws of quantum physics instead of Newton's classics for objects the largest, and as a result, nanomaterials are used in the manufacture of microsensors and electronic chips in modern devices, which have high technical specifications.

I.10.6. Optical properties

Optical properties are considered one of the most important properties characterized by nanomaterials, as they have captured the attention of optics scientists, as the sizes of nanoparticles affect the electronic structure, as a result of energy changes through the transfer of the electron from the transport band to the valence band, as absorbance and the energy gap are

related to changes in these transitions **figure (I.5)**. As for other changes, such as changing size, they will change both the electronic and physical properties. To clarify further, the conduction and color changes in semiconductors. For example, pure gold grains, which have a diameter of 200 nm and a golden color, then reduce them to less than 20 nm to become colorless (transparent), and as the increase miniaturization, its color changes gradually from green, then orange, then red. This property contributes to the manufacture of device screens with high resolution, contrast, and purity of colors.

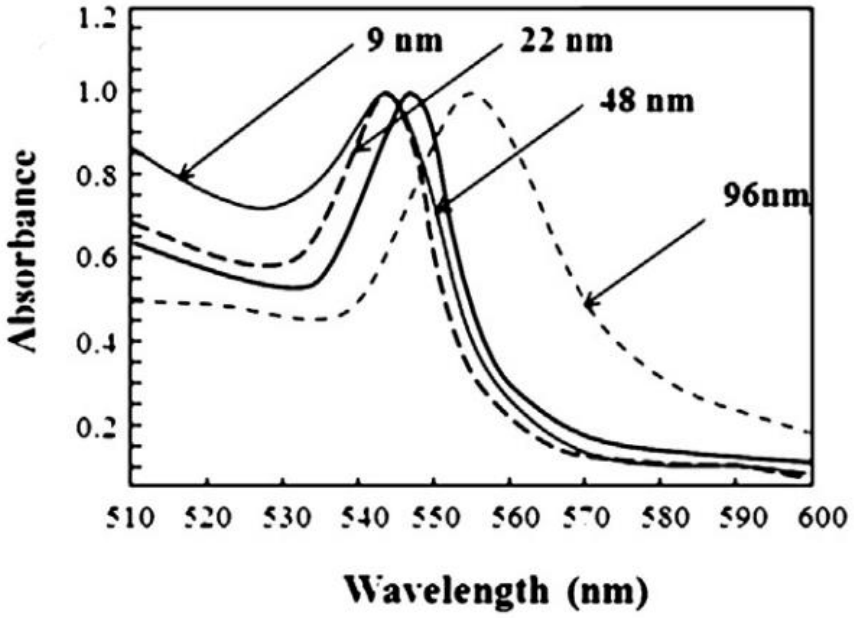

Figure I.5 : Absorbance curves for nanoparticles of different sizes.

I.11. Preparation of nanomaterials

When materials are prepared and manufactured in nanometer sizes, they acquire exceptional electrical, optical, and magnetic qualities and properties that are not available to them when they are in the tangible size, despite the identical chemical composition in both cases, due to the new arrangement that the atoms take. The different properties of the prepared nanomaterials depend on the size of their granules, and also depend on method used in producing the nanomaterial. There are many methods for manufacturing materials at the nanoscale, which depend mainly on reducing the grains of the material or what are called top-down approaches, as well as on the assembly of the atoms of the material or what is known as bottom-up approaches. Thus, there are

many methods for preparing nanomaterials and they can be classified into three categories: Preparation by physical methods, preparation by chemical methods, and preparation by mechanical methods. We will provide an explanation of each of the approaches followed in addition to some of the methods used in the production of these nanomaterials as follows [35]:

- **The method is top-down**

The preparation of nanomaterials is considered a top-down approach by reducing the size of the material from the centimeter scale down to the most common and widely used nanoscale dimensions, due to its ability to prepare various nanomaterials in large quantities. Among the preparation methods is the mechanical grinding method, as there is many literature that has used grinding mechanical. Mechanical methods are used in various ways to prepare magnetic materials, including the literature[36][37], in addition to the synthesis of nano-drugs in the pharmaceutical industry[38][39], and to prepare materials for electronic applications[40-42]. However, the literature that uses this method is sparse, and this is due to the limited control over the formation and size of nano-grains and also the preparation process takes time. For a long time, up to 20 hours[36].

- **The method is bottom-up**

Most researchers use bottom-up approaches due to the absence of the aforementioned drawbacks related to the top-down approach. This method relies on preparing larger blocks of atomic structure [43], that is, moving from a lower scale to the nanoscale, and in this case it relies mainly on chemicals.

Below we mention among the most widely used and common applied methods for preparing nanomaterials.

I.11.1. Preparation by physical methods

I.11.1.1. Ablation method using laser beams (laser ablation method)

In it, a high-energy pulsed laser is used on a solid target. This process is performed in a vacuum room. The laser beam interacts with the target, and then the particles fly away, forming plasma and depositing on the base, forming thin strips, **Figure (I.6)**[27][44][45].

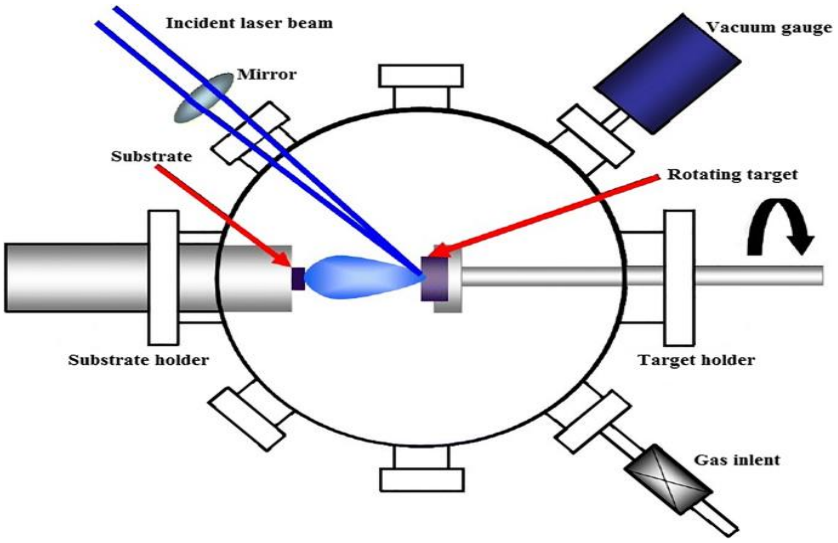

Figure I.6 : Laser ablation method[46].

I.11.1.2. Physical vapor deposition (PVD) method

Physical vapor deposition (PVD) is one of the vapor phase approaches, where thin, nano-thick layers are obtained by evaporating the solid material to be deposited at high temperatures and under vacuum, then condensing the vapor on the substrates and depositing the coating by heterogeneous nucleation growth of crystals. In the beginning, the crystals compete to grow and form in a variety of directions to condense at the end of deposition as preferential sites for growth, as the high temperature increases the chemical reaction and evaporation of the solvents. The PVD method is used to collect nanoparticles, where the material of the thin films and the type of substrate are important factors that aid in deposition. Among the literature that used this method are Figgemeier and Ogi[47][48], and it is possible to deposit many types of materials in the form of thin layers and nanostructures using various PVD processes, for example, electron beam physical vapor deposition, evaporative deposition, cathode arc deposition, and ion plating, in addition to improved sprays, and these are used Coatings are used in various applications such as optics, automotive, medical, firearms, paints, etc. The physical vapor deposition method was also used in 2010 by NASA scientists at the NASA Glenn Research Center in Cleveland Ohio[35][49][50].

I.11.2. Preparation by chemical methods

I.11.2.1. Sol-gel Method[50][35][16]

Sol-Gel methods are among the most common methods for synthesizing particles, as this method goes through two stages: The liquid phase (sol), then after a period of time the material evaporates, turning into the gel phase, and therefore it is called the sol-gel method. Its importance lies in the ability to control the nanostructure during the initial manufacturing by controlling the size of the particles and the homogeneity of their distribution, and it begins This method involves dissolving powdery raw materials, or what are known as precursors, to turn into a colloidal solution, which is similar to a fluid containing sediments of ultra-fine solid nanoparticles to gradually develop into a gel. Then, the incoherent gelatinous material can be isolated and the nanoparticles can be obtained using factors such as filtration, drying, or Centrifugation is an easy-to-use and low-cost method. The solution is used to dip the surfaces of materials to protect them from corrosion, as well as to deposit its particles in the form of layers and to produce ultra-fine nanoparticle powders. This method was used especially with metal oxides[51-53], but in contrast it has some disadvantages such as the high cost of precursors[54][55], and low Purity coupled with long reaction times, which can hamper scaling up the technology to a viable level[56].

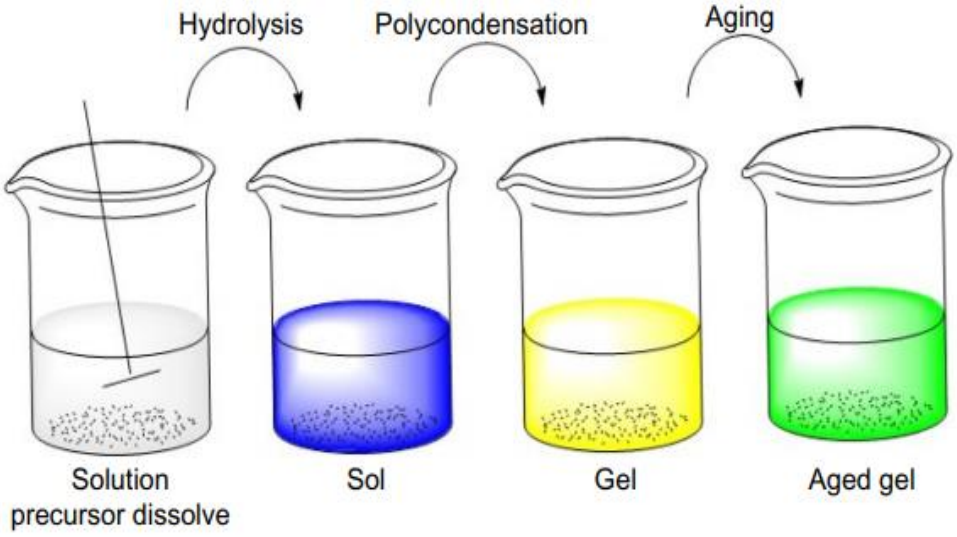

Figure I.7 : How to prepare nanoparticles using sol-gel technology[57].

I.11.2.2. Hydrothermal Method

The hydrothermal method is considered one of the most common methods for preparing nanoparticles, and it received great attention from scientists in various specialties. It was used for the first time by the British geologist Roderick Murchison during 1792-1871 to describe the formation of minerals and rocks through changes in the Earth's crust by the influence of water in the presence of pressure. And high temperatures, as the hydrothermal method has been used to synthesize nanomaterials in many literatures[58-61] as a result of the presence of water as the main reaction medium to dissolve the materials and recrystallize them under high temperature and pressure instead of harmful solvents. Therefore, it is consid a green or sustainable technology, and the shape can also be controlled by controlling the vapor pressure resulting from the reaction using either high or low pressure. This technology relies mainly on the chemical reactions of materials in the middle of the heated solution and the surrounding pressure and temperature. In particular, the solution is placed in an autoclave device consisting of a steel pressure vessel under high temperature and pressure. And increases the solubility of the metal and the crystals precipitate and grow on the substrate. One of the advantages of this technology is that it can produce nanomaterials with minimal material loss. The distribution of crystals and their size can also be controlled by controlling parameters such as reaction time and temperature. The type of solvent and precursor, in addition to the fact that unstablenanomaterials can be produced in the presence of high temperature. The hydrothermal method has been used by many researchers to produce nanomaterials such as nanotubes, graphene sheets, nanodiscs, in addition to casings hollow nanoscale. Multiple types of raw materials can also be used, such as metals[62], carbon[63][64], metal oxides[65-69], sulfides[70], phosphates[71][72], hydroxides[73], and accordingly. It is clear how versatile this technology is and how it relates to a variety of applications[35][57][74].

I.11.3. Preparation by mechanical methods

I.11.3.1. Ball milling method

Preparing nanomaterials at the lowest cost represents a major challenge, and methods have been developed from the bottom up and from the top down to produce these materials, as high-energy ball milling is a widely used method among the top-down production approaches. The mechanical grinding method relies on producing nanomaterials in the form of a powder whose

size ranges from 3 to 25 nm, by placing the material under very high energy and grinding it with steel balls in a vertical, vibrating, or planetary manner. It has been used to manufacture nano-aluminum alloys, corrosion-resistant paint, and many others. Of other nanocomposites [75-77].

I.11.3.2. Mechanical structure method

The method involves crushing coarse grains consisting of micrometer particles of several mixtures, obtaining the smallest microstructure sizes from nanoscale deposits with the appearance of bulky materials, where the nature of gases and temperature also greatly affect the composition of the final product [50][78][76].

I.12. Nanotechnology applications

Nanotechnology is considered one of the promising technologies that is expected to lead to major changes in various fields, especially medical fields and industrial fields such as the field of communications and information, the field of energy and its technologies, in addition to the field of food preservation and manufacturing. Perhaps the extensive use of nanotechnology has been in the medical and scientific fields, as well as It can contribute to finding new materials and products, as nanotechnology currently assumes the creation of new materials and their synthesis at the molecular and atom level. That is, the idea of using nanotechnology is to rearrange the atoms that make up the materials in their correct position, and whenever the atomic arrangement of the material changes, it changes. Resulting from it to a large extent. Nanotechnology has already entered into application, and a dye-sensitive nanocrystalline cell was used to generate an electric current in solar cells. Materials made of nanoparticles that keep floor surfaces shiny were also produced by the American company nanophase, also, nanoparticles of TiO_2 were produced and added to the glass, which work to resist dirt, by the Japanese company Nippon. And not only that, but a waterproof layer with nanoparticles covering the leaves, protecting them from getting wet, was made at the lowest cost by Sally Ramsey, and in the field of electronics, nanotechnology will help in greatly reducing the size of electronic devices. A theory of resistance was discovered, which appears when dealing with electric current and magnetic fields at the atomic level, by the French scientist Ver and the German scientist Grünberg, which is called giant magnetic resistance, which contributed to saving data and information in hard disks and increasing their storage capacity very significantly by transforming the fields magnetism into

an electric current so that the computer can read it. As for the field of communications and information, nanotechnology is used in the manufacture of cables, networks, and circuits that can achieve a breakthrough in this field, in terms of the carrying capacity and efficiency of these circuits, and this appears in the size of the product or its high efficiency, as well as In modern devices such as computers and mobile phones, food nanotechnology is also considered an emerging field of interest that opens up a whole world of new possibilities for the food industry, as food security is among the most important issues that people care about, as anti-microbial and anti-fungal nanoparticles made from the metals silver, magnesium and zinc have been used, in the covers of food preservative containers, they are characterized by being more durable, heat-resistant, and lighter than others. Nano chips also represent insulating materials to prevent food spoilage and the absorption of oxygen. In addition, glass and cardboard containers have been produced that contain nano-covers that act as a barrier that prevents the passage of flavors and gases. Nanomaterials are also used to significantly accelerate chemical reactions. For example, metal nanocatalysts undergo high catalytic treatment, as nanocatalysts are important in the chemical industries, environmental treatment, and petroleum refining. An electrocatalyst consisting of nickel metal nanocomposites has been used for the electrocatalytic oxidation of methane, where Methane can be electrochemically oxidized to produce syngas, electricity and heat, while causing very low environmental pollution. Nanomedicine is considered one of the most important fields of application of nanotechnology, and even the most important of all, due to its direct connection to human life and health. The recent development in nanotechnology has helped change the medical rules used in preventing, diagnosing, and treating diseases. Nanotechnology, for example, provides new methods from drug carriers inside the human body are able to target different cells in the body, monitor disease sites, inject drugs, order cells to secrete appropriate hormones, and also confront the most deadly diseases in humans. Diagnostic devices can also benefit from advances in nano applications in the field of electronics, such as imaging devices. Magnetic resonance imaging, X-ray imaging devices, and ultrasound imaging devices[16][29][32].

I.13. Conclusion

Through the above, we have touched on generalities about nanotechnology and the most important information about this modern technology, to provide an understanding of the behavior of nanomaterials and the change in their properties compared to traditional materials. We also conclude through this chapter that the rapid development of nanotechnology and science has led to the progress and development of other technologies and industries. It is one of the most important technologies today and in the future, and nanotechnology has become the forefront of the most important fields because of its ability to manufacture electronic devices with the smallest size and the highest efficiency in terms of speed and quality in performing various operations, and in improving human service in all areas of life, and this can be achieved improvement by modifying the scale of microstructure, in addition to giving great hope for future scientific revolutions in physics, chemistry, biology, engineering, etc. Therefore, must work to take advantage of the distinct properties of nanomaterials to create innovations and inventions that benefit humanity in many scientific and industrial fields and to speed up and facilitate life in various aspects.

References

[1]هديل نبيل سليم غياضة، متطلبات النانو تكنولوجي المتضمنة في كتب الكيمياء للمرحلة الثانوية ومدى اكتساب طلبة الصف الحادي عشر لها، أطروحة ماجستير، الجامعة الاسلامية-غزة، 2017.

[2] Dr. Mortimer L. Downey, Dr. Duncan T. Moore, Gary R. Bachula, Delores M. Etter, Dr. E. Fenton Carey, Lori A. Perine, Committee on Technology National Science and Technology Council, NATIONAL NANOTECHNOLOGY INITIATIVE: Leading to the Next Industrial Revolution, A Report by the Interagency Working Group on Nanoscience, Engineering and Technology, Washington, D.C, 2000.

[3] Leydecker, s, Nano Materials in Architecture Intrior and Architecture Design, Birkhauser. Germany, 2008.

[4] على حربة، العمارة في ظل تقنية النانو، مجلة جامعة البحث، م المجلد39-ا، ص 83–115، 2017.

[5] Abdullaeva, Zhypargul. Nano-and biomaterials: compounds, properties, characterization, and applications. John Wiley & Sons, 2017.

[6] Durán-Lobato, Matilde, et al. "Nanotechnologies for the delivery of biologicals: Historical perspective and current landscape." Advanced Drug Delivery Reviews 176, 2021.

[7] Stephanopoulos, George, and Gintaras V. Reklaitis. "Process systems engineering: From Solvay to modern bio-and nanotechnology: A history of development, successes and prospects for the future." Chemical engineering science 66.19, 4272-4306, 2011.

[8] Bardosova, Maria, and Tomas Wagner, eds. Nanomaterials and nanoarchitectures: a complex review of current hot topics and their applications. Springer, 2015.

[9] Reineke, Joshua, ed. Nanotoxicity: methods and protocols. Humana Press, 2012.

[10] Shatkin, Jo Anne. Nanotechnology: health and environmental risks. Crc Press, 2017.

[11] Tolochko, N. K. "History of nanotechnology." Encyclopedia of Life Support Systems (EOLSS), 2009.

[12] Hornyak, G. L., Dutta, J., Tibbals, H. F., & Rao, A, Introduction to nanoscience. CRC press, 2008.

[13] Granek, Galina, and Giora Hon. "Searching for asses, finding a kingdom: The story of the invention of the scanning tunnelling microscope (STM)." Annals of Science 65.1, 101-125, 2008.

[14] Hulla, J. E., S. C. Sahu, and A. W. Hayes. "Nanotechnology: History and future." Human & experimental toxicology 34.12, 1318-1321, 2015.

[15] Richard Jones, Nanotechnology and visions of the future (part 1), Soft Machines, 2007.

[16] أ.د.محمد شريف الاسكندري، تكنولوجيا النانو من أجل غد أفضل، عالم المعرفة الكويت، 2010.

[17] Aqel, Ahmad, et al. "Carbon nanotubes, science and technology part (I) structure, synthesis and characterisation." Arabian Journal of Chemistry 5.1, 1-23, 2012.

[18] Iijima, Sumio, and Toshinari Ichihashi. "Single-shell carbon nanotubes of 1-nm diameter." nature 363.6430, 603-605, 1993.

[19] أ.منير نايفة، النانو تكنولوجي (مقدمة في فهم علم النانو تكنولوجي)، مطابع الدار العربية للعلوم- بيروت، 2009.

[20] Monthioux, Marc, and Vladimir L. Kuznetsov. "Who should be given the credit for the discovery of carbon nanotubes?." Carbon 44.9, 1621-1623, 2006.

[21] Hullmann, Angela. "Measuring and assessing the development of nanotechnology." Scientometrics 70.3, 739-758, 2007.

[22] NAZAR HUSSAIN KALWAR, SYNTHESIS, CHARACTERIZATION AND APPLICATION OF NICKEL NANOPARTICLES, A THESIS SUBMITTED TOWARDS THE PARTIAL FULFILLMENT OF THE REQUIREMENT FOR THE AWARD OF DOCTOR OF PHILOSOPHY IN ANALYTICAL CHEMISTRY, National Centre of Excellence in Analytical Chemistry, University of Sindh, Jamshoro – PAKISTAN, 2013.

[23] Murty, B. S., et al. "Unique properties of nanomaterials." Textbook of nanoscience and nanotechnology, 29-65, 2013.

[24] Schwarz, James A., Cristian I. Contescu, and Karol Putyera, eds. Dekker encyclopedia of nanoscience and nanotechnology. Vol. 5. CRC press, 2004.

[25] Bayda, Samer, et al. "The history of nanoscience and nanotechnology: from chemical–physical applications to nanomedicine." Molecules 25.1, 112, 2019.

[26] Condon, Anne. "Designed DNA molecules: principles and applications of molecular nanotechnology." Nature Reviews Genetics 7.7, 565-575, 2006.

[27] نهى علوي الحبشي، ماهي تقنية النانو؟: مقدمة مختصرة بشكل دروس مبسطة، المملكة العربية السعودية، 2011.

[28] Hossain, Kaizar, and Shaik Rameeja. "Importance of nanotechnology in civil engineering." European Journal of Sustainable Development 4.1, 161-161, 2015.

[29] أ.د. محمود محمد سليم صالح، تقنية النانو وعصر علمي جديد، المملكة العربية السعودية، 2015.

[30] Kreyling, Wolfgang G., Manuela Semmler-Behnke, and Qasim Chaudhry. "A complementary definition of nanomaterial." Nano today 5.3,165-168, 2010.

[31] Lövestam, Göran, et al. "Considerations on a definition of nanomaterial for regulatory purposes." Joint Research Centre (JRC) Reference Reports 80; 00-41, 2010.

[32] Bashir, Sajid, and Jingbo Liu. "Nanomaterials and their application." Advanced Nanomaterials and Their Applications in Renewable Energy; Elsevier Inc.: Amsterdam, The Netherlands, 1-50, 2015.

[33] Gong, Shu, and Wenlong Cheng. "One-dimensional nanomaterials for soft electronics." Advanced Electronic Materials 3.3, 1600314, 2017.

[34] Hatem, S., Nanotechnology Research Center. Faculty of Engineering, Alexandria University, P 12, 2010.

[35] Selina Vi Yu Tang, BSc, Synthesis of Nanomaterials for Biomedical Applications, Thesis submitted to the University of Nottingham for the degree of Doctor of Philosophy January 2014.

[36] Thuan, Nguyen Chi, Pham Thanh Phong, and Nguyen Xuan Phuc. "Magnetic properties of $La_{0.7}Ca_{0.3}MnO_3$ nanoparticles prepared by reactive milling." Journal of alloys and compounds 479.1-2 828-831, 2009.

[37] Sampathkumaran, E. V., et al. "Magnetism of fine particles of Kondo lattices, obtained by high-energy ball-milling." Journal of Physics: Condensed Matter 23.9, 2011.

[38] Laaksonen, Timo, et al. "Intact nanoparticulate indomethacin in fast-dissolving carrier particles by combined wet milling and aerosol flow reactor methods." Pharmaceutical research 28, 2403-2411, 2011.

[39] Basa, Shradhanjali, et al. "Production and in vitro characterization of solid dosage form incorporating drug nanoparticles." Drug development and industrial pharmacy 34.11, 1209-1218, 2008.

[40] Chen, Zhongxue, et al. "Facile synthesis and stable lithium storage performances of Sn-sandwiched nanoparticles as a high capacity anode material for rechargeable Li batteries." Journal of Materials Chemistry 20.34, 7266-7271, 2010.

[41] HALLMANN, S., FINK, M. J. & MITCHELL, B. S. The mechanochemical formation of functionalized semiconductor nanoparticles for biological, electronic and superhydrophobic surface applications. Houston, TX. 2011.

[42] Zaghib, Karim, et al. "A new synthetic route of LiFePO4 nanoparticles from molten ingot." ECS Transactions 33.27, 23, 2011.

[43] ROTELLO, V. M. Nanoparticles: Building Blocks for Nanotechnology, Kluwer Academic/Plenum Publishers. 2004.

[44] Filipponi, Luisa, Duncan Sutherland, and Interdisciplinary Nanoscience Center. "Introduction to nanoscience and nanotechnologies." NANOYOU Teachers Training Kit in Nanoscience and Nanotechnologies, 1-29, 2010.

[45] Amendola, Vincenzo, et al. "Top-down synthesis of multifunctional iron oxide nanoparticles for macrophage labelling and manipulation." Journal of Materials Chemistry 21.11, 3803-3813, 2011.

[46] Naser, Hameed, et al. "The role of laser ablation technique parameters in synthesis of nanoparticles from different target types." Journal of Nanoparticle Research 21, 1-28, 2019.

[47] Ogi, Takashi, et al. "Synthesis of nanocrystalline GaN from Ga2O3 nanoparticles derived from salt-assisted spray pyrolysis." Advanced Powder Technology 20.1, 29-34, 2009.

[48] Figgemeier, E., et al. "Titanium dioxide nanoparticles prepared by laser pyrolysis: Synthesis and photocatalytic properties." Applied Surface Science 254.4, 1037-1041, 2007.

[49] Shahidi, Sheila, Bahareh Moazzenchi, and Mahmood Ghoranneviss. "A review-application of physical vapor deposition (PVD) and related methods in the textile industry." The European Physical Journal Applied Physics 71.3, 2015.

[50] TOUNSIA AIT AHCENE, ELABORATION, ETUDE NANOSTRUCTURALE ET PROPRIETES ELECTRIQUES DE NANOMATERIAUX DU SYSTEME ZnO - Bi_2O_3 , Pour obtenir le titre de DOCTORAT D'ETAT EN PHYSIQUE, Université Mentouri de Constantine, 2007.

[51] Bezzi, G., et al. "A novel sol–gel technique for hydroxyapatite preparation." Materials Chemistry and Physics 78.3, 816-824, 2003.

[52] Senthilkumaar, S., and R. Thamiz Selvi. "Synthesis and characterization of one dimensional ZnS nanorods." Synthesis and Reactivity in Inorganic, Metal-Organic, and Nano-Metal Chemistry 38.9, 710-715, 2008.

[53] Isasi-Marín, J., et al. "Structural, magnetic and luminescent characteristics of Pr3+-doped ZrO_2 powders synthesized by a sol–gel method." Journal of Physics D: Applied Physics 42.7, 2009.

[54] Chen, Chien Chon, Chin-Hua Cheng, and Chung-Kwei Lin. "Template assisted fabrication of TiO_2 and WO_3 nanotubes." Ceramics International, 39.6, 6631-6636, 2013.

[55] Tang, Guogang, et al. "Template-assisted hydrothermal synthesis and photocatalytic activity of novel TiO_2 hollow nanostructures." Ceramics International 39.5, 4969-4974 , 2013.

[56] Tighe, Christopher J., et al. "Scale up production of nanoparticles: continuous supercritical water synthesis of Ce–Zn oxides." Industrial & Engineering Chemistry Research 52.16, 5522-5528, 2013.

[57] Rane, Ajay Vasudeo, et al. "Methods for synthesis of nanoparticles and fabrication of nanocomposites." Synthesis of inorganic nanomaterials. Woodhead Publishing, 121-139, 2018.

[58] Ioku, Koji, Masahiro Yoshimura, and Shigeyuki Somiya. "Post sintering of apatite ceramics from fine powders synthesized under hydrothermal conditions." Journal of the Ceramic Society of Japan 96.1109, 109-110, 1988.

[59] Sōmiya, Shigeyuki, and Rustum Roy. "Hydrothermal synthesis of fine oxide powders." Bulletin of Materials Science 23, 453-460, 2000.

[60] Adschiri, Tadafumi, Katsuhito Kanazawa, and Kunio Arai. "Rapid and continuous hydrothermal crystallization of metal oxide particles in supercritical water." Journal of the American Ceramic Society 75.4, 1019-1022, 1992.

[61] Adschiri, Tadafumi, Yukiya Hakuta, and Kunio Arai. "Hydrothermal synthesis of metal oxide fine particles at supercritical conditions." Industrial & engineering chemistry research 39.12, 4901-4907, 2000.

[62] Aksomaityte, Gabriele, Martyn Poliakoff, and Edward Lester. "The production and formulation of silver nanoparticles using continuous hydrothermal synthesis." Chemical engineering science 85, 2-10, 2013.

[63] Nassar, Mostafa Y. "Size-controlled synthesis of $CoCO_3$ and Co_3O_4 nanoparticles by free-surfactant hydrothermal method." Materials letters 94, 112-115, 2013.

[64] Ni, Shibing, Xuelin Yang, and Tao Li. "Hydrothermal synthesis and photoluminescence properties of $SrCO_3$." Materials Letters 65.4, 766-768, 2011.

[65] Adschiri, Tadafumi, et al. "Hydrothermal synthesis of metal oxide nanoparticles at supercritical conditions." Journal of Nanoparticle Research 3, 227-235, 2001.

[66] Cabanas, Albertina, et al. "A continuous and clean one-step synthesis of nano-particulate $Ce1- xZrxO_2$ solid solutions in near-critical water." Chemical Communications 11, 901-902, 2000.

[67] Cabañas, Albertina, et al. "Synthesis of nanoparticulate yttrium aluminum garnet in supercritical water–ethanol mixtures." The Journal of supercritical fluids 40.2, 284-292, 2007.

[68] Leybros, Antoine, et al. "CFD simulation of ZnO nanoparticle precipitation in a supercritical water synthesis reactor." The Journal of Supercritical Fluids 70, 17-2, 2012.

[69] Lester, E. D., et al. "Controlled continuous hydrothermal synthesis of cobalt oxide (Co_3O_4) nanoparticles." Progress in Crystal Growth and Characterization of Materials 58.1, 3-13, 2012.

[70] Liu, Yuanfang, et al. "Hydrothermal synthesis of square thin flake CdS by using surfactants and thiocarbohydrate." Materials research bulletin 36.7-8, 1231-1236, 2001.

[71] Chaudhry, Aqif A., et al. "Instant nano-hydroxyapatite: a continuous and rapid hydrothermal synthesis." Chemical communications 21, 2286-2288, 2006.

[72] Lester, Edward, et al. "Producing nanotubes of biocompatible hydroxyapatite by continuous hydrothermal synthesis." CrystEngComm 15.17, 3256-3260, 2013.

[73] Wang, Qiang, et al. "Synthesis of ultrafine layered double hydroxide (LDHs) nanoplates using a continuous-flow hydrothermal reactor." Nanoscale 5.1, 114-117, 2013.

[74] Gan, Yong X., et al. "Hydrothermal synthesis of nanomaterials." Journal of Nanomaterials, 1-3, 2020.

[75] Yadav, Thakur Prasad, R. Manohar Yadav, and D. Pratap Singh. "Mechanical milling: a top down approach for the synthesis of nanomaterials and nanocomposites." Nanoscience and Nanotechnology 2.3, 22-48, 2012.

[76] Dutta, J. and Hofmann, H. Nanomaterials, Electronic Book, 2005.

[77] Rajput, Namita. "Methods of preparation of nanoparticles-a review." International Journal of Advances in Engineering & Technology 7.6, 2015.

[78] Tulinski, Maciej, and Mieczyslaw Jurczyk. "Nanomaterials synthesis methods." Metrology and Standardization of Nanotechnology: Protocols and Industrial Innovations, 75-98, 2017.

Chapter II

Basics of electronic spin technology and its applications

Chapter II : Basics of electronic spin technology and its applications

II.1. Introduction

Over the past few decades, a new research topic known as spintronics has flourished, and this in turn has led to developments in information and communication technologies, in which electron spin as well as charge are addressed and is closely related to the quantum property of the electron, resulting in features smaller than 100 nanometers in size and miniaturizing semiconductor electronic devices while increasing their capabilities, performance, reliability and functionality, as recent studies have shown that it is possible to work on the rotation of charge carriers and use this quantity to modify the electrical and optical properties of semiconductor structures. The working principle of Spintronique devices is based on a simple scheme, by storing written information in the spins as rotating in a specific direction (up or down) and connecting them to mobile electrons to carry the information along the wire and read it at the station. The spin direction of the conduction electrons persists for a relatively long time (nanoseconds) during which the electron momentum decays, making these devices already in industrial use as storage and memory applications and as magnetic field sensors for hard disk read heads [1].

II.2. The electron spin

II.2.1. Electron discovery

In 1897, British physicist Joseph Thomson was able to discover the electron through its kinetic activity, using cathode rays while conducting vacuum tube experiments. It is considered among the elementary particles that were discovered before other components of the atom, and even before the atom itself. It was later called the atom. “Electron” was based on a proposal by Irish physicist George Stoney, which gained worldwide acceptance[2]. Thomson also learned about some of the properties of the particle of matter (the electron). He expected it to be two thousand times smaller than the hydrogen ion, which is the lightest atomic particle ever discovered, and which enabled scientists to understand the nature of electric current and the atomic structure of matter [3].

II.2.2. The internal angular momentum of an electron

Experimental evidence has shown that the electron has angular momentum independent of its orbital angular momentum. These experiments suggest only two possible states for this angular momentum, and they follow the pattern of a 1/2 angular momentum quantum. Angular momentum and magnetic momentum can indeed arise from a rotating ball of charge. But this classical conception cannot fit the size or nature of the spin of the electron. The electron spin property must be considered as quantum epistemic without a detailed classical analogy. The quantum number associated with the electron spin follows the characteristic pattern[4] :

$$S=\sqrt{S(S+1)}\hbar, \qquad S=\frac{1}{2}, \qquad m_s= \pm\frac{1}{2} \qquad \text{(II.1)}$$

II.3. Self-Spin

When certain elementary particles move through a magnetic field, they are deflected in a way that suggests they have small magnetic properties. In the classical world (classical physics), a rotating charged body has magnetic properties very similar to those exhibited by these elementary particles, so physicists described elementary particles as they are particles that have a self-spin.

But it is misleading to conjure up an image of the electron as a small, rotating object. Instead, one must accept the observed fact that the electron is deflected by being exposed to a magnetic field. If one insists on the image of a rotating object, real contradictions will emerge. Unlike a small tossed ball, for example, the spin of an electron does not It never changes, and has only two possible directions. In addition, the idea that electrons and protons are rigid “bodies” that can “spin” in a vacuum is difficult to maintain in itself given what we know about the rules of quantum mechanics, yet the term “self-spin” is still used [5].

II.4. The scientific and technical perspective of self-winding

Starting in the 1920s, scientists Otto Stern and Zalthergeiach from the University of Hamburg conducted a series of important experiments on a beam of atomic particles, knowing that all moving charges produce magnetic fields. They proposed measuring the magnetic fields produced by electrons revolving around the nuclei in atoms. But what surprised the two scientists was that the electrons themselves behaved as if they were rotating around themselves very quickly, producing small magnetic fields independent of those magnetic fields resulting from their orbital

movement around the nucleus. The term "self-spin" was soon used to describe this apparent rotation of subatomic particles.

Self-spin is considered a strange physical quantity. It is similar to the rotation of a planet around itself, as it gives the particle angular momentum and a small magnetic field. Based on the known sizes of the particles, the surfaces of these charged particles must move faster than the speed of light in order to produce the measured magnetic moments. In addition, This determines the spin that has specific discrete values, and these factors create all sorts of complications that make spin one of the most difficult aspects of quantum mechanics.

In a broader sense, self-spin is a fundamental property that affects the arrangement of electrons and nuclei in atoms and molecules, giving it great physical importance in chemistry and solid-state physics. Likewise, spin is a fundamental consideration in all interactions between subatomic particles, whether in high-energy particle beams, or in liquids with the low temperature or weak flow of particles from the Sun is known as the solar wind. In fact, many if not most physical processes, ranging from the smallest nuclear scales to the largest astrophysical distances, depend heavily on particle interactions and the self-spin of those particles. Self-roll represents the total angular moment of an object. The self-spin of elementary particles is similar to the self-spin of macroscopic bodies. In fact, the self-spin of a planet is the sum of the values of the self-spin moments and the orbital angular moments of all its elementary particles, as well as the self-spin of other complex bodies such as atoms and protons (made up of quarks) [6].

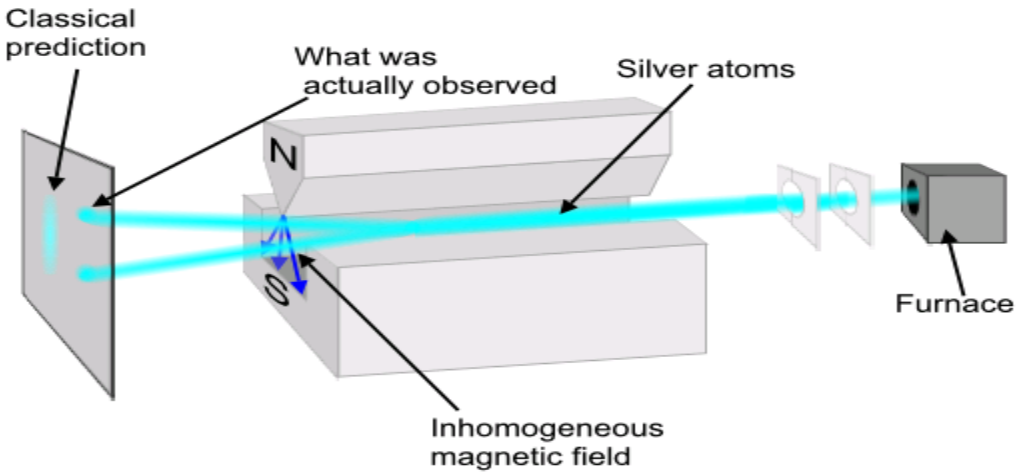

Figure II.1 : Stern-Gerlach experiment.

II.5. Definition of electronic spin

Spin, in quantum mechanics, can be observed somewhat vaguely, which does not have a very precise classical counterpart. However, it turns out that the rotation of the electron around itself is responsible for the origin of magnetism, and the magnetic moment can take values S= ± 1/2 and this is according to the direction of the magnetic field. The rotation of an electron around itself in a counterclockwise direction is also known as a spin up electron. If it rotates in a clockwise direction, it is called a downspin electron[5].

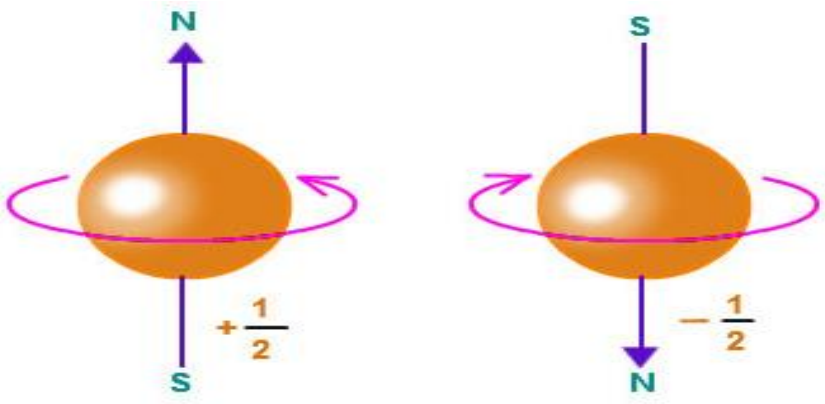

Figure II.2 : Electronic spin (Up=+1/2, Dn=-1/2) [7].

II.6. Basic principles of spintronics

The basic principle of electron spin includes the spin-dependent properties of the electron in addition to its charge- and mass-dependent properties, as it considers the angular momentum of the particle that cannot be lost or gained. It also makes possible the possibility of its use in purely quantum applications such as quantum computers due to the quantum nature of spin. Which represents two possibilities for the two naturally occurring states “0” and “1” in logical operations.

II.6.1. Spin electronics and magnetism

Electric charges, which are electrons and holes in semiconductors, are used to transmit and capture information. This is in classical electronics. In addition to their charge, they possess a magnetic moment, which is rotation. This spin of the electron causes the appearance of magnetism in magnetic materials, where the number of lower-spin and upper-spin electrons

differs, and these electrons are the same as the electrons participating in electrical transmission. However, the similarity of the number of upper-spin electrons with the number of lower-spin electrons leads to the incompatibility of magnetic fields and the emergence of so-called non-magnetic materials, whether metallic, semiconducting or insulating, as this difference is considered the first basic principle of spin electrons[8-11].

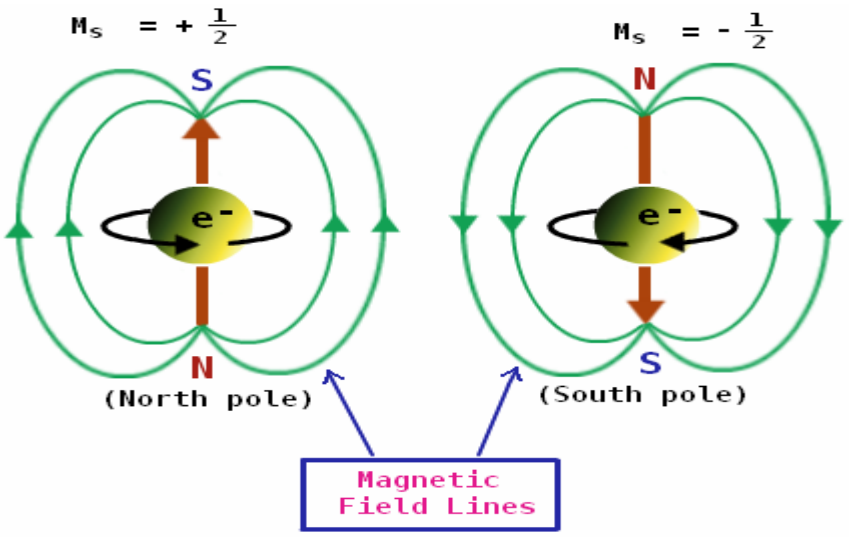

Figure II.3 : A diagram of the electron spin that determines the direction of the magnetic lines and poles formed[12].

II.6.2. The direction of the electronic spin is preserved

Electrons spread in metals and their movement slows down as a result of the presence of crystalline defects. Despite the collisions they are exposed to, propagation is neglected with a reversal in the spin directions of the electrons. Therefore, the lower and upper spin electrons generate two electric currents in parallel, and this is called Mott approximation[13].

II.6.3. Spread of electrons according to spin

The diffusion of electrons in magnetic materials such as iron and nickel varies depending on their spin, since these materials have an unequal number of electrons with an upper spin and a lower spin that form a local magnetic field. Therefore, the propagation potential of the current-conducting electrons will be either completely parallel to the local magnetic field or anti-parallel (reverse).

II.6.4. Electron spin accumulation

When an electric current passes from a magnetic material to a non-magnetic material, an insulating region will appear in which electrons accumulate. This is because the number of upper-spin and lower-spin electrons is different in magnetic materials, while their number is equal in non-magnetic materials. As the buffer zone accumulates upper-spin and lower-spin electrons, but they are not as different as they are in the magnetic material, nor are they equal like the non-magnetic material.

II.7. spintronics phenomena

II.7.1. Great magnetic resistance

The discovery of the greatest magnetic resistance (GMR) quickly attracted attention due to its potential applications in exploiting electronic spin, as it was discovered in 1988 in Orsay, Germany, on multiple, alternating layers of very thin layers of iron and chromium, where chromium is a non-magnetic material and the iron was magnetized. In different directions according to each layer. Studies of great magnetic resistance have doubled in many laboratories and at the experimental level Stuart Parkin and others have demonstrated the presence of GMR in Fe/Cr, Co/Cr and Co/Ru layers prepared by the simple method by spraying. The electrical resistance of a conductor changes when it is applied to a magnetic field, which is called magnetic resistance. This magnetic resistance is amplified by multiple magnetic layers made up of alternating layers of magnetic and non-magnetic metals, which is GMR, or giant magnetic resistance[14-16].

Conduction currents were applied to the Cr/Fe model, where chromium represents a non-magnetic material and iron was magnetized in different directions. According to the applied current, the following cases resulted:

II.7.1.1. Cross stream perpendicular to the plane of layers (CPP)

In most metals, electrons are subject to inelastic and elastic collisions. Neglecting the possible processes of electron re-rotation, it can be considered that the current is transmitted in the metal by two types of electrons: upper-spin electrons and lower-spin electrons, in which the electronic spin information is preserved. At the level of transmission distance, this distance is called the propagation length.

When an electric current passes between two layers of iron metal such that the two layers are aligned in parallel and are magnetized in opposite directions and in the middle is a layer of non-magnetic chromium CPP (AP) metal, this causes an imbalance in the spin groups between the two metals, and this is due to an imbalance in the number of electrons spinning up and down, which leads to the emergence of a transition region in which the spin is coordinated, this idea was first introduced independently by Van Son and Johnson. In this case, the upper-spin electrons cross the first layer, but face severe resistance when they reach the last layer, while fewer of lower-spin electrons that can cross the first layer can easily cross the last layer. In the case of magnetization of the two layers in the same direction CPP (P) by passing the electric current, the upper-spinned electrons will be able to cross the first layer and will not find any resistance as they pass through the layers. However, on the other hand, the lower-spinned electrons will find strong resistance at the first layer, and some electrons will pass through it to be able to pass the next layer with ease and without any resistance[13][17-20].

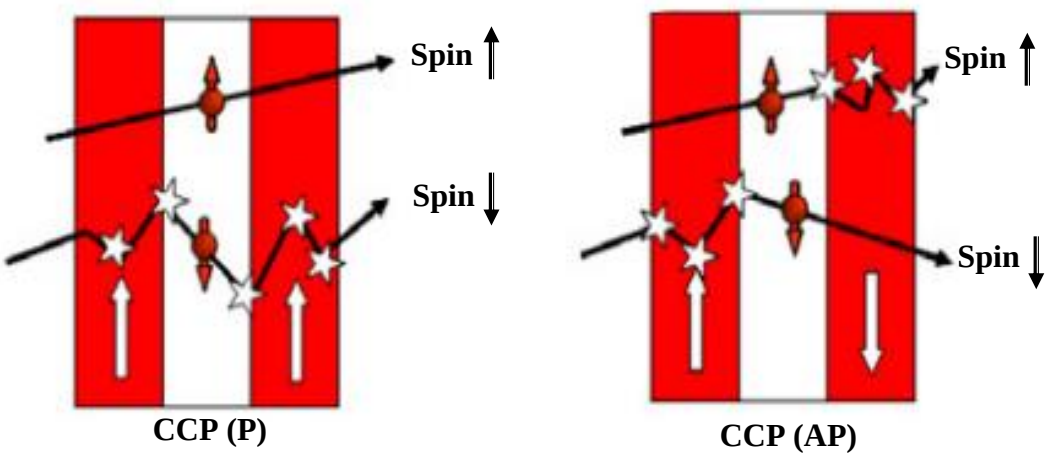

Figure II.4 : A diagram showing the path of electrons in a CPP configuration and the terms AP and P corresponding to parallel and anti-parallel magnetization.

II.7.1.2. Current parallelism in layers plane (CIP)

The propagation of electric current in parallel over layers such that the magnetization of the two iron layers is opposite in direction is somewhat more complicated, as the difference in propagation potential for each type from types of carriers in a ferromagnetic metal must be taken into account. In this case CIP (AP), the electrons move through all layers in a random manner, regardless of their spin, as a result of being exposed to strong resistance that hinders their movement. At the end of the layers, only electrons with self-spin that are compatible with the magnetization of the layer are able to cross outside the path. In the case of magnetization of the two layers of iron in the same direction CIP (P), the electrons with a spin that is compatible with the magnetization of the two layers will pass easily and will not be exposed to any resistance that hinders their movement, while electrons with a spin that is opposite to the magnetization of the two layers will be exposed to severe resistance and a small number will escape through it. As the resistance of each channel includes the average of the different diffusion processes that the electrons undergo throughout their journey, and through the various cases it becomes clear that the electrons in the CPP (AP) mode are exposed to the greatest magnetic resistance[21][13][17-20].

Figure II.5 : A diagram showing the path of electrons in a CIP configuration and the terms AP and P corresponding to parallel and anti-parallel magnetization.

II.7.2.Transition Zone

During the formation of the simple case geometry (CPP), which consists of two magnetic iron metal layers, aligned in parallel and asymmetrical as a result of the different spins of the conduction carriers, either up or down, with a layer of normal, from non-magnetic metal in the middle, as shown in the **figure (II.6)**. In this case, the current electrons move between the layers from the first layer with spin to the top, through the interlayer (ordinary metal), to the second layer with spin to the bottom. As a result of the electrons passing through the middle layer, the spin groups in the two layers are disturbed due to the difference in the number of spin electrons between the two layers. This is because magnetic metals have a different number of electrons with upper and lower spins compared to non-magnetic metals, which are equal. Electrons accumulate in this region to gradually harmonize the spin and it is called the transition region. The system moves from a state of spin imbalance to a state of spin balance, where the maximum magnetism resistance (GMR) depends on the spin buildup and it increases in this configuration (CPP) compared to the CIP model, which does not contain the spin buildup phenomenon as a result of the transfer of electrons parallel with the layers[17][22].

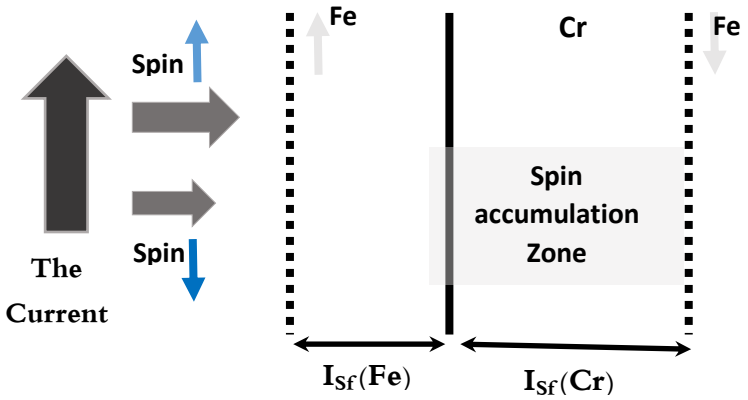

Figure II.6 : Schematic diagram showing the spin accumulation region in the case of the Fe/Cr layer.

II.7.3.Tunnel magnetic resistance TMR

Some disadvantages of high magnetic resistance may appear in practical applications, such as the need to use advanced techniques to measure resistance, including superconducting contacts. In addition, it is generally difficult to separate layers magnetically. To facilitate these difficulties, a simple structure was created, which is called a tunnel junction, which consists of two layers. Two magnets separated by an insulating material and connected to two probes for current and voltage. The magnetism is determined in the first layer and the direction of magnetization in the second layer is controlled according to the magnetization of the first layer. The ferromagnetic state is determined by measuring the intensity of the current, where the high current represents the ferrous layer and the low current represents the antimagnetic layer. When the current passes through the first magnetic layer, the electrons whose spin is directed in the direction of the magnetization of the layer will be able to pass through, and accumulate in the insulating area to form a tunnel. Then two cases are considered:

- If the second layer has magnetization in the same direction as the first layer (P), the electrons pass through the insulator through the tunneling effect, and the magnetoresistance is weak.
- If the second layer contains magnetization in the opposite direction of the first layer (AP), the electrons will not be able to cross the second layer. However, only some electrons are able to cross the barrier, and therefore the current that crosses is weak and the magnetic resistance is large, as shown in the f**igure(II.7)**[23][24].

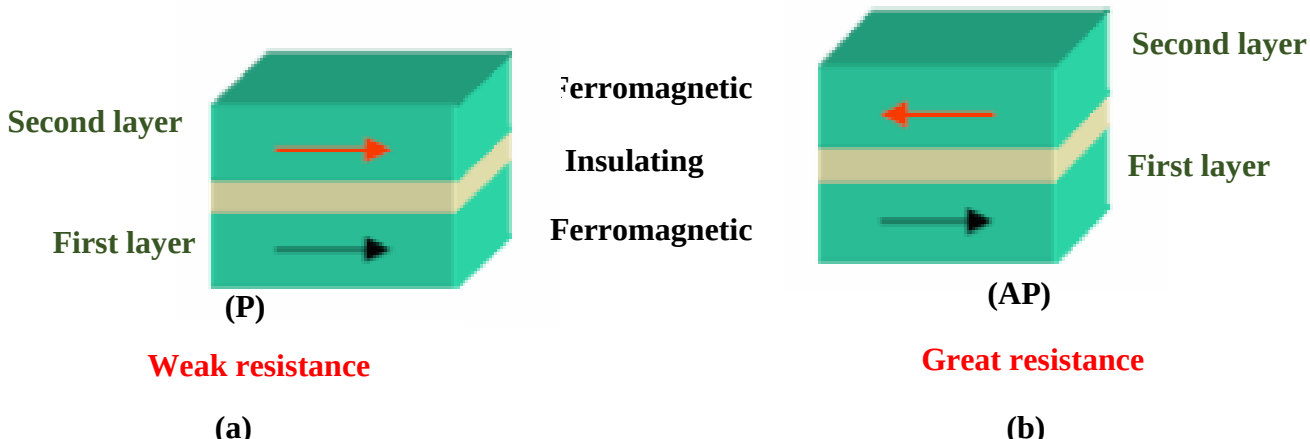

Figure II.7 : A diagram showing a magnetic tunnel intersection in parallel and antithetical states.

II.7.4. Spin electron transfer through carbon nanotubes and nanowires

Functional performance is related to the property of metals and ferromagnets with spin electrons. Work is being done to combine the field of molecular electronics and their spin, and this is likely to lead to many advantages in the field of industry due to the use of electronic spin mechanisms, and in this race towards organic spin devices, as An important place is the use of carbon nanotubes, which are ideal carriers with significantly long coherence length. They are virtually defect-free graphene sheets with coiled particles of enormous aspect ratios. Carbon nanotubes are an ideal playground for examining both GMR and TMR. Because of their bonding with other materials, it would be expected that two tubes with different anisotropy would bond to a magnetic surface in a similar way, and it has been reported TMR like transport via carbon nanotubes has already been reported experimentally by several researchers[24-28].

The bonding between other materials and nanotubes is among the properties that are relevant to the physics related by agreement of radially the Fermi level to the tube axis, where the transport between the nanotube and a magnetic metal is determined by the overlap between the corresponding Fermi surfaces **figure (II.8)**, in case (a) when the Fermi wave vector $K_F^{\uparrow}$and $KF^{\downarrow}$is larger than the Fermi wave vector of the carbon nanotube. There is always a k-vector for the magnetic metal that matches the Fermi wave vector for both spins. Therefore, the two spins, can be crossed in the tube and the total resistance is independent of the spin and is small. As for case (b) when the Fermi wave vector $K_F^{\uparrow}$ and $K_F^{\downarrow}$ is smaller than the Fermi wave vector of the carbon nanotube, there are no states available for the metal contact whose wave vectors exactly match the Fermi wave vector of the carbon nanotube, and the spin electrons can propagate out of the Fermi surface into states with large longitudinal momentum. It can also be expected that increasing the temperature may lead to a reduction in the resistance of the spin-up electrons, while leaving the spin-down electrons unchanged. As for case (c), when the Fermi wave vector $K_F^{\downarrow}$ is smaller than the Fermi wave vector of the nanotube At the same time, the Fermi wave vector of the carbon nanotube is greater than $K_F^{\uparrow}$, the majority of the electrons will be able to enter the carbon nanotube and become completely polarized. An increase in temperature can also lead to a deterioration in polarity, and this is due to the fact that the high energy states are occupied by the spin electrons. Rotational polarization also depends on the identity of the

number of occupied states with longitudinal momentum and the type of the carbon nanotube[24] [4].

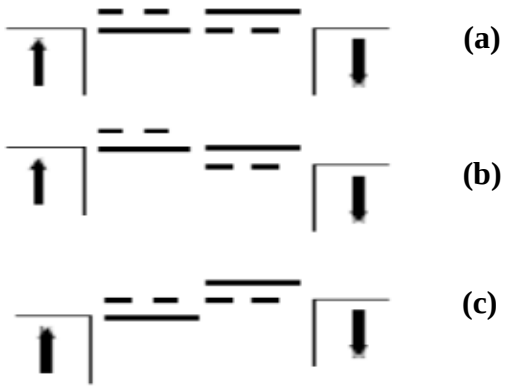

Figure II.8 : A diagram showing the alignment of planes at the magnetic contact point.

II.8. Electro-spin applications

Spintronics applications depend on taking advantage of the spin of electrons, by developing electronic materials that are characterized by the transfer of spin instead of its charge only in materials based on semiconductors, which consist of magnetic semiconductors and ferromagnetic metals, as traditional electronic devices depend on the transfer of electrical charge. Through holes and electrons without exploiting the spin. The advantages of these devices over traditional non-magnetic devices are their speed in data processing, their low energy consumption, as well as their small size. It is possible to create data storage devices that operate at the speed of light and at the size of an atom, as well as computer memories that are thousands of times denser and faster. In the near future, it is expected that devices based on spin electronics will spread. Hence, we must deal with the contradictory and sometimes ambiguous quantum mechanics, and the dominance of wave properties over the behavior of electrons with their quantum properties, which is the spin that is closely related to magnetism. Among the spintronic devices are the quantum computer and the magnetic resistance random access memory (RAM-M) with TMR technology, spin scanner and spin transistor, in addition to sensors, biomedical applications, quantum computing, etc[29].

- The difference between a traditional transistor-based computer and a quantum computer lies in the use of quantum mechanical phenomena such as entanglement and superposition to represent the data operations it performs, and it will be able to solve some problems faster, and this is because the basic unit of information (quantum qubit) is not binary but rather quaternary, and this property arises as a result directly due to its commitment to the laws of quantum mechanics, it exists in states corresponding to a mixture or superposition of the classical logical state 0 or 1, that is, it can exist in the form of 0 and 1 or in the form of 0 or 1 with the presence in each case of a numerical coefficient, and the coding information is determined within a single quantum qubit and exists In a superposition from 0 to 1 for use by a quantum computer, since each electronic spin represents one qubit, the superposition can also change randomly from 0 to 1 as a result of interaction with the environment, disrupting the superposition or decoherence states, and it happens quickly because the electric force Between the strong and long-range charges, this is a disadvantage in contrast to conventional semiconductor devices. To develop these quantum devices, quantum computing research has been supported by many government and military funding agencies, although it is still in its infancy. Experiments have already been conducted in which quantum computing processes have been used, and theoretical and scientific research is still continuing in this field [29].
- RAM-M is considered one of the first spin-electronic devices that were invented, as it does not lose stored information after turning off the power, as it relies on the integration of a magnetic tunnel junction, which is a device with two layers of metallic ferromagnets with a thin insulating layer in the middle. When an electric current crosses the device, a small number of electrons are able to cross the insulating layer through the process of quantum tunneling despite the presence of strong resistance. The tunneling current is hindered when the two magnetic layers have opposite directions and allowed when their directions are identical, and information is stored as magnetic poles instead of charges electric[31][32].

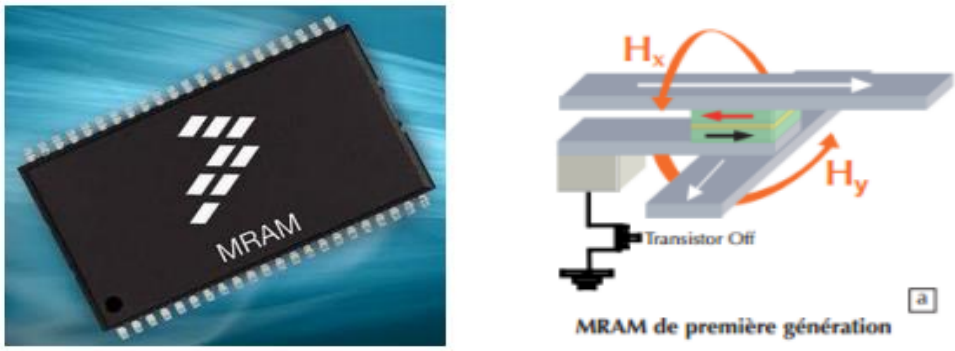

Figure II.9 : Magnetic resistance random access memory (RAM-M).

- The spin scanner is considered an innovative and effective technology for detecting cancer cells while they are still very small. Its principle is based on the use of a beam of polarized electrons with a uniform spin in a specific direction. The spin of electrons is detected by analyzing the polarization of the spin of the electron beam using a Muller polarimeter. This experiment must also be in a medium with an external magnetic field, by shedding a strong magnetic field on the patient's body in order to attract the cells, and then inserting A spin-polarized electron beam is directed toward the unaffected part of the body. The change in the direction of the spin is detected using a polarimeter. After that, a spin-polarized electron beam is inserted toward the part that underwent surgery. If the first spin cancels the second spin, the The result is zero, which indicates that the cancer cells have been removed from the body, and in this way it effectively detects the presence of cancer cells in the specific area.
- Quantum transistors are characterized by detecting spin states without the need to apply an electric current. It also uses spin states up and down to generate binary data, where the upper electronic spin represents 0 and the lower electronic spin represents 1. It also uses a "spin-flip" mechanism to change the state of the diode from 0. To 1, in addition to the fact that the electronic spin is semi-permanent, which helps to develop detectors that are much smaller but more sensitive than others, and therefore it is expected that these devices can store more data in less space and consume less energy, in addition to using less expensive materials. Quantum transistors are often used in the production of computer RAM, and more sensitive sensors are also being created for cars.

The use of electronic spin in new devices is revolutionizing the twenty-first century, as it is capable of changing life towards an unexpected digital atomic world, and this will make things cheaper, smaller, and more useful to all of humanity [33][34].

II.9. Conclusion

In this chapter, we have discussed the basic concepts of electronic spin technology, which is considered one of the most promising techniques for miniaturizing semiconductor electronic devices and even leads to features smaller than 100 nanometers in size. We have also touched on its applications in future electronic devices. Electronic spin technology, or what is known as "Spintronics" devices, is considered among the new branches of electronics in which the spin of the electron is processed, in addition to the charge, and thus dealing with the quantum property of the electron, which leads to obtaining smaller and more affordable devices, and this is what prompted us to do more research in this field.

References

[1] Joseph T. Finley, Spintronics Using Low Magnetization Materials, Submitted to the Department of Electrical Engineering and Computer Science in partial fulfillment of the requirements for the degree of Doctor of Philosophy, University of California Berkeley, 2020.

[2] Xania, the Discoveries of Electrons Protons and Neutrons, Inorganic chemistry, PP 1-8, 2021.

[3] Othman Hassan, Joseph Thomson, the atomic scientist and discoverer of the electron, Al-Khaleej Newspaper, May 2019.

[4] OUMSALEM Abdellah, Titre de thèse Le transport de spin dans les nanomatériaux application les ordinateurs quantiques, Université Hassiba Ben Bouali de Chlef, 2008.

[5] Benmebrouk Lazhar, Introduction to Electronic Spin Science and Nanotechnology, Kasdi Merbah University, Ouargla, 2016.

[6] Ahmed Mimon Ash-Shazlie, Mohammad Al-Sabbagh, Sara Harba, Fadi Hamwi, Basem Ashour, What is self-winding, Syrian researchers, 2015.

[7] Spintronics electronic Tutorials – Mepits, August 2015.

[8] P. W. Anderson, D.J. Thouiess, E. Abraharns, D. S. Fisher, New method for a scaling theory of localization, PH YSICAL RK VIEW B, VOLUME 22, NUMBER 8, 1980.

[9] David Vanderbilt, Soft self-consistent pseudopotentials in a generalized eigenvalue formalism, PHYSICAL REVIEW B, Rapid Communications, VOLUME 41, NUMBER 11, 1990.

[10] David Vanderbilt, Optimally smooth norm-conserving pseudopotentials, PHYSICAL REVIEW B, VOLUME 32, NUMBER 12, 1985.

[11] Emmanuel ARRAS, Étude théorique de la structure et de la stabilité des alliages GeMn dans le cadre de la spintronique, pour obtenir le grade de DOCTEUR DE L'UNIVERSITÉ DE GRENOBLE - JOSEPH FOURIER, 2006.

[12] Syed Hasan Shirazi, Free electrons, Quora, 2021.

[13] N . F. Mott, F.R.S., H. H, The Resistance and Thermoelectric Properties of the Transition Metals, niversity of Bristol, 1936.

[14] M. N. Baibich, J. M. Broto, A. Fert, F. Nguyen Van Dau, and F. Petrof, Giant Magnetoresistance of (001)Fe/(001)Cr Magnetic Snperlattices, PHYSICAL REVIEW LETTERS, VOLUME 61, NUIMBER 21, 1988.

[15] Fert, Albert, Les débuts de la spintronique-Travaux précurseurs et magnétorésistance géante, Reflets de la Physique, 15, 5-10, (2009).

[16] Cibert, Joël, Jean-François Bobo, and Ulrike Lüders, Development of new materials for spintronics, Comptes Rendus Physique 6, 9, 977-996, (2005).

[17] Valet, T., and A. J. P. R. B Fert, "Theory of the perpendicular magnetoresistance in magnetic multilayers.", Physical Review B, V.48,N. 10, (1993).

[18] Johnson, Mark, and R. H. Silsbee, "Thermodynamic analysis of interfacial transport and of the thermomagnetoelectric system.", Physical Review B, V.35,N.10, (1987).

[19] Van Son, P. C., H. Van Kempen, and P. Wyder, "Boundary resistance of the ferromagnetic-nonferromagnetic metal interface.", Physical Review Letters,V. 58, N.21, 1987.

[20] Ziese, Michael, and Martin J. Thornton, eds. Spin electronics. Vol. 569. Springer, 2007.

[21] Bournel, Arnaud. "Electronique de spin et semiconducteurs".

[22] Zhang, Shufeng, and Peter M. Levy, "Conductivity perpendicular to the plane of multilayered structures.", Journal of Applied Physics, V. 69, N.8, 4786-4788, (1991).

[23] Parkin, S. S. P., N. More, and K. P. Roche, "Oscillations in exchange coupling and magnetoresistance in metallic superlattice structures: Co/Ru, Co/Cr, and Fe/Cr.", Physical review letters, V.64, N.19, (1990).

[24] Tsukagoshi, Kazuhito, Bruce W. Alphenaar, and Hiroki Ago, "Coherent transport of electron spin in a ferromagnetically contacted carbon nanotube.", Nature 401.6753, 572-574, (1999).

[25] Zhao, B., et al, "Spin-dependent transport in multiwalled carbon nanotubes.", Journal of applied physics, V.91, N.10, 7026-7028, (2002).

[26] B. Zhao, I. M¨onch, H. Vinzelberg, T. M¨uhl, and C. Schneider, 'Quantum spin transportation in Ga/As' Appl. Phys. Lett. 80, 3144 (2002).

[27] Sahoo, S., et al, "Electrical spin injection in multiwall carbon nanotubes with transparent ferromagnetic contacts", Applied Physics Letters 86.11, (2005).

[28] A. Jensen, J. Nygard, and J. Borggreen, in Toward the controllable quantum states, Proceedings of the International Symposium on Mesoscopic Superconductivity and Spintronics, H. Takayanagi and J. Nitta , 33 (2003).

[29] Brown, P. J., et al, "The magnetization distributions in some Heusler alloys proposed as half-metallic ferromagnets", Journal of Physics: Condensed Matter, V. 12, N.8, (2000).

[30] Ross, Caroline A, "Patterned magnetic recording media, " Annual Review of Materials Research, V. 31, N.1, (2001).

[31] Daughton, J. M. "Magnetoresistive memory technology, Thin Solid Films, 216, 1, 162-168, (1992).

[32] Bussmann, K., et al, "Switching of vertical giant magnetoresistance devices by current through the device", Applied physics letters, 75,16, 2476-2478, (1999).

[33] Albert, F. J., et al, "Spin-polarized current switching of a Co thin film nanomagnet", Applied Physics Letters, 77, 23, 3809-3811, (2000).

[34] Grollier, Julie, et al, "Spin-polarized current induced switching in Co/Cu/Co pillars", Applied Physics Letters, 78, 23, 3663-3665, (2001).

Chapter III

Laboratory synthesis of nanomaterials and analysis methods

Chapter III: Laboratory synthesis of nanomaterials and analysis methods

III.1. Introduction

In this chapter, we will be interested in presenting the practical aspect of how to prepare thin layers of magnesium oxide and silicon dioxide using the hydrothermal method. This will address the stages of their preparation in terms of using natural resources as raw materials, assembling them, then mixing the solutions and preparing the appropriate substrates for film deposition. Their thickness is measured at deposition temperatures of 150, 200, and 300 degrees Celsius in the presence of a change in the strength of the applied external magnetic field, and then their composition is examined to ensure the deposition of (MgO-SiO_2) films with good specifications, using various devices to measure and analyze the properties of thin layers. This process can be summarized according to the following steps:

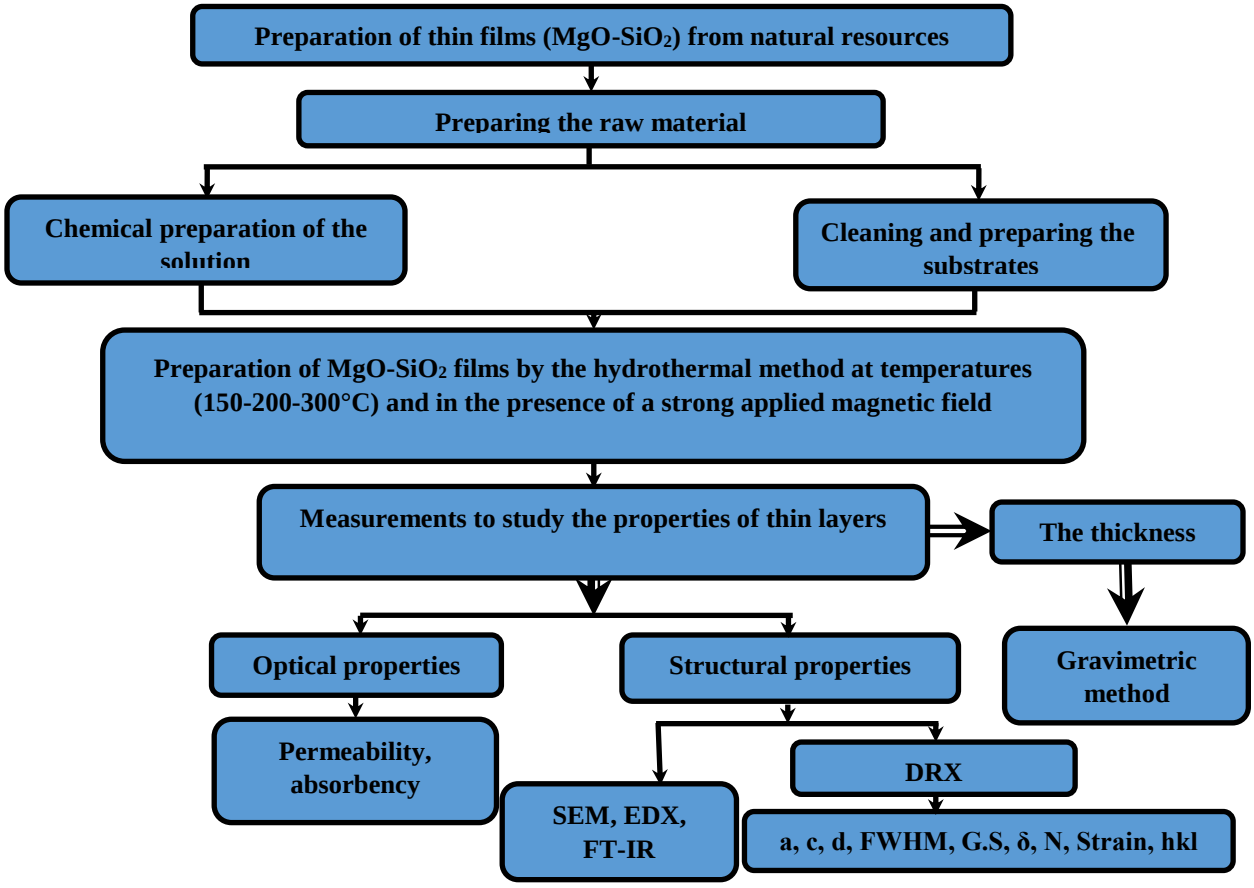

Figure III.1 : Steps for experimental work.

III.2. Preparation of thin films (MgO-SiO_2) from natural resources

III.2.1. Preparing the raw material

The raw material was collected by searching for a certain number of rocks in the Ouargla region. The rocks are distinguished by their color and size. In our study, a sample of brown rock was taken, and then the geographical location was determined using the application's GPS coordinates, which took the following values. : X=5.53, y=31.80, h=192 m. To prepare this sample for use, we polished it in order to get rid of the impurities accumulated in its outer layer and increase its purity using a polishing device of the type (MECAPOL-P255 U). Then it is crushed and broken to reduce its size to a few grains whose dimensions range from millimeters to centimetres, and to obtain a fine powder. It is very similar to soft flour in shape and is ready for use. It is placed in a mechanical grinding device for about a quarter of an hour.

Figure (III.2) represents the procedures taken to prepare the rock sample.

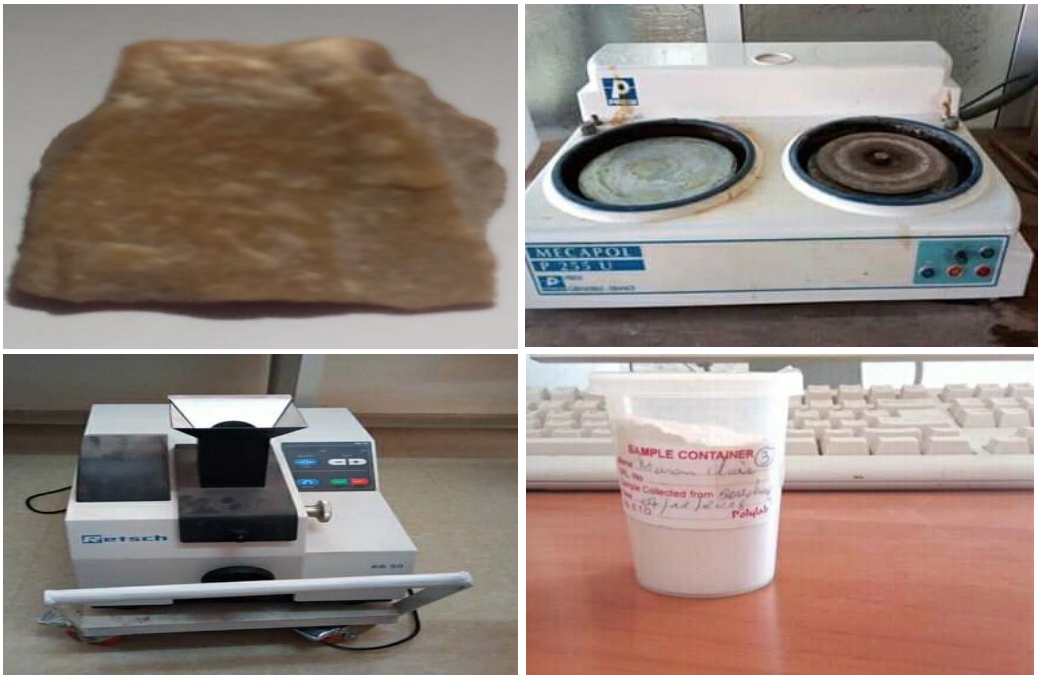

Figure III.2 : Stages of rock sample preparation.

The molecular and crystalline structure of the rock sample was identified and studied, and its components were identified using a group of chemical and physical spectroscopic analysis methods, represented by the X-ray diffraction technique using the DRX device, and X-ray fluorescence (XRF), and FT-IR absorption spectroscopy, and it turned out that the rock sample consists mainly of α-quartz with a concentration of 69%. It also contains other compounds in relatively weak concentrations, and as XRF technology showed the concentrations of the chemical elements that make up the sample in atomic concentration, it was found that it contains 24.07% of magnesium and 21.83% of silicon in addition to indium with 19.67% and rhodium with 14.40%, while Other elements appeared in weak percentages not exceeding 5%, and FT-IR technology confirms that most of the bonds appearing in the sample indicate the presence of the quartz compound.

III.2.2. Chemical preparation of the solution

The chemical solution was prepared and a homogeneous liquid was obtained by placing a mass of 5 mg of sodium bicarbonate ($CHNaO_3$) and copper (Cu), after which 10 mg of potassium chromium oxide (K_2CrO_4) and the rock material were placed, which was weighed using a sensitive balance from Type (DENVER INSTRUMENT SI-114). Then it is dissolved in a volume of 20 ml of ion-free water and the solution is mixed with a magnetic mixer for 10 minutes in order to obtain complete dissolution and thus obtain an aqueous solution. The solution is left for 24 hours at room temperature to ensure its homogeneity and stability. The properties of these elements can be summarized. Chemicals in **table (III.1)** are as follows:

Table (III.1): Properties of materials needed for the chemical preparation of the solution [12-17].

Element	chemical formula	Shape and color	molar mass (g/mol)	Volumetric mass (g/ Cm^3)	melting point (°C)
Sodium bicarbonate	$CHNaO_3$	Solid white in colour	84.01	2.20	109
copper	Cu	auburn	63.546	8.96	1.085
potassium chromium oxide	K_2CrO_4	yellow	194.19	2.73	968

Figure (III.3) shows the chemicals for preparing the solution and the final solution prepared.

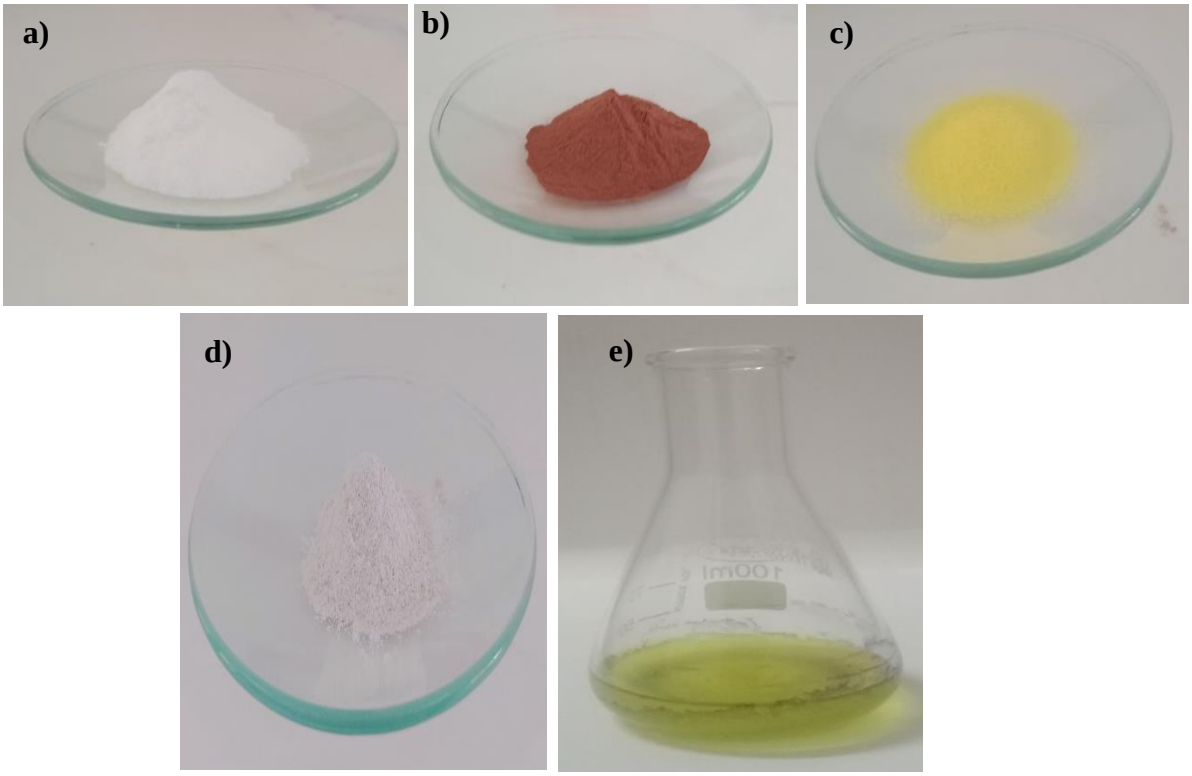

Figure III.3 : Chemical materials for preparing the solution, (a) Sodium bicarbonate ($CHNaO_3$), (b) Copper (Cu), (c) Potassium chromium oxide (K_2CrO_4), (d) Rock material, (e) The prepared solution.

III.2.3. Preparing the substrates

The substrates used in the membrane preparation process are heat-resistant glass substrates. We used Microscope Slides type substrates supplied by the German company SUPE RIOR, and their dimensions are approximately 76 x 26 x 1 mm^3. It is known that measurements and physical properties are affected by the surface condition of the substrate, so the process of cleaning these substrates went through several stages after they were cut into parts to obtain substrates free of impurities by removing fats and traces of dust and thus facilitating the process of good adhesion of the solution in the form of thin layers.

First, it is washed with plain water and one of the washing powders to get rid of any remaining suspended materials. Then we wash it under running water to ensure the powder is removed. After that, it is immersed in nonionic water for 15 minutes and placed in a beaker containing acetone solution. Finally, it is washed again with nonionic water for 5 minutes. After the cleaning process is carried out, the substrates are dried well, weighed using a sensitive scale, and placed in a special container for glass substrates before the deposition process is carried out.

III.3. Preparation of MgO-SiO_2 films by hydrothermal technique

After preparing the solution and preparing the substrates and cleaning them well, the substrate was placed in the solution in a Teflon container, then the solution and the substrate were placed in a drying oven and heated at a different deposition temperature (150-200-300 degrees Celsius), as the deposition was performed at growth times of 120 minutes when exposed Two external magnetic fields have the same direction. In the second stage, two external magnetic fields are applied so that the external magnetic field has a direction opposite to the direction of the other field. After the specified period of time, the substrates are removed and rinsed in non-ionized water. This method is considered low-cost and easy to handle. Compared with other methods due to limitations of the equipment and the process itself, making it difficult to produce on a large scale[18].

III.4. Measurements to study the properties of thin layers

III.4.1. Measuring the thickness of films

There are many methods for measuring the thickness of thin films, as it is considered one of the important parameters for studying and determining physical properties, including the gravimetric method, whereby the glass substrates were weighed before the material deposition process using a high-sensitivity balance, and after deposition, the difference in weight was then determined to obtain the thickness of Through the following equation[19]:

$$t = \frac{m_2 - m_1}{\tilde{n}_{total} \cdot s} \qquad \textbf{(III.1)}$$

whereas:

m_1: Weight of substrate before film deposition (g).

m_2: Weight of substrate after deposition (g).

s: Membrane area (cm^2).

$\tilde{n}_{total}$: Total density of the film material (g/cm^3).

III.5. Techniques for studying structural properties

III.5.1. Diffraction X-ray technology (DRX)

X-ray diffraction technology is used to characterize crystalline materials and learn many structural information, including determining the shape of the primary cell, its dimensions, its crystalline structure, in addition to its composing atoms and the preferred direction of crystal growth. Since solid materials are classified according to their crystal structure into crystalline materials and random materials, and to judge that a material is crystalline does not depend on its appearance, even if this belief was assumed in the past, but rather depends mainly on the regularity of its atoms and molecules in the periodic arrangement at the microscopic level, and this is what crystallography confirmed in 1913. This is based on X-rays. Crystalline materials are divided into two categories, including monocrystalline materials whose structure is a repetition of the unit cell in three dimensions. That is, the atoms of monocrystalline materials are arranged in a regular geometric arrangement and in a periodic form, thus possessing a kind of symmetry. Polycrystalline materials are materials whose arrangement ends regular periodicity at the grain

boundaries, which constitute the border between the granular organization of single crystals of matter and those adjacent to it. As for the random materials (Amorphous Materials), they are materials whose atoms are combined randomly without a specific system and their structure does not have a repetition of the unit cell, and thus they form a complex formation and its condition is not Thermodynamically stable[20][21]. X-rays are considered electromagnetic waves that occupy the region between gamma rays and ultraviolet rays, and their wavelengths range between 0.01 and 100 Å, which is much shorter than that of visible light. Therefore, they are used in crystal diffraction experiments for the possibility of comparing their wavelengths with the separation distances between atoms in the crystal.

The principle of this technique is based on directing a beam of monochromatic X-rays onto the surface of a membrane. Peaks appear at specific angles as a result of the deviation of part of this beam from parallel crystal planes. The intensities of these peaks vary depending on the direction and number of these planes. It was demonstrated by scientist Bragg that the position of the diffracted X-ray beams can be determined by the crystal, and that these X-rays only exist at positions where the diffracted rays interfere constructively at parallel planes, he also developed a simple model of the crystal structure shown in the **figure (III.4)**. What is distinguished from these peaks is the crystalline state, as each peak represents a crystalline level at which diffraction occurred, while the random state of X-ray diffraction patterns is characterized by the absence of sharp peaks[22][23], and this is summarized according to the following Bragg relationship:

$$n\ddot{e} = 2\, d_{hkl} \sin \grave{e} \qquad \textbf{(III.2)}$$

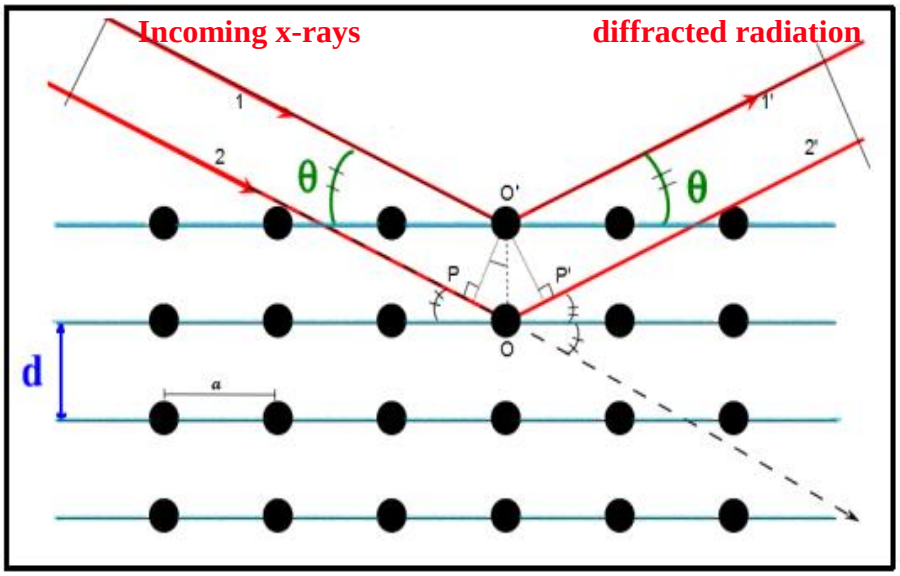

Figure III.4 : Schematic diagram of X-ray diffraction on crystal planes in Bragg conditions[24].

During this study, an EMPYREAN PANalytical X-ray diffraction (XRD) device with a wavelength ($\lambda_{\hat{e}_{\acute{a}}cu} = 1.54060$ Å) electrical voltage of 45 KV and a current intensity of 40 mA. All diffraction patterns for the samples were recorded using the device shown in **figure (III.6)**, it is located at the research center level of the physical-chemical analysis at the University of Laghouat, where was used of angle 2θ in the range (10-90°) in this setup, the sample is securely placed on the holder for study and analysis using X-rays. The sample can be rotated around a vertical axis at a specific angle θ, with each rotation angle being recorded by the detector 2θ. It's important to note that the holder and the detector are mechanically compatible. After the X-rays are emitted from the source, they deviate from parallel crystal planes on the surface of the sample and are received by the counter. The angle of incidence changes step by step during the measurement, and the actual intensity of the reflected beam is recorded by the detector at each step. This occurs when Bragg's condition is met, resulting in peaks in the diffraction pattern for the intensity of the reflected beam[25-27].

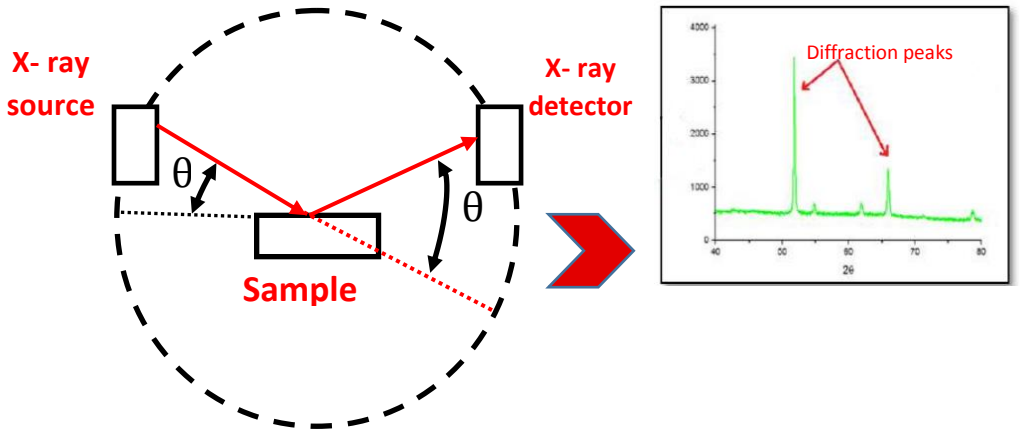

Figure III.5 : A diagram showing the diffraction of X-rays [28].

The X-ray diffraction diagram shows the intensity of the diffraction lines and their corresponding angles, and through it many structural information is determined for the deposited films, such as their crystalline structure and the preferred direction of their growth under ideal conditions. By determining the diffraction angles, the interfacial distances of the atomic surfaces (d_{hkl}) can be calculated, as well as the lattice constants of each crystalline structure, which It is a description of the dimensions of the unit cell in the crystal lattice, in addition to the possibility of calculating the grain size through the Scherer's relationship of the equation (IV.5). By knowing the grain size, the dislocation density is calculated (δ), which represents the number of dislocation lines that cross a unit area in the crystal, in addition to calculating the number of crystals per unit area. When X-rays are reflected from each part of the crystal at angles different from the other part, that is, the reflection resulting from different parts of the crystal is at different angles, this indicates that the interspace distance is not equal between the atomic surfaces at each point of the crystal, and from this the presence of distortions in the crystal becomes clear. The percentage of deformation during the growth of the membrane arising in compression or network expansion can be calculated through the relationship (IV.8)[29-31][19].

Figure III.6 : Used X-ray diffraction machine (DRX).

III.5.2. Scanning electron microscopy (SEM)

The scanning electron microscope is considered one of the effective techniques for identifying the nature and morphology of the surface of membranes, and this technique is characterized by being non-destructive to the sample. It was developed to overcome the optical problems in optical microscopes, represented by the Rayleigh criterion, which is the standard that describes the limit in the size of structures observed using visible light in addition to the effect of the optical lens aperture. In its formation of magnified images, it relies on electrons instead of light waves because they have wavelengths much smaller than visible light, where the working principle of the microscope depends on directing an electron beam from the source of electrons (cathode) to pass through electromagnetic lenses, which work to focus the beam on a small part of the surface of the sample to be studied. The collision of the electron beam with surface atoms causes many reactions and the emission of secondary particles to be detected and captured to determine the sample's topography and composition. The quality of the images is affected by the uneven number of bounced electrons and falling electrons, and then the charging process occurs

for the sample. To avoid this negative effect, the sample is coated with a thin metal layer that reduces the electrons absorbed by the sample, so that this microscope works in a vacuum to obtain three-dimensional and more accurate images by directing the electron as intended and not interacting with air molecules, and the chemical elements of the sample surface are identified through the unit attached to the energy dispersive X-ray spectroscopy (EDX) in the scanning electron microscope[32-34]. **Figure (III.7)** shows the schematic diagram of the scanning electron microscope.

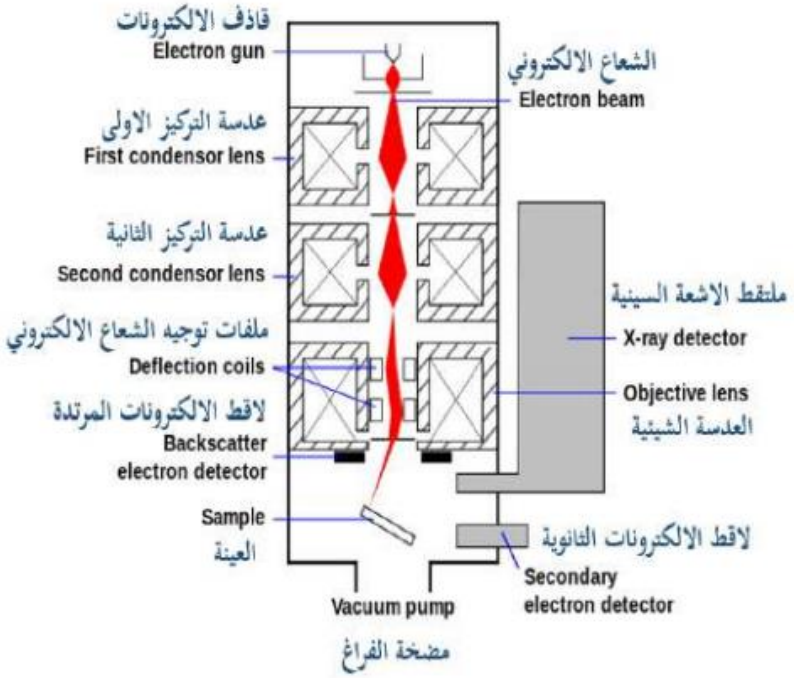

Figure III.7 : Schematic of a scanning electron microscope (SEM) [35][36].

In this study, we used a ZEISS EVO 15 device equipped with an electronic emitter from a Lanthanum hexaboride cathode (LaB_6) instead of a tungsten filament, which is located at the level of the research center for physical-chemical analysis at the University of Ouargla, as shown in **Figure (III.8)**.

Figure III.8 : Used scanning electron microscope (SEM).

III.5.3. Fourier transform infrared absorption (FTIR) spectroscopy

FTIR technology, or Fourier transform infrared spectroscopy, is among the widely used technologies due to its importance in determining the molecular structure of materials without damaging them and at the lowest cost. It is also used to detect changes that occur to molecules as a result of their interaction, by identifying the chemical bonds that make up the molecular structures. For materials, it is suitable for the three states of matter (solid, liquid, gaseous), as its principle depends on the absorption of infrared rays passing through the sample, so its atoms are excited, causing a vibrational movement of the atoms to occur at the molecule level, and the vibrational movement results from the movement of two atoms or a group of atoms, and this leads to a periodic change in the length of chemical bonds[37][38]. The photon that has an energy equal to the transfer energy is absorbed by the molecule, this absorption characterizes the bonds between atoms and appears in the form of bands in the spectrum, and since each molecule has a specific vibrational energy that differs from another molecule. This energy is measured and the molecule is identified, as vibrational movements are divided into two types, including stretching vibrations, which express a change in the distance between atoms on the bond axis without changing the angles between the bonds. Their types include simple stretching, which represents

the stretching of a single bond, and double stretching, which represents the stretching of more than one bond. At the same time, the expansion in this case can be symmetrical, such as the expansion or contraction of the two bonds occurring together. It can also be asymmetrical, which includes the opposition between the two bonds, such as one bond expanding and the other contracting simultaneously[39-41]. As for the second type of vibrational movements, they are bending vibrations, which are represented by In the change in the angle between the two bonds resulting from the movement of atoms in or outside the level of the two bonds, its types are divided into four types, including rocking bending, in which, at its level of equilibrium, the structural unit swings left and right. As for the concussive bend, the structural unit oscillates back and forth outside the equilibrium plane. In addition to scissor bending, the movement of which is characterized by the movement of scissors, which is represented by in the movement of the two bonds towards convergence and divergence between them, and torsional bending, in which the atoms outside their equilibrium plane are twisted around the bond between them and the rest of the molecule[42-45], as shown in the **figure (III.9)**.

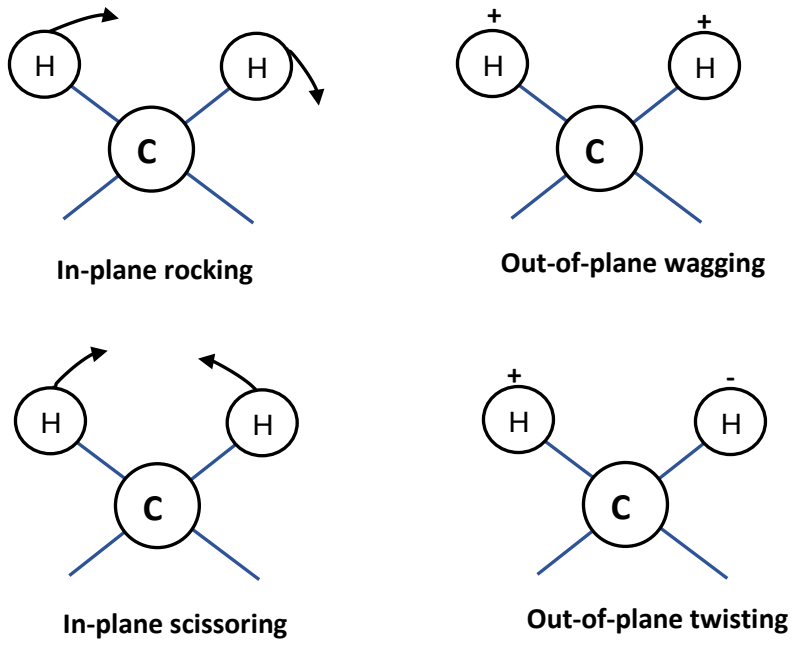

Figure III.9 : Types of bending vibrations.

In the current study, a Cary 600 series FTIR Spectrometer equipped with a Fourier transform was used, as shown in **figure (III.10)**, through which the spectra were recorded by sending a beam of infrared wavelengths from the source in the confined field. Between 400 and 4000 cm^{-1}, it is directed to a plate and divided into two equal beams. One beam is directed to a fixed mirror and another to a moving mirror to be reflected again and pass through the sample, and then the detector receives it and records it. Using an immediate mathematical conversion process, the received signal is transformed into the desired spectrum. The absorbed wavelengths of the absorption peaks in the infrared absorption spectra are determined and attributed to the functional groups of each substance, through the use of available references to enable one to know the chemical compounds and the type of atoms and bonds that make up the molecule[46].

Figure III.10 : Infrared spectrometer used.

III.5.4. Optical measurements

Optical measurements depend on measuring the absorbance and transmittance spectra of ultraviolet and visible rays, through which the valuables of the energy bands and the type of electronic transitions are determined. Absorbance expresses the decrease in the energy of electromagnetic radiation after it passes through the sample. The basic degree depends on the thickness and nature of the membrane and can be formulated according to the relationship (**III.3**), as for transmittance, it expresses the ratio of the intensity of the penetrating radiation (I_T) and the incident radiation (I_0), as shown in the relationship (**III.4**)[47][48].

$$A = I_A/I_0 \qquad \text{(III.3)}$$

I_A and I_0 represent the radiation intensity before and after it falls on the sample, respectively.

$$T = I_T/I_0 \qquad \text{(III.4)}$$

Optical measurements were made using a Cary Series UV Vis 100 spectrometer, which is located at the level of the research center for physical-chemical analysis at the University of Ouargla. Its working principle is based on the fact that compounds absorb UV-visible light at specific wavelengths by sending light From a source with a wide range of wavelengths, consisting of a tungsten lamp for visible light and a deuterium lamp for ultraviolet light. The transmitted light then passes through a monochromatic consisting of a prism that allows only a specific wavelength or a range of wavelengths of light to pass through. This beam heads towards a semi-reflecting mirror and is divided into two beams, one beam is considered a reference and the other passes through the sample. Ultraviolet and visible rays interact with the molecules in the sample and non-absorbed rays are captured by the detector and their intensity is measured.

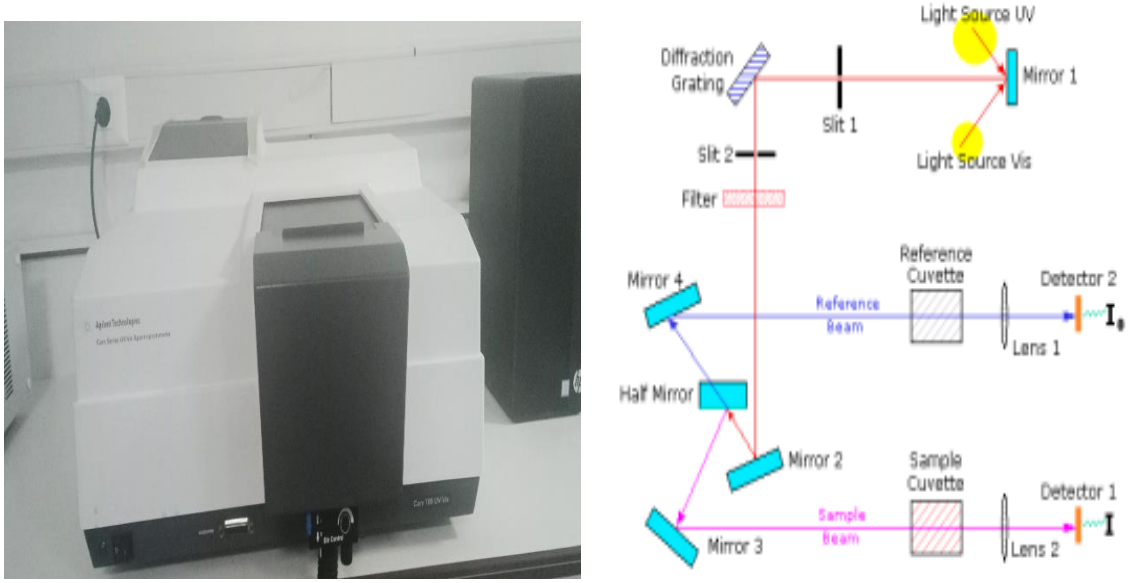

Figure III.11 : Illustration of the ultraviolet-visible spectroscopy model (UV-VIS) and the device used[49].

Many optical constants are determined through transmittance and absorption spectra. Based on the values of the latter, the absorption coefficient (α), which represents the decrease in the percentage of incident radiation energy per unit distance in the direction of wave propagation within the medium, is calculated. To determine it, we use the Bouguer Lambert-Beer relationship, which is known as the Beer and explained as follows:

$$\mathbf{T} = \mathbf{e}^{-á.\mathbf{d}} \qquad \textbf{(III.5)}$$

This relationship is used by neglecting reflection in all cases (air-layer, air-substrate, layer-substrate), and knowing the thickness, the absorption coefficient for each permeability value can be determined by the following relationship[50][51]:

$$á(\mathbf{Cm})^{-\mathbf{1}} = \frac{\mathbf{1}}{\mathbf{d(Cm)}}\mathbf{ln}(\frac{\mathbf{100}}{\mathbf{T}(\%)}) \qquad \textbf{(III.6)}$$

Where: (d) Film thickness in (Cm), (T) Optical transmittance.

The nature of the electronic transfers occurring in the energy bands, which can be direct or indirect, depends on the values of the absorption coefficient. When an electron at the top of the valence band absorbs a photon with an energy equal to or greater than the energy of the gap, it moves to a vacant place at the bottom of the conduction band, directly and vertically at the same point in space k occurs in what are called direct transfers. However, when the electron moves from the top of the valence band to the bottom of the conduction band in a non-vertical manner, then the electronic transfers are indirect[52], and the energy band gap (Eg), which is considered one of the important optical constants, is also calculated using the (Tauc) model, which is represented by drawing the relationship Graphs between (hν) and $(\alpha h\nu)^2$. In addition, the energy gap is not completely empty in pure semiconductors, as it is interspersed with local levels arising from crystalline defects[53].

III.6. Conclusion

In this chapter, the basic stages of thin film deposition of magnesium oxide and silicon dioxide ($MgO\text{-}SiO_2$) prepared from natural resources using the hydrothermal technique were discussed, as it is considered one of the techniques characterized by several degrees of freedom, due to the simple assembly process and convenient operation. In addition, the substrate solution is subjected to a suitable hydrothermal treatment to form stable crystalline phase films on the substrate and thus does not require thermal treatment of the films after crystallization or interaction of the film with the atmosphere. The films with high purity and good homogeneity will also be obtained, and this is what It was also reported by growing thin films of ZnO by the hydrothermal method, which were of high quality, with a smooth surface and no obvious fluctuation[54]. On the other hand, we discussed methods for analyzing the structural, morphological, and optical properties of the prepared films.

References

[1] Sodium Bicarbonate, Material Safety Data Sheet, 2009.

[2] Sodium Bicarbonate, Safety Data Sheet, according to Federal Register rules and Regulations, Vol. 77, 2012.

[3] Sodium Bicarbonate, Genesis Alkali, LLC, V3.2, 2019.

[4] S. W. Holman, R. R. Lawrence and L. Barr, Melting Points of Aluminum, Silver, Gold, Copper, and Platinum, Proceedings of the American Academy of Arts and Sciences, Vol. 31, pp. 218-233, 1896.

[5] GERD ANGER, JOST HALSTENBERG, KLAUS HOCHGESCHWENDER, CHRISTOPH SCHERHAG, ULRICH KORALLUS, HERBERT KNOPF, PETER SCHMIDT, MANFRED OHLINGER, Chromium Compounds, Vol. 9, 2012.

[6] Potassium chromate, Material Safety Data Sheet, 2010.

[7] Guijun Yang and Soo-Jin Park, Conventional and Microwave Hydrothermal Synthesis and Application of Functional Materials: A Review, materials, 2019.

[8] Oge Anazia, Chemistry of Zirconia and Its Bioanalytical Applications, A Thesis Presented to The Faculty of the Department of Chemistry Western Kentucky University Bowling Green, Kentucky, 2009.

[9] Dr. Naima Abdel Qader Ahmed, Dr. Muhammad Amin Suleiman, Crystallography and X-rays, Cairo,2005.

[10] B.en.G.Streeman,"Solid State Electronic Devices"2nd Edition ,PrenticeHall,Inc.,Englewood Cliffs ,N.J.(1980).

[11] M. H. Brodsky," Amorphous Semiconductors", 2nd Edition SpringerVerlag, Germany,(1979).

[12] Dr.Ali H.Ataiwi, Dr.Alaa A. Abdul-Hamead, Study Some of the Structure Properties of ZrO2 Ceramic Coats Prepared by Spray Pyrolysis Method, Eng. & Tech. Journal, Vol.27, No.16, 2009.

[13] D. Bowen and B. K.Tanner," High Resolution X-ray Diffractometry and Topography", Taylor & Francis e-Library, (2005).

[14] W. D. Callister," Fundamentals of Materials Science and Engineering", 5 Th Edition, John Wiley & Sons, Inc, New York,(2001).

[15] Salah YAHIAOUI, L'effet de la molarité des différentes sources d'étain sur les propriétés des couches minces d'oxyde d'étain SnO2 élaborées par Spray Ultrasonique, Mémoire pour obtenir le diplôme de Magister, Université Mohamed Khider – Biskra, 2014.

[16] Powder diffraction Files Search Manual Minerals joint committee on powder diffraction standares,USA, (2003).

[17] Deane K. Smith and Ron Jenkins, The Powder Diffraction File: Past, Present, and Future, Journal of Research of the National Institute of Standards and Technology, Volume 101, Number 3, May–June 1996.

[18] PREETI SAGAR NAYAK, B K SINGH, Instrumental characterization of clay by XRF, XRD and FTIR, Bull. Mater. Sci., Vol. 30, No. 3, June 2007, pp. 235–238.

[19] B. D. CULLITY, ELEMENTS OF X-RAY DIFFRACTION, , University of Notre Dame, 1956.

[20] Abdel-Fattah Ahmed El-Shazly, Solid-state physics.

[21] Chaojun Wang, Multiscale Modeling and Simulation of Nano crystalline Zirconium Oxide, Ph.D,Thesis, Engineering Mechanics Dissertations, University of Nebraska,(2009).

[22] Goldstein, J.I., D.E. Newbury, J.R. Michael, N.W. Ritchie, J.H.J. Scott, and D.C. Joy, Scanning electron microscopy and X-ray microanalysis, Springer, 2017.

[23] K. C. A. SMITH, B.A., C. W. OATLEY, M.A., MSc, The scanning electron microscope and its fields of application, University of Cambridge, 1955.

[24] Essam Abbas Khudair, Preparation of polycrystalline thin films of zinc oxide - indium oxide as a gas sensitizer using the chemical pyrolysis method, Master Thesis, Wasit University, 2015.

[25] Brandon Cheney, Introduction to Scanning Electron Microscopy, Department at San Jose State University.

[26] Oatley, C., D. McMullan, and K. Smith, The development of the scanning electron microscope. Elsevier: Amsterdam, Netherlands, 1985.

[27] I. REHMAN and W. BONFIELD, Characterization of hydroxyapatite and carbonated apatite by photo acoustic FTIR spectroscopy, JOURNAL OF MATERIALS SCIENCE: MATERIALS IN MEDICINE 8 (1997) 1 — 4.

[28] J. Madejova, FTIR techniques in clay mineral studies, Vibrational Spectroscopy 31 (2003) 1–10.

[29] Ben Belkacem, N., Synthèse et caractérisation de complexes mixtes de cobalt (III) avec l'éthylènediamine, une série d'acides aminés et des bases azotées, UMMTO, 2012.

[30] Barbara H. Stuart, INFRARED SPECTROSCOPY: FUNDAMENTALS AND APPLICATIONS, University of Technology, Sydney, Australia, 2004.

[31] Dr. Ahmed Khamis Mohamed Salama, Spectroscopy between theory and practice, College of Science in Zulfi - Qassim University, Kingdom of Saudi Arabia, 2010, 109-84.

[32] F. Bosch Reig, J.V. Gimeno Adelantado, M.C.M. Moya Moreno, FTIR quantitative analysis of calcium carbonate (calcite) and silica (quartz) mixtures using the constant ratio method. Application to geological samples, Talanta 58 (2002) 811-821.

[33] Theodor Schneller, Rainer Waser, Marija Kosec, David Payne, Chemical Solution Deposition of Functional Oxide Thin Films, Springer Wien Heidelberg New York Dordrecht London, 2013.

[34] Derrick M. R., Stulik D. and Landry J. M, Infrared Spectroscopy in Conservation Science, the J. Paul Getty Trust, The Getty Conservation Institute, (1999).

[35] Polfer N. C. and Dugourd P, Laser Photodissociation and Spectroscopy of Mass-separated Biomolecular Ions, Lecture Notes in Chemistry 83; Springer International Publishing Switzerland, (2013).

[36] Sulabha K. Kulkarni, Nanotechnology: Principles and Practices, Springer Cham Heidelberg New York Dordrecht London, 2015.

[37] B.G.Yacobi, Semiconductor Materials, Kluwer Academic Publishers , New York, (2004).

[38] Marzook Alshammary, Optical and Magneto-Optical Properties of Doped Oxides, Thesis submitted to the University of Sheffield for the degree of Doctor of Philosophy, the university of Sheffield, 2011.

[39] ATTALLAH MOURAD, Elaboration et caractérisation des couches minces d'oxyde de silicium, obtenues par voie sol-gel, PRESENTE POUR OBTENIR LE DIPLOME DE MAGISTER EN PHYSIQUE, UNIVERSITE MENTOURI-CONSTANTINE, 2010.

[40] Charles S. Wiliams and Orvillia. Bechlund, A short course for Engineers and Scientists, John Wiley et sons (1972).

[41] D.Mencaraglia, Thèse de doctorat d'état, paris VI (1987).

[42] s. a M. Zee, Fahr Ghalib Hayati, Hussain Ali Ahmed, Semiconductor devices physics and technology, University of Al Mosul,Dar Al-Hikma for printing and publishing, 1990.

[43] J. Tauc, Amorphous and liquid Semiconductors, Plenum press, London, N.Y., (1974).

[44] Huaihao Wu, Zuofu Hu, Bin Li, Hailong Wang, Yunfei Peng, Dongzhan Zhou, Xiqing Zhang, High-quality ZnO thin film grown on sapphire by hydrothermal method, Materials Letters, 2015.

Chapter IV

Analyzes the characteristic of installed nanomaterials

Chapter IV: Analyzes the characteristic of installed nanomaterials

IV.1.Introduction

In this last chapter, we will present the results of the study of thin layers of magnesium oxide and silicon dioxide (MgO-SiO_2), which were prepared from natural resources and by the hydrothermal method on glass substrates, and we changed the deposition temperature (150-200-300°C) and the strength of the applied external magnetic field to prepare novel membranes that contribute significantly to new uses and applications, then we try to analyze and interpret each of them separately and seek to combine them, this analysis is based on studying the effect of both the deposition temperature and the strength of the applied magnetic field on the structural properties by studying the X-ray diffraction pattern and knowing its crystal structure on the one hand, on the other hand, study the various properties of these membranes, such as morphological, structural, optical and electrical properties by SEM, EDX, FT-IR, and UV-Visible, respectively.

IV.2.Structural properties of (MgO-SiO_2) thin films

Magnesium oxide is a highly ionized solid that crystallizes in a rock salt structure[1], with a cubic crystal structure[2]. It is considered one of the most common types in nature[3], it belongs to the family of alkaline earth metal oxides. The structure of magnesium oxide corresponds to two cubic sublattices of ions centered on the face, which are displaced from the lattice according to one of the lateral directions of the lattice.

- Coordinates of Mg atoms (0,0,0).

- The coordinates of the O atoms are $(\frac{1}{2}, \frac{1}{2}, \frac{1}{2})$.

The lattice is a face-centered cubic crystal structure with magnesium ions at the vertices of the lattice and oxygen ions between each pair of magnesium ions[4]. Having a network constant of the same value (a = 4.193) and a melting point of (3600°C) [5], and as It is shown in the **figure (IV.1)**.

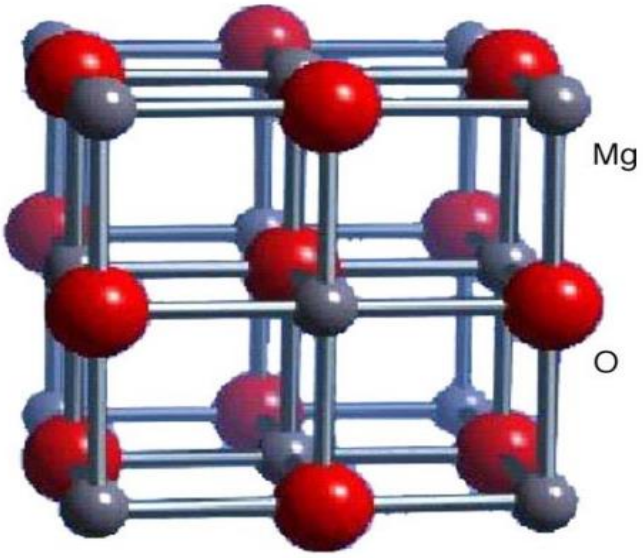

Figure IV.1 : The primary cell of magnesium oxide.

Silicon dioxide is considered one of the silica oxides. Its chemical formula is SiO_2, Silicon is the most abundant element in the Earth's crust after oxygen. It is mainly found in certain rocks or in the form of the silicate ion SiO_3^{-2} linked to a positive ion, which gives sodium silicate Na_2SiO_3, potassium K_2SiO_3, or calcium $CaSiO_3$ to metals are more common [6], silicon dioxide is also very common in its natural state in minerals. The thin layers of silicon dioxide can be converted from the amorphous state into the ∝-quartz crystalline phase by increasing the annealing temperature (also called rock crystal). SiO_2 crystallizes as quartz in the triaxial quadrilateral, tetrahedrons are connected in the three planes of space such that a Si^{+4} ion with ionic radius 0.39 Å is surrounded by four oxygen atoms with ionic radius 0.66 Å, arranged at the upper part from a faces quadruple semi-regular. Each tetrahedron is linked to four oxygen atoms, meaning that the basic building block of silica is a silicon atom surrounded by four oxygen atoms that form the heads of the tetrahedron to crystallize in the hexagonal system[7-9].

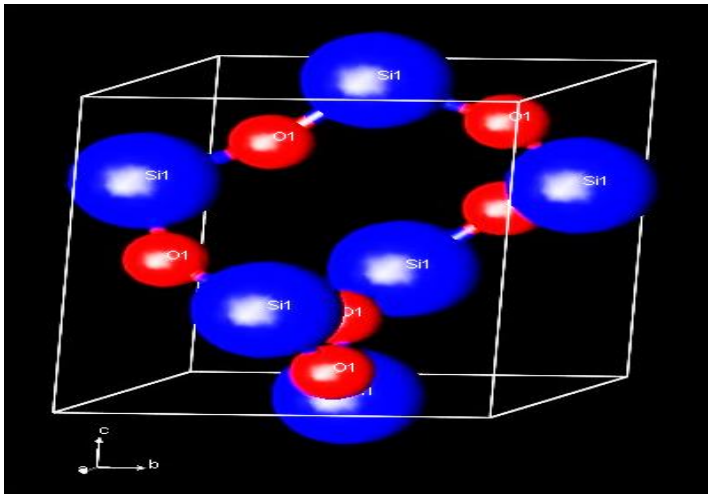

Figure IV.2 : Crystal structure of quartz[10].

We studied the structural properties of MgO-SiO_2 films prepared, using the X-ray diffraction technique and revealed through the results diagnosis for different temperatures (150-200-300°C) that all the deposited films have a polycrystalline structure, where the X-ray diffraction patterns shown in **figure (IV.3)** of MgO-SiO_2 films when two external magnetic fields are projected with the same direction show the presence of several clear peaks at diffraction angles 26.58°, 43.31°, 48.66°, which exactly match the peaks of MgO and of it has a cubic crystal structure according to the ICSD card (**I**norganic **C**rystal **S**tructure **D**atabase) number 9378-015-98, in addition to the angular position 29.43° corresponding to level (0 1 1) for SiO_2 films with a hexagonal crystalline structure, according to the card ICSD Card No.98-015-5252, also the preferential direction of growth is [0 0 2] at the peak (2θ= 43.37°) of the MgO peak.

Figure (IV.4) shows the X-ray diffraction patterns for the prepared films in the case of applying two external magnetic fields, such that the external magnetic field has a direction opposite to the direction of the other field and for various deposition temperatures, and it shows the presence of peaks of varying intensity for the levels (0 1 1), (1 1 1), (0 0 2), (0 0 3) at angles 29.45°, 39.20°, 43.38°, and 50.47°, which relate to the structure of the membranes MgO and SiO_2 according to ICSD Card no. 9378-015-98 and no. 98-015-5252 respectively, also, all the prepared layers are polycrystalline in nature, and we notice the dominance of the (0 0 2) plane of (MgO) at the angle 43.38° over the rest of the planes, making it the plane with the preferential direction of crystal growth, where the diffraction intensity is the highest possible, which

represents the vertical direction of the substrate surface, and this direction is due thermodynamically to the formation of the lowest surface energy [11]. and this can be explained by the drift model, which states that nucleation corresponding to different orientations occurs during the initial stage of membrane deposition and each nucleus competes for growth but only those nuclei that have the fastest growth rate in the substrate can survive[12]. where the molecules migrate to the growth surface and the number of adsorbed Mg and O atoms that are highly mobile at the substrate temperature and can easily move to balanced atomic sites on the surface is improved, it means that the (0 0 2) plane of MgO is strongly stabilized. Thus the dominance of the preferential orientation [0 0 2] occurs when the substrate temperature is sufficiently optimal to arrange the atoms with minimal defects and maximum packing density, the thermal energy of the substrate is also expected to provide energy for the migration of the surface atoms to form a stable preferential layer[1].

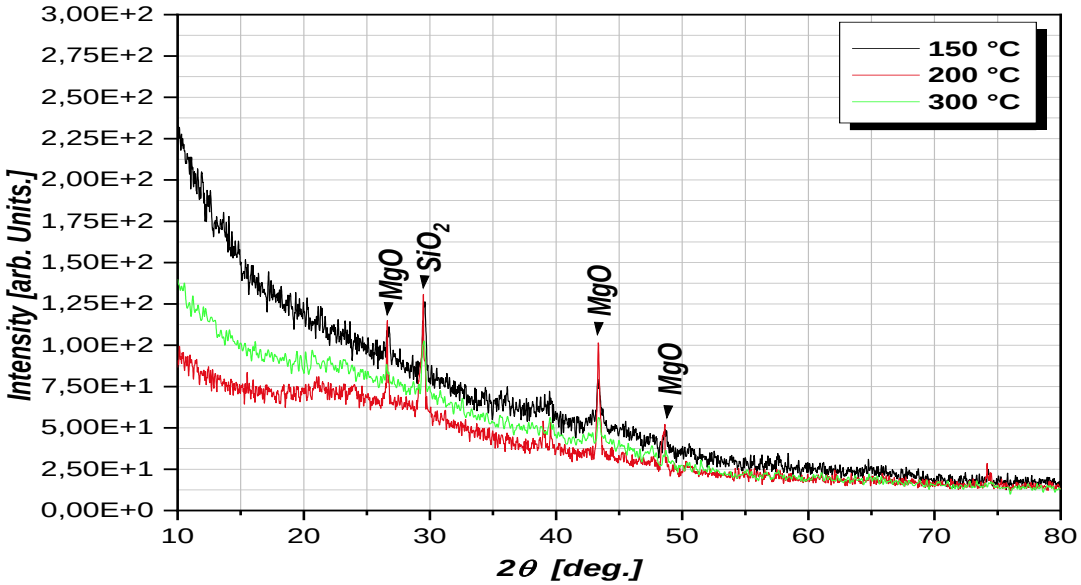

Figure IV.3 : X-ray diffraction (XRD) schemes for prepared membranes as a function of deposition temperature and in the presence of two external magnetic fields so that they have the same direction.

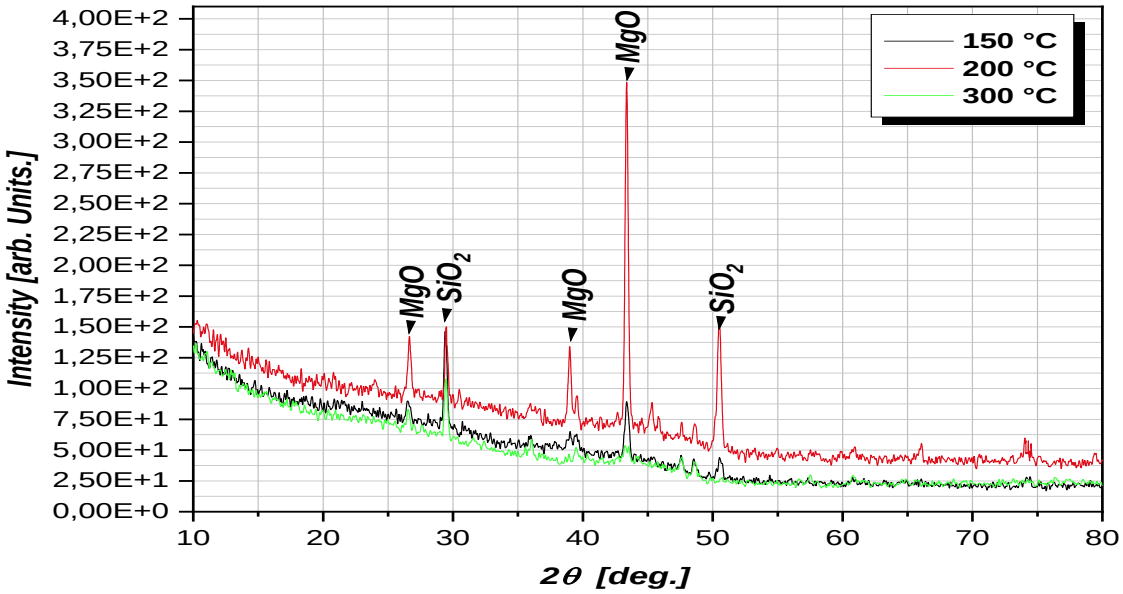

Figure IV.4 : X-ray diffraction (XRD) schemes for prepared membranes as a function of deposition temperature and in the presence of two external magnetic fields so that the external magnetic field has the opposite direction to that of the other field.

We notice from the X-ray diffraction patterns in both cases and deposited at temperatures (150-200-300°C), that the peak intensity of (MgO) and (SiO_2) increases when two external magnetic fields are applied, so that the external magnetic field has a direction opposite to the direction of the other field. At the expense of the peaks of other crystallographic directions and decreases slightly with increasing deposition temperature, this is due to the increase in the corresponding FWHM and may be attributed to the recrystallization potential, with the exception of the films deposited at 200 degrees Celsius, it increases and represents the highest increase in intensity, and this indicates that there are some levels that are favorable for the growth of crystals, so the intensity of this peak increases accordingly, this can be explained by the fact that FWHM decreases which confirms that the deposition at that degree and the intensity of the applied magnetic field has led to crystal regularity and thus increased the degree of crystallization of the membrane material and the decrease of the crystal defects formed in the membrane in preparation.

We also notice that there is a displacement in the locations of the characteristic peaks (0 0 2), (0 1 1) for (MgO) and (SiO_2) at the angular positions of 43.34° and 29.45° respectively for the films prepared for different deposition temperatures after applying two external magnetic fields, so that The external magnetic field has a direction opposite to that of the other field than before shedding two external magnetic fields so that they have the same direction and that this displacement is trending towards greater values for 2θ and the interpretation of this displacement is due to the decrease in the corresponding lattice constants and the decrease in the distance between the crystalline levels (d), hence, an increase in the diffraction angle, and thus a shift of the distinct peaks towards the right in the diffraction pattern due to its connection to an inverse relationship according to Bragg's law[12], when comparing the obtained results and the interview to the 2θ diffraction angles of the locations of the characteristic peaks of the prepared membrane models with the values contained in the standard material examination card ICSD Card No. 98-015-9378 and as shown in **table (IV.1)** and **table (IV.2)**, we find that the values of the interfacial distances between the crystal planes were largely identical to their values in the card.

Table (IV.1): X-ray diffraction results for films prepared at different deposition temperatures in the presence of two external magnetic fields with the same direction.

Material	N°	samples		2è (deg.)	d (Å) Measured	d (Å) Standard	(hkl)	FWHM (deg)
	1	**MgO**	150 °C	43.31	2.088	2.096	(0 0 2)	0.39
	2		200 °C	43.37	2.085	-	(0 0 2)	0.31
	3		300 °C	43.45	2.081	-	(0 0 2)	0.47
	1	**SiO_2**	150 °C	29.43	3.033	3.027	(0 1 1)	0.23
	2		200 °C	29.51	3.025	-	(0 1 1)	0.11
	3		300 °C	29.59	3.018	-	(0 1 1)	0.62

Table (IV.2): X-ray diffraction results for films prepared at different deposition temperatures in the presence of two external magnetic fields, where the external magnetic field has an opposite direction to the direction of the other field.

Material	N°	samples		2è (deg.)	d (Å) Measured	d (Å) Standard	(hkl)	FWHM (deg)
	1	MgO	150 °C	43.34	2.086	2.096	(0 0 2)	0.37
	2		200 °C	43.38	2.084	-	(0 0 2)	0.29
	3		300 °C	43.46	2.080	-	(0 0 2)	0.43
	1	SiO_2	150 °C	29.45	3.032	3.027	(0 1 1)	0.18
	2		200 °C	29.54	3.021	-	(0 1 1)	0.08
	3		300 °C	29.60	3.016	-	(0 1 1)	0.54

IV.2.1.Determine compositional parameters

IV.2.2. Determine the crystal lattice constants

To calculate both the lattice constants (a) and (c) for magnesium oxide and silicon dioxide ($MgO\text{-}SiO_2$) films, we can use the following expressions (IV.1), (IV.2), (IV.3), (IV.4) [12] [2] [13]:

$$n\lambda = 2d_{hkl}.\sin\theta \quad \textbf{(IV.1)}$$

$$d = \frac{a}{\sqrt{(h^2+k^2+l^2)}} \quad \textbf{(IV.2)}$$

$$a = \frac{\lambda}{\sqrt{3}\sin\theta} \quad \textbf{(IV.3)}$$

And

$$c = \frac{\lambda}{\sin\theta} \quad \textbf{(IV.4)}$$

Where: d is the distance between the crystal planes.

(hkl): Miller coefficients.

(θ): Bragg angle.

λ: X-ray wavelength (λ=1.5406 Å).

Through the results we obtained and listed in **table (IV.3)**, we found that there is good agreement with the values of the constants in the card ICSD Card No. 98-015-9378 and ICSD Card No. 98-015-5252, slight decrease in the values of the network constants (a_0, c_0) was observed with increasing deposition temperature, which ranged between 4.162-4.174, 3.485-3.503 and 6.036-6.067, respectively -**Figure (IV.5)-** also, the values of the inter-crystalline distances between the crystal planes, d, decrease with the increase in the deposition temperature, which can be attributed to the difference in the angular position of the prominent peak, and it turns out that the angular positions increase with increasing temperature. In general, the angular position shifts toward the lower and upper sides due to the increase and decrease of the corresponding mesh parameters. It was also observed that it decreased when two external

magnetic fields were applied, such that the external magnetic field had a direction opposite to the direction of the other field. This can be attributed to further realignment of the granules and the strong interaction between the substrate and the solution atoms.

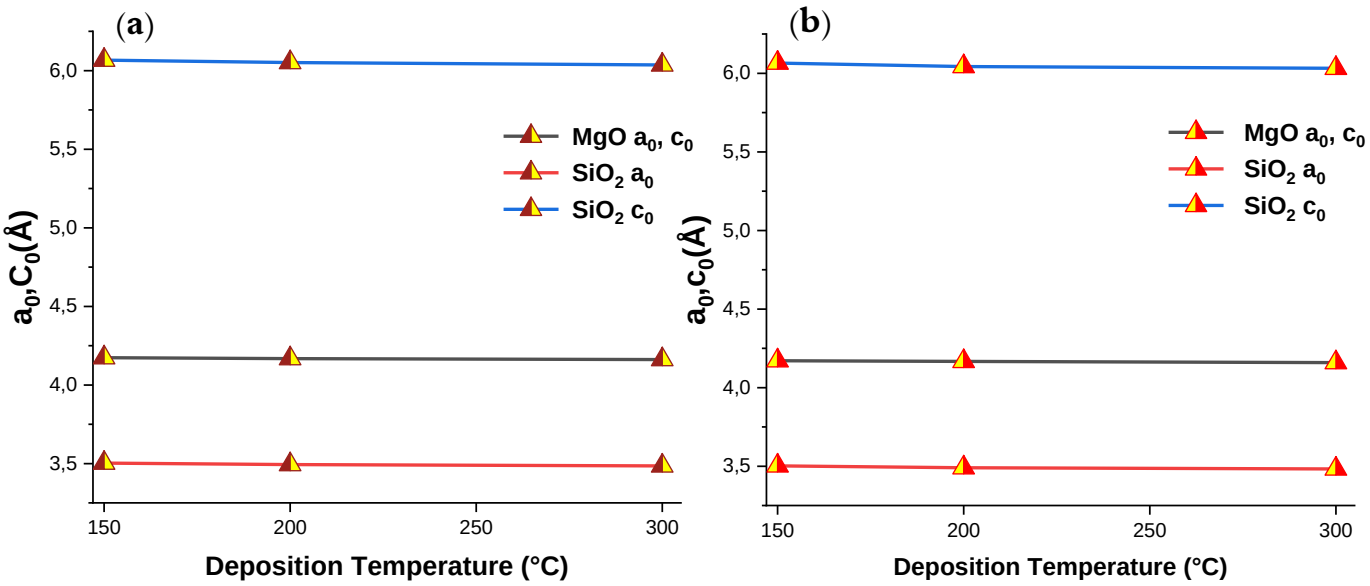

Figure IV.5 : Lattice constants (a_0, c_0) as a function of changing the deposition temperature and in different coordinates: (a) in the presence of two external magnetic fields so that they have the same direction, (b) in the presence of two external magnetic fields so that the external magnetic field has a direction opposite to the direction of the other field.

IV.2.3. Average grain size

By calculating the values of the average grain size of the prepared layers as a function of the deposition temperature based on Scherer's Formula, which is explained as follows [14]:

$$G.S = \frac{\kappa\lambda}{B.\cos\theta} \qquad \textbf{(IV.5)}$$

where:

G.S: Crystalline size (nm).

κ: The network formation constant is called the sparking constant and is equal to 0.9.

B: Maximum half at width full in radians.

λ: X-ray wavelength (Å).

We note that the average grain size values, which are presented in **table (IV.4)** for samples prepared when two external magnetic fields are applied, such that the external magnetic field has a direction opposite to the direction of the other field, are greater than their counterparts for samples prepared when two external magnetic fields are applied, such that they have the same direction, it was found that the grain size of (MgO) and (SiO_2) falls within the range 20.09-30.14 nm, 15.40-115.54 nm and the range 18.24-27.73 nm, 13.33-77.02 nm, respectively, this indicates that the films prepared in both cases are nano-crystalline, it was also observed that the average grain size tends to decrease with increasing deposition temperature, and this in turn causes an increase in the diffraction angle (2θ) and an increase in the width at the peak at mid-intensity this is shown in **figure (IV.6)** and **figure (IV.7)**, however, the opposite behavior was observed for thin films deposited at 200 degrees Celsius, which led to the cancellation of some grain boundaries when the grains coalesced to form crystals of larger size, as well as the cancellation of existing defects after the growth process occurred and rearranging the crystalline grains, and improving the crystallinity of the material, where the granules take enough energy to grow and arrange within the network. The changes in FWHM and corresponding grain size may be attributed to the crystallization of the deposited films as well as crystal growth and nuclide formation. The improvement in crystallinity of MgO-SiO_2 thin films may provide the activation energy to occupy the minimum energy site of adsorbed atoms due to the fusion of islands by increasing surface and volume diffusivity[15-17] [12].

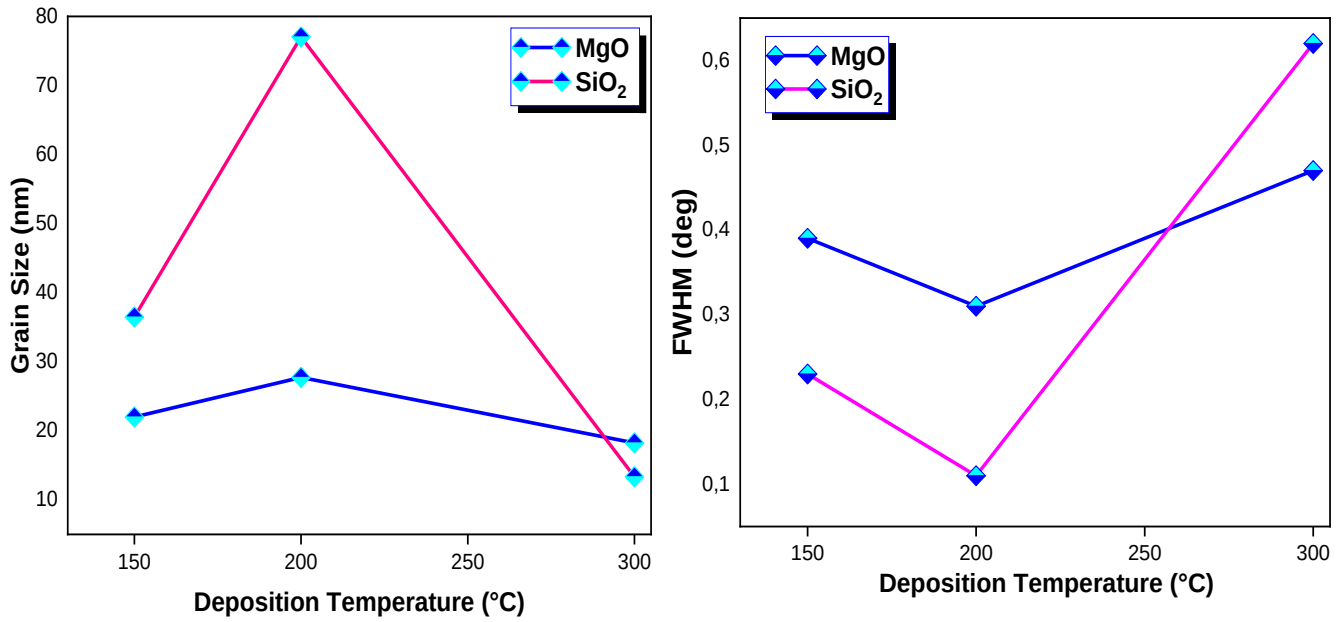

Figure IV.6 : The relationship between FWHM and grain size rate as a function of different deposition temperatures and in the presence of two external magnetic fields that have the same direction.

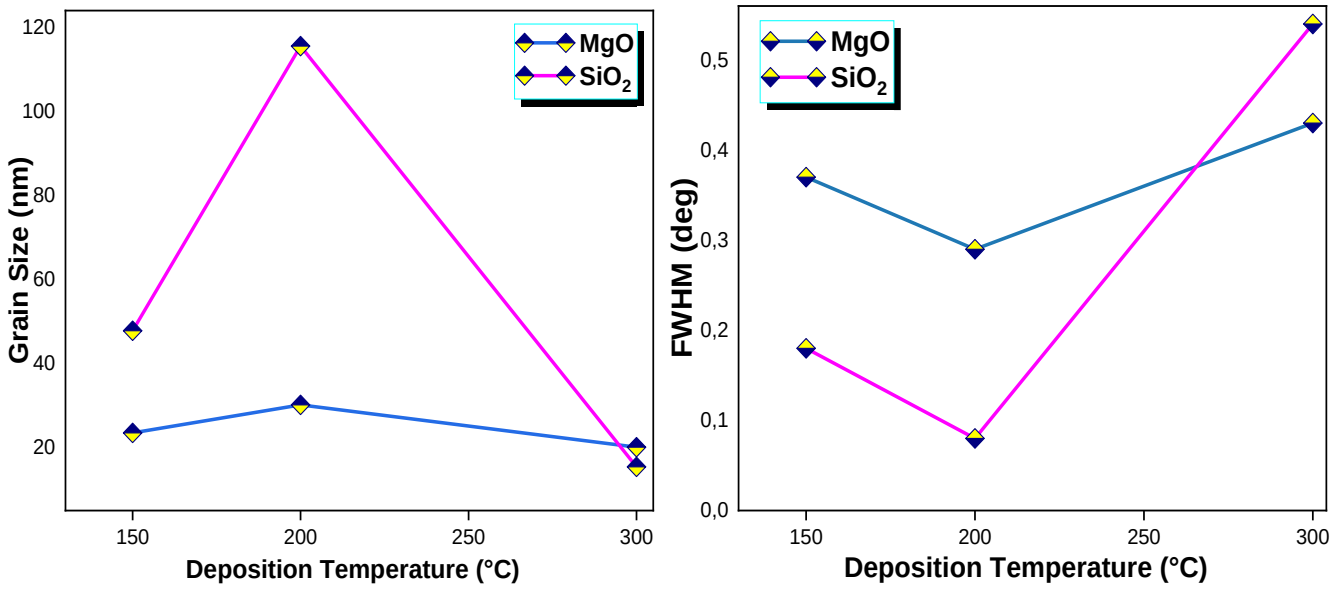

Figure IV.7 : The relationship between FWHM and grain size rate as a function of different deposition temperatures and in the presence of two external magnetic fields, such that the external magnetic field has a direction opposite to the direction of the other field.

IV.2.4. Number of crystals and dislocation density

The dislocation density (δ) and number of crystallites of the prepared MgO-SiO_2 films were calculated by the following two expressions:

$$\delta = \frac{1}{G.S^2} \quad \textbf{(IV.6)}$$

$$N = \frac{t}{G.S^3} \quad \textbf{(IV.7)}$$

Where t: Thin membrane thickness.

The results showed differences in the dislocation density (δ) and the number of granules per unit area (N) as a function of the granular size, and this is shown in the **table (IV.3)**, an increase was observed with increasing deposition temperature, and the values ranged from 1.30×10^{15} m^{-2} to 3×10^{15} m^{-2}, and from 0.16×10^{15} m^{-2} to 5.64×10^{15} m^{-2}. The number of crystals per unit area (N) was also found in the range (12.53-29.3) $\times 10^{16}$ m^{-2}, and the range (0.591-75.15) $\times 10^{16}$ m^{-2} for (MgO) and (SiO_2) respectively, this is due to the decrease in grain size except for thin films at 200 °C which led to the formation of larger-sized crystals. These values rise when two external magnetic fields are shone so that they have the same direction, so that we note that both the values of the dislocation density and the number of granules have inverse proportion to the grain size, this means that the apparent increase in granular size improves the crystal structure and thus reduces the dislocations by reducing the granular boundaries found therein as shown in **figure (IV.8)** and **figure (IV.9)**[12] [18].

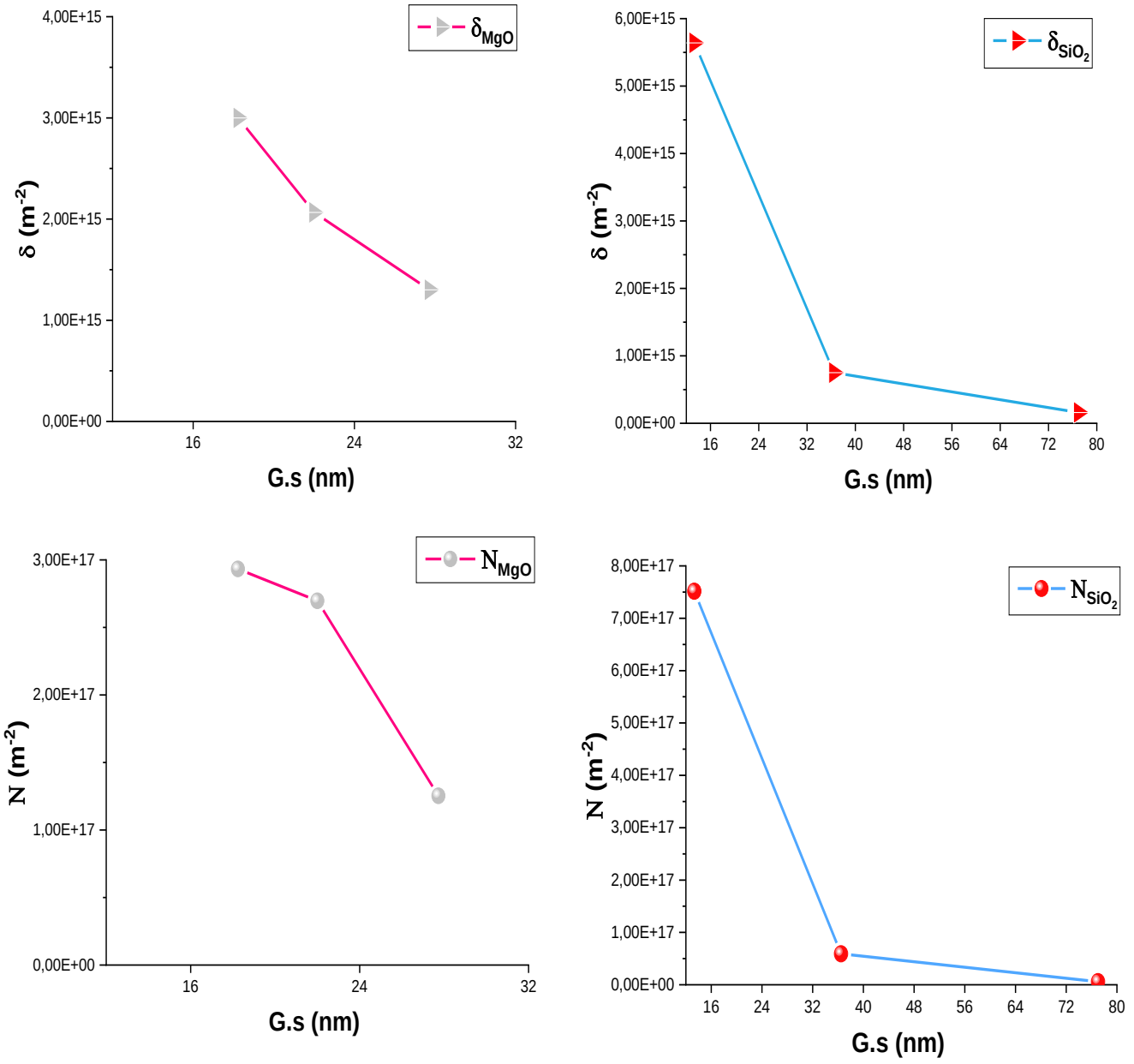

Figure IV.8 : Changes in the density of dislocations and the number of crystals as a function of the granular size rate in the presence of two external magnetic fields that have the same direction.

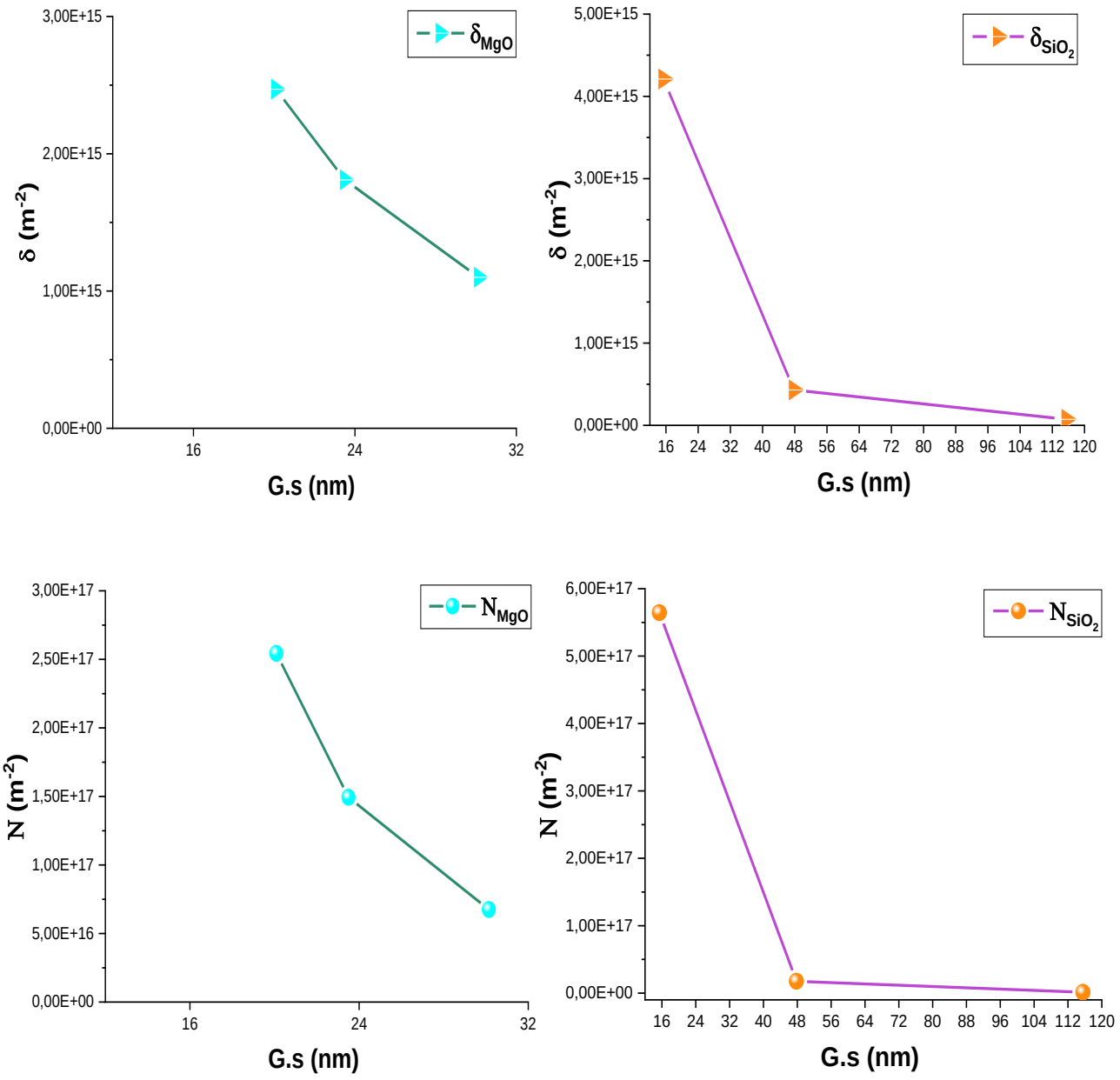

Figure IV.9 : Changes in the density of dislocations and the number of crystals as a function of the granular size rate in the presence of two external magnetic fields, such that the external magnetic field has a direction opposite to the direction of the other field.

IV.2.5. Crystal distortion

Figure (IV.10) shows the difference in the deformation of the material as a function of the deposition temperature, and this deformation of the crystals (Strain) was calculated through the following relationship[19]:

$$Strain = |d_{XRD} - d_{ASTM}| / d_{ASTM} \quad \textbf{(IV.8)}$$

Where:

d_{ASTM}: The amount of interfaced distance in the card [deg].

d_{XRD}: The amount of interfaced distance calculated [deg].

Through the data shown in **table (IV.3)**, deformation of crystals (MgO) and (SiO_2) has been shown to increase as the deposition temperature increases, a relative increase was also observed when two external magnetic fields were shone so that they would have the same direction, and this is due to the increase in stress on the crystalline levels and the occurrence of compression with changes in the interfaced distances (d), the decrease in crystal distortion in certain areas is also due to its decrease and is illustrated by the following form[18].

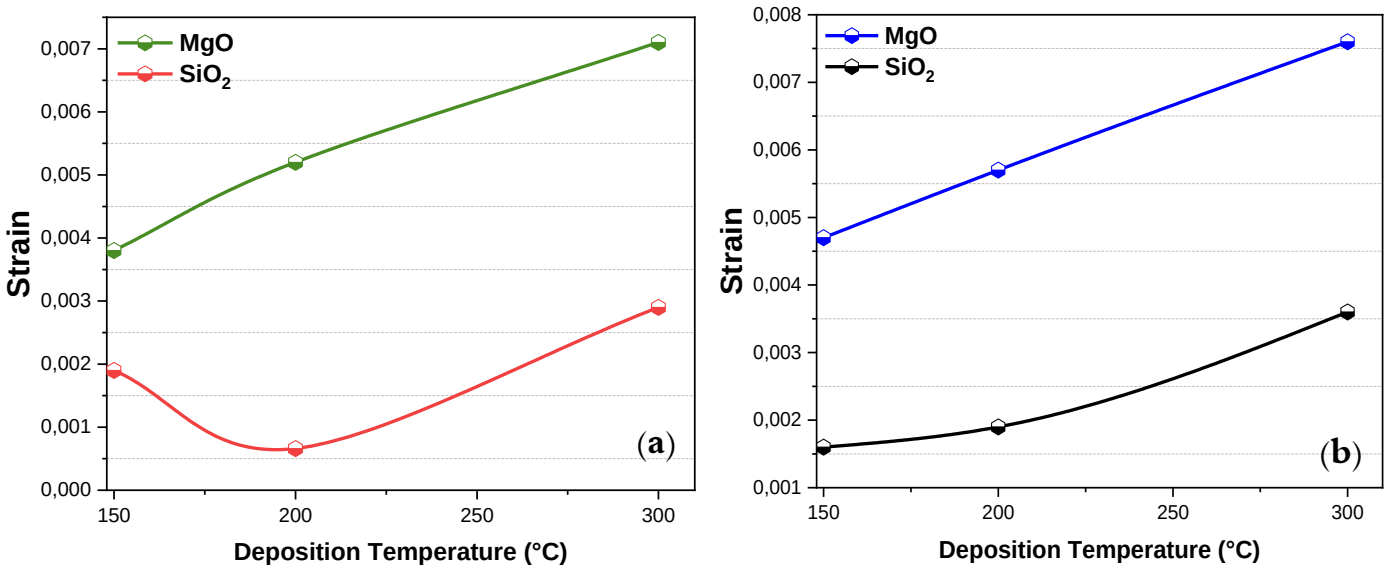

Figure IV.10 : Crystals distortion as a function of changing the deposition temperature and in different coordinates: (a) in the presence of two external magnetic fields so that they have the same direction, (b) in the presence of two external magnetic fields, such that the external magnetic field has a direction opposite to the direction of the other field.

Table (IV.3): it represents the crystal lattice constants, granular average size, density of dislocations, number of crystals and the crystal distortion of films prepared at different deposition temperatures in the presence of two external magnetic fields so that they have the same direction.

samples	2è (deg)	a (Å)		c (Å)		Grain Size (nm)	$\delta \times 10^{15}$ m^{-2}	$N \times 10^{16}$ m^{-2}	Strain $\times 10^{-2}$	(hkl)
		Obs.	Stand	Obs.	Stand					
MgO 150 °C	43.31	4.174	4.193	4.174	4.193	22.00	2.066	26.97	0. 38	(0 0 2)
MgO 200 °C	43.37	4.168	-	4.168	-	27.73	1.30	12.53	0.52	(0 0 2)
MgO 300 °C	43.45	4.162	-	4.162	-	18.24	3	29.33	0.71	(0 0 2)
SiO_2 150 °C	29.43	3.503	3.850	6.067	7.220	36.48	0.75	05.91	0.19	(0 1 1)
SiO_2 200 °C	29.51	3.494	-	6.051	-	77.02	0.16	0.585	0.066	(0 1 1)
SiO_2 300 °C	29.59	3.485	-	6.036	-	13.33	5.64	75.15	0.29	(0 1 1)

Table (IV.4): it represents the crystal lattice constants, granular average size, density of dislocations, number of crystals and the crystal distortion of films prepared at different deposition temperatures in the presence of two external magnetic fields, such that the external magnetic field has a direction opposite to the direction of the other field.

samples	2è (deg)	a (Å)		c (Å)		Grain Size (nm)	$\delta \times 10^{15}$ m^{-2}	$N \times 10^{16}$ m^{-2}	Strain $\times 10^{-2}$	(hkl)
		Obs.	Stand	Obs.	Stand					
MgO 150 °C	43.34	4.171	4.193	4.171	4.193	23.5	1.81	14.93	0.47	(0 0 2)
MgO 200 °C	43.38	4.167	-	4.167	-	30.14	1.10	6.75	0.57	(0 0 2)
MgO 300 °C	43.46	4.159	-	4.159	-	20.09	2.47	25.43	0.76	(0 0 2)
SiO_2 150 °C	29.45	3.502	3.850	6.065	7.220	47.81	0.43	01.77	0.16	(0 1 1)
SiO_2 200 °C	29.54	3.490	-	6.043	-	115.54	0.074	0.119	0.19	(0 1 1)
SiO_2 300 °C	29.60	3.483	-	6.032	-	15.40	4.21	56.45	0.36	(0 1 1)

IV.3.Morphological properties of thin layers (MgO-SiO_2)

The scanning electron microscope (SEM) was used to study the morphological properties of the thin layers of magnesium oxide and silicon dioxide (MgO-SiO_2) prepared by hydrothermal method on the glass substrates, and the extent of the effect of changing the deposition temperature (150-200-300°C) in the presence of a change in the strength of the applied magnetic field, where **figure (IV.11)** shows microscopic images of surface samples shown in the two-dimensional high zoom taken by SEM in the same zoom 50μm and in the presence of two external magnetic fields so that they have the same direction, and we note that the membranes possess clear fullness surfaces and that molecular granules of different shapes are separated by interstitial spaces and distributed in different sizes, and it is clear from the **figure (IV.11.b)** that the surface of the membrane contains small granular particles and with a small number. The average particle size has an effect on the density of the membrane material distribution, so we notice an increase in the density of the material distribution on the surface of the sample at a temperature of 200 °C with relatively large granular particles, and at the temperature of 300 °C we note that the sample has a homogeneous surface with small-sized granules as shown in the **figure (IV.11.c)** and **figure (IV.11.d)**, and through this, we find that the formation of the topographic surface of the membrane depends basically on the deposition temperature and the extent of dissolution of the materials chosen for deposition in the solution, they affect the crystal dimensions as well as affect their geometric shape, but when two external magnetic fields are applied, such that the external magnetic field has a direction opposite to the direction of the other field, it becomes clear that there is a noticeable homogeneity and condensation of the physical distribution of the surface of the samples, and this appears on the surface of the sample at 200 °C, where the granular particles become small in size with a high density as their growth and crystallization increase, and when the temperature increases to 300 °C, the membrane surface becomes more homogeneous in distribution and free of islands and voids with the gradually for grains coalescing, as shown in **figure (IV.12.b)** and **figure (IV.12.c)** [44].

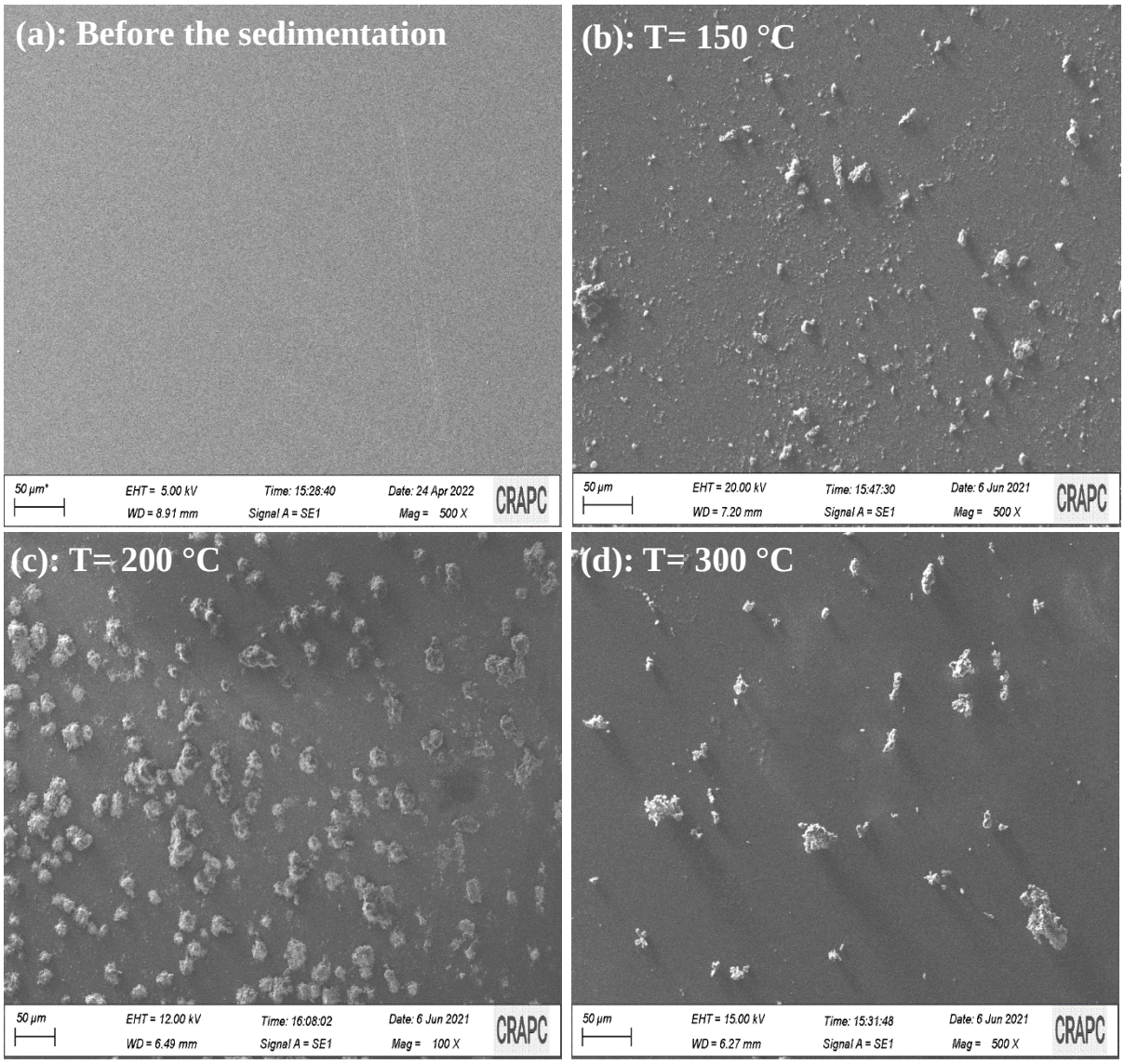

Figure IV.11 : SEM images of the layers prepared at different sedimentation temperatures and in the presence of two external magnetic fields so that they have the same orientation.

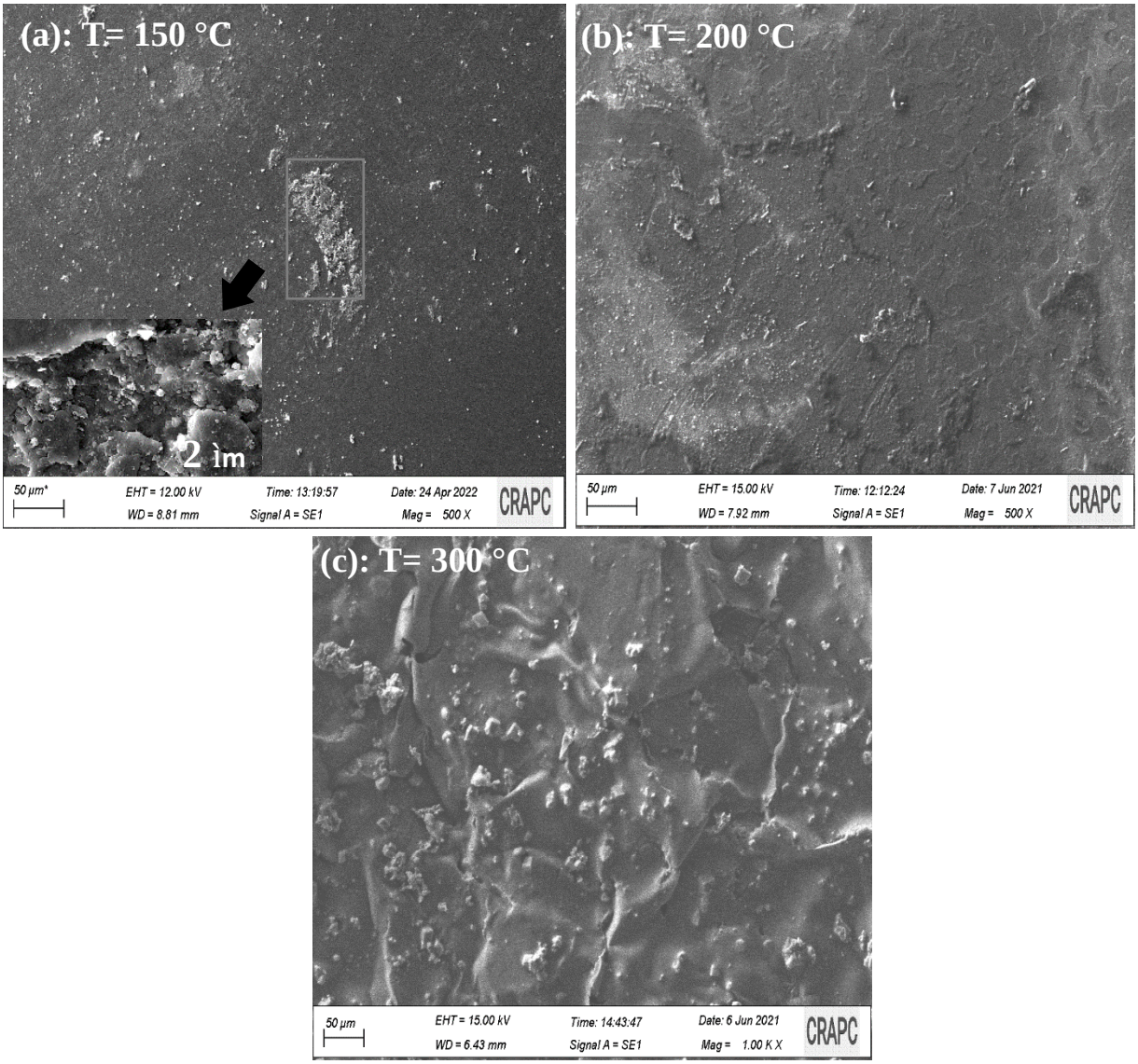

Figure IV.12 : SEM images of the films prepared at different sedimentation temperatures and in the presence of two external magnetic fields so that the exterior magnetic field has an opposite orientation to the direction of the other field.

IV.4.Properties of compositional analysis of thin layers (MgO-SiO_2)

Measurements of the radiation dispersion energy (EDX) of the thin layers of the wiped points were performed by the electronic package of the scanning electron microscope resulting from the cross effect between the charged particles and the membrane material and to be received by the detector, since each chemical element has a set of distinctive peaks in the X-ray spectrum, the chemical components of the membrane are determined through the energy of the X-ray produced and the approval of the energy difference between atomic orbits, and these measurements have proven to us the presence of carbon (C), oxygen (O), sodium (Na), magnesium (Mg), and silicon (Si) within the thin layers at different temperatures and in the change of magnetic field strength, and in addition, the element calcium (Ca) appears, and this is likely to be a result of the glass substrate, and as shown by the emission lines spectra in **figure (IV.13)** for MgO-SiO_2 films when two external magnetic fields are applied so that they have the same direction, as for the membranes, in the case of applying two external magnetic fields such that the external magnetic field has a direction opposite to the direction of the other field and this is shown in **figure (IV.14)**, and in addition to the weights of the mass and atomic elements (Wt% and at%) present in the **tables (IV.5)**, **tables (IV.6)**, and our study therefore shows the confirmation of the elements to be found.

Tables (IV.5) and **(IV.6)** represent the weight percentages and atomic percentages of the chemical elements in the energy range studied.

Table (IV.5) : represents the atomic and mass ratios of the chemical elements of the layers prepared at different sedimentation temperatures in the presence of two external magnetic fields so that they have the same direction.

Chemical Element	The heated sample (°C)					
	150		200		300	
	Wt%	At %	Wt%	At %	Wt%	At %
Carbon	2.57	4.97	2.24	3.88	5.04	10.55
Oxygen	38.58	54.04	43.54	56.54	33.04	51.92
Natrium (Sodium)	10.39	10.13	14.47	13.08	13.66	14.95
Magnesium	2.32	2.14	2.43	2.08	1.31	1.84
Silicon	29.19	23.29	27.09	20.04	6.97	6.24
Calcium	5.18	2.90	4.59	2.38	6.73	4.22

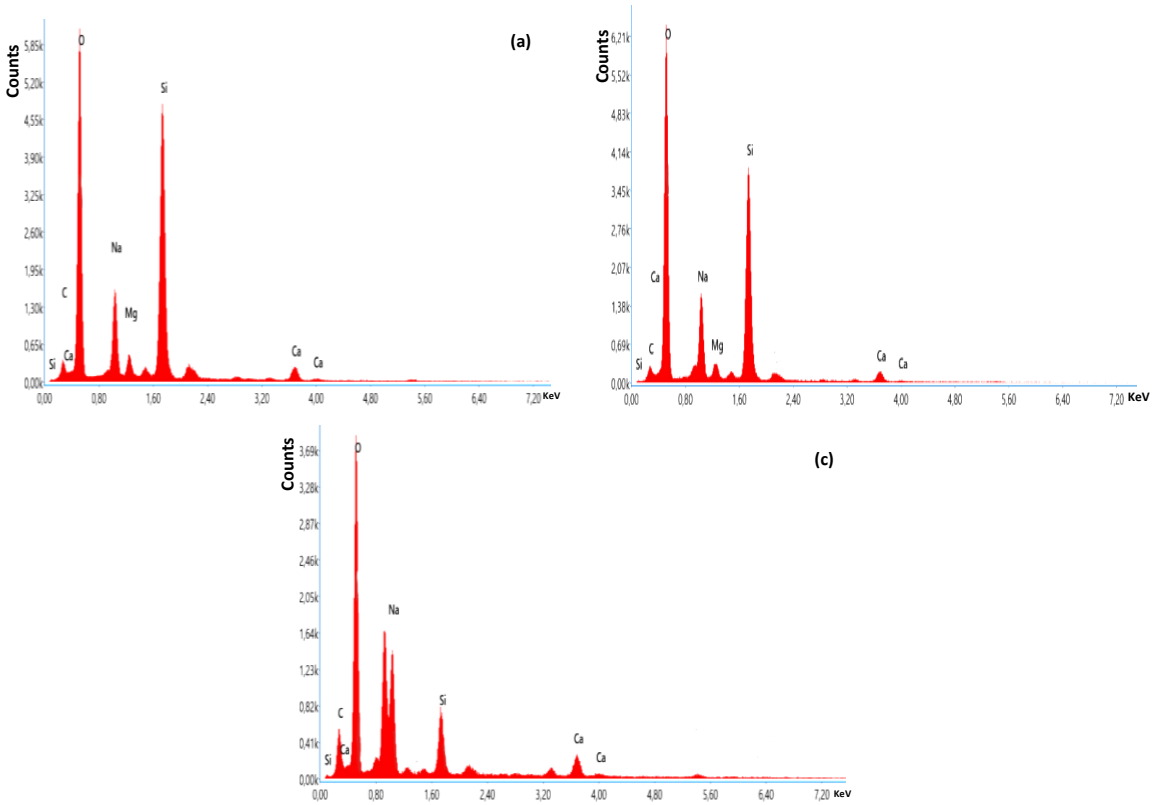

Figure IV.13 : EDX spectra of films prepared at different deposition temperatures and in the presence of two external magnetic fields with the same orientation

((a): T=150 °C, (b): T= 200 °C, (c): T=300 °C).

Table (IV.6) : represents the atomic and mass ratios of the chemical elements of the membranes prepared at different deposition temperatures in the existence of two exterior magnetic fields, so that the exterior magnetic field has an opposite orientation to the direction of the other field.

Chemical Element	The heated sample (°C)					
	150		200		300	
	Wt%	At %	Wt%	At %	Wt%	At %
Carbon	0.00	0.00	12.72	20.91	4.99	8.43
Oxygen	37.00	50.41	40.95	50.53	42.00	53.25
Natrium (Sodium)	12.34	11.70	11.84	10.16	21.60	19.06
Magnesium	2.83	2.54	1.93	1.57	1.77	1.48
Silicon	38.44	29.84	18.56	13.04	18.46	13.33
Calcium	7.22	3.93	2.66	1.31	1.84	0.93

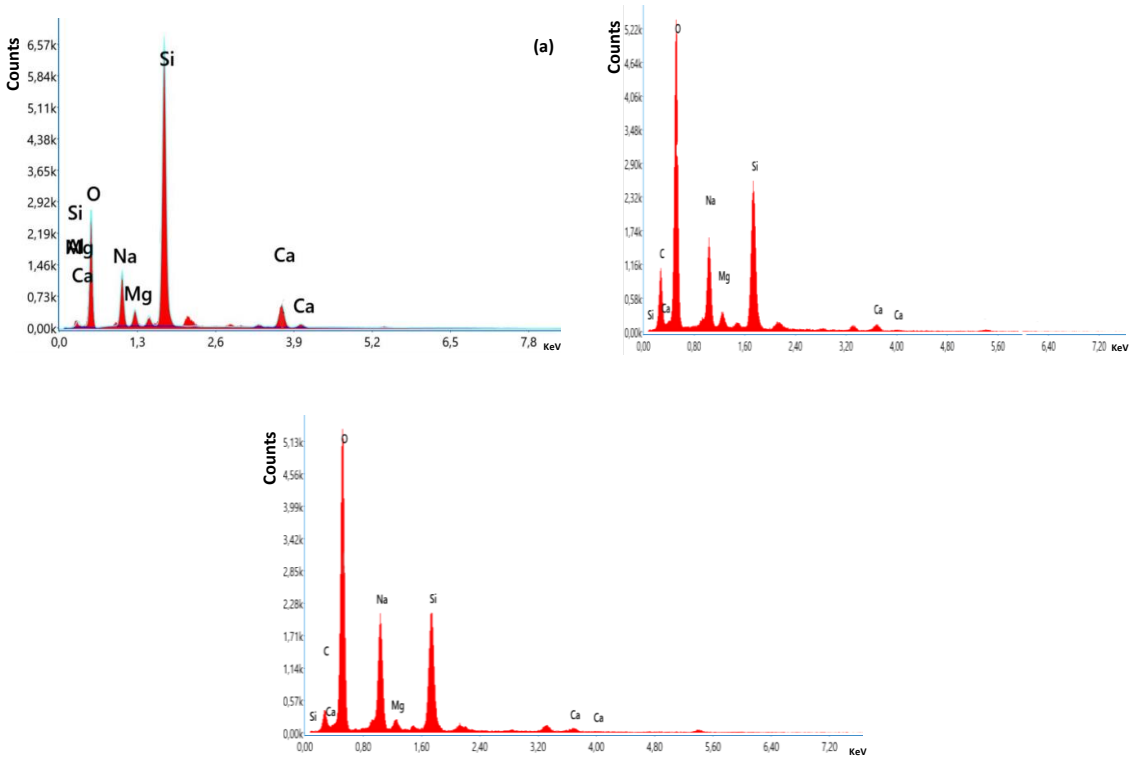

Figure IV.14 : EDX spectra of films prepared at different deposition temperatures and in the presence of two external magnetic fields such that the external magnetic field has an opposite direction to that of the other field ((a): T=150 °C, (b): T= 200 °C, (c): T=300 °C).

IV.5. Molecular structure properties of thin layers ($MgO\text{-}SiO_2$)

FT-IR measurements were made for magnesium oxide and silicon dioxide ($MgO\text{-}SiO_2$) films by measuring the transmittance spectrum as a function of wavenumber to determine the molecular structures that are formed from atoms bonded together for crystalline, amorphous, organic and inorganic materials, these bonds have central vibrations and each molecule has a set of harmonic vibrations that can be identified. To qualitatively analyze these membranes, the absorbed wavelengths corresponding to the chemical group present in them are determined, and then the corresponding functional group is determined. We use this property to track chemical bonding studies of thin layers prepared, using infrared spectroscopy with a range of 4000-500 cm^{-1}.

Figure (IV.15), (IV.16) shows the infrared absorption spectra of films prepared upon a change in deposition temperatures and the strength of the applied magnetic field. The following chemical bonds (Mg-O), (Si-O), (C-H), (CO_3^{-2}), (-OH) were identified based on the absorption spectra of the rays and this through their vibration sites and thus conclusion of chemical bonds, and as shown in the **table (IV.7)**, which shows the type of links and vibration patterns in addition to their corresponding frequency.

Most of the chemical bonds that appeared in all the FTIR spectra of the thin layers indicate that they contain magnesium oxide and silicon dioxide, which is completely consistent with previous spectroscopic results, and in addition, other links have been found that are due to some organic impurities.

Below is a presentation of the results of this spectroscopic measurement of thin layers ($MgO\text{-}SiO_2$) obtained using infrared Spectrometer (FT-IR).

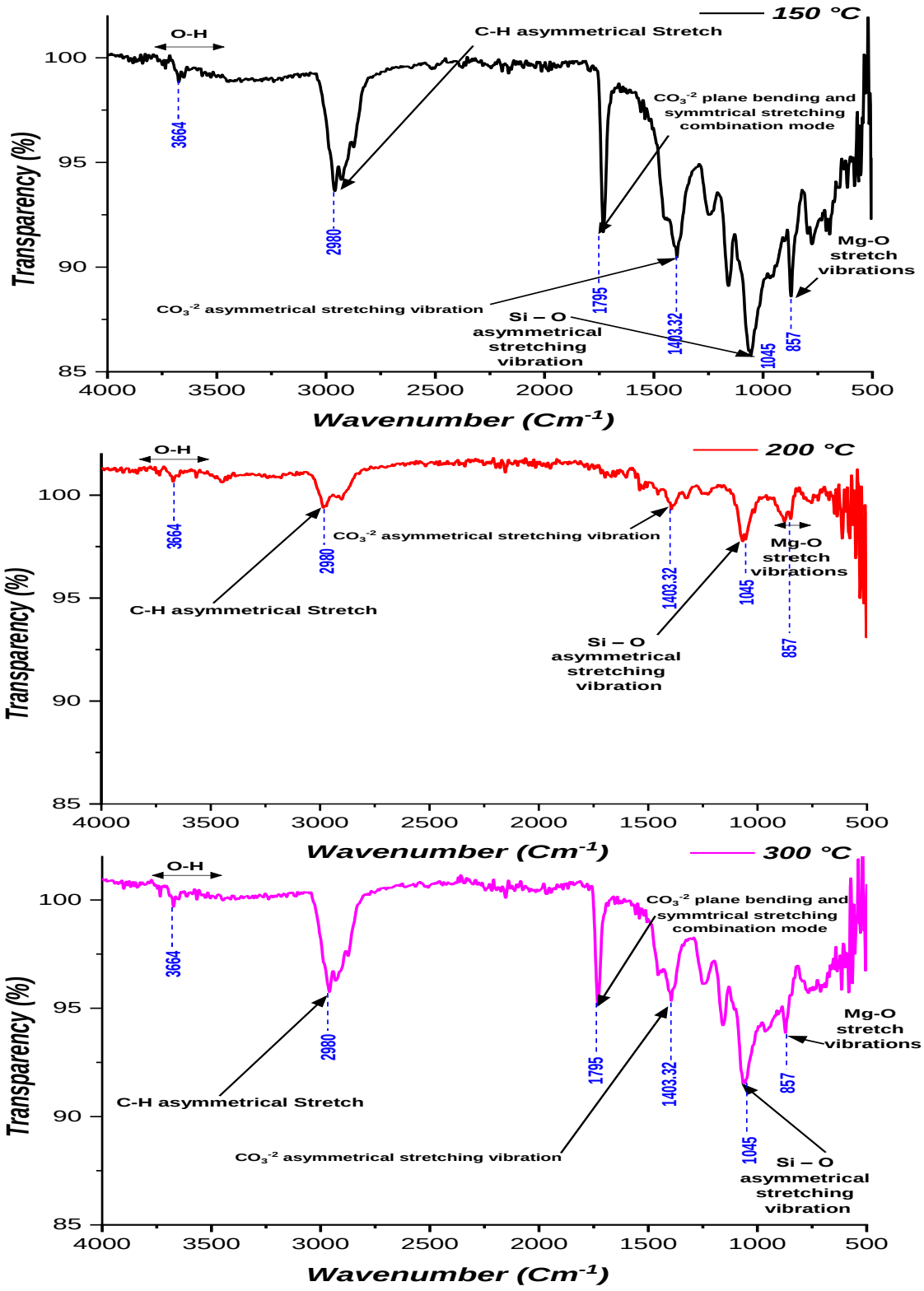

Figure IV.15 : The infrared absorption spectrums of prepared membranes change at different deposition temperatures and in the presence of two external magnetic fields so that they have the same direction.

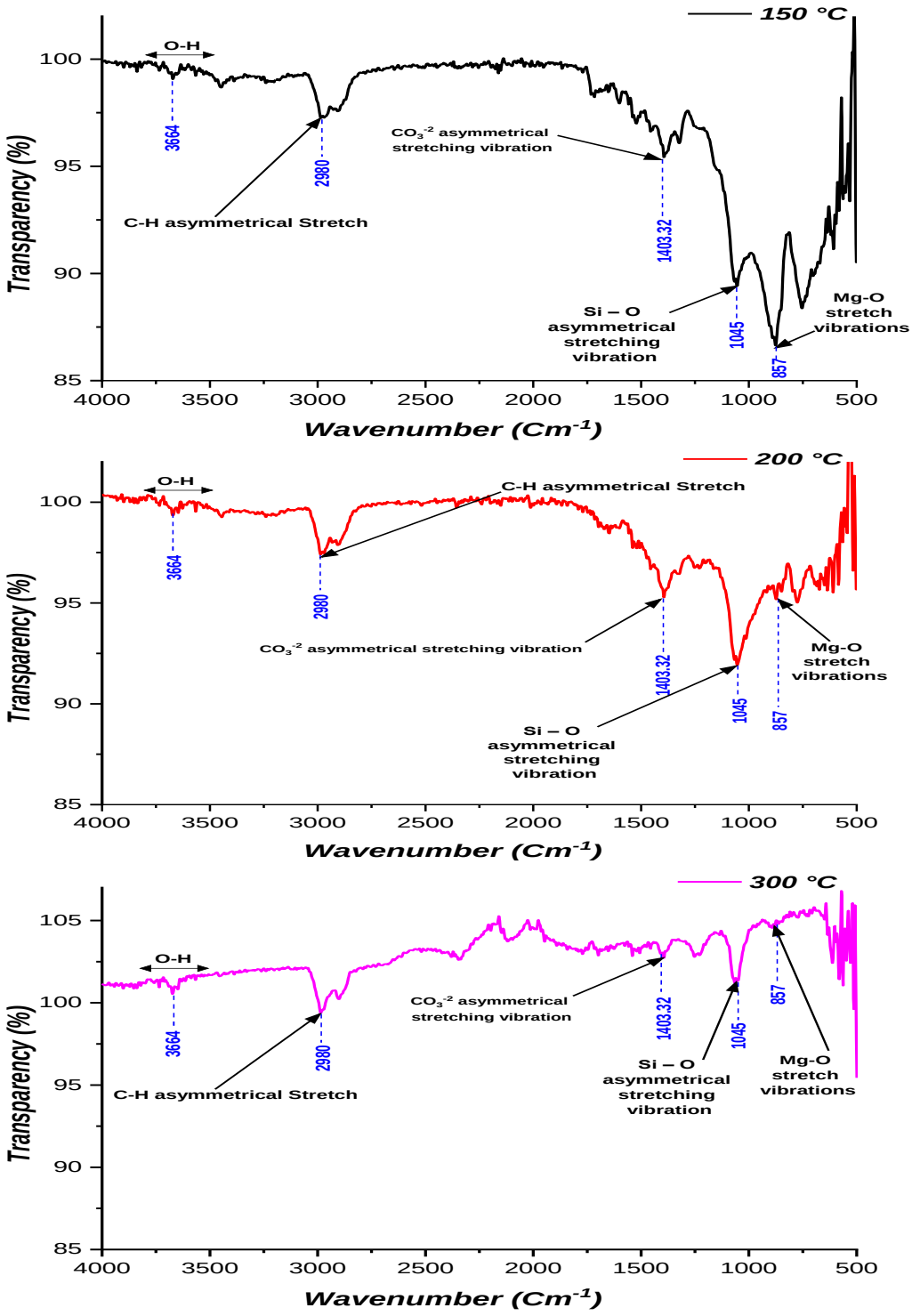

Figure IV.16 : The infrared absorption spectrums of prepared membranes change at different deposition temperatures and in the presence of two external magnetic fields such that the external magnetic field has an opposite direction to that of the other field.

The absorption at the peak at 1045 cm^{-1} indicates the asymmetric stretching vibration of the Si-O bond, which indicates the presence of quartz[21-25], the absorption band was also observed at the peak 857 cm^{-1} which is an indicator of the vibration of the Mg-O expansion bond[26], the intensities of these absorptions vary from one sample to another some of them decrease in intensity, while others disappear and this is due to the difference in their compositions.

Several weak-intensity absorption tapes were also observed at about 3664cm^{-1} which are attributed to the vibration of the stretch of the hydroxyl-OH group and participation in hydrogen bonds with water molecules[27-28], the absorption band at the 2980 cm^{-1} peak indicates an asymmetrical stretching of the C-H bond, which is an indication of the presence of organic impurities[27] [29-31], while the absorption bands 1403.32 cm^{-1} and 1404.12 cm^{-1} indicate the asymmetric expansion vibration of the carbonate ion CO_3^{-2}, these vibrations appeared in all samples, which leads us to say that they constitute all samples. However in the case of two external magnetic fields that have the same direction and at 150-300 °C deposition temperatures, the presence of an amount of calcite as impurities ($CaCO_3$) was observed at the peak at 1795 cm^{-1}, which is attributed to the vibration combining bending in the equilibrium plane and symmetrical expansion of CO_3^{-2} ions[30].

Table (IV.7) : Molecular structure of the prepared films metals and their corresponding vibrations at different deposition temperatures and different magnetic field strengths were determined using FTIR.

Wave number (Cm^{-1})		*Compound*	*Molecular bond and type of vibration*
3800-3200	3664	Absorbed water	**O-H Stretch vibration**
	2980	Organic impurities	**C-H asymmetrical Stretch**
	1795	Calcite	**CO_3^{-2} plane bending and symmetrical stretching combination mode**
1476-1392	1403.32 1404.12	Calcite	**CO_3^{-2} asymmetrical stretching vibration**
	1045	Quartz	**Si–O asymmetrical stretching vibration**
	857	Magnesium oxide	**Mg–O Stretch vibration**

It is clear from the information obtained and listed in the **table (IV.7)** that there are three main vibrations: Asymmetric Vibration, Symmetric Vibration, and Bending Vibration, mostly, stretching vibrations occur at higher frequencies than bending vibrations. In addition, asymmetric stretching vibrations occur at a higher frequency than symmetrical stretching vibrations.

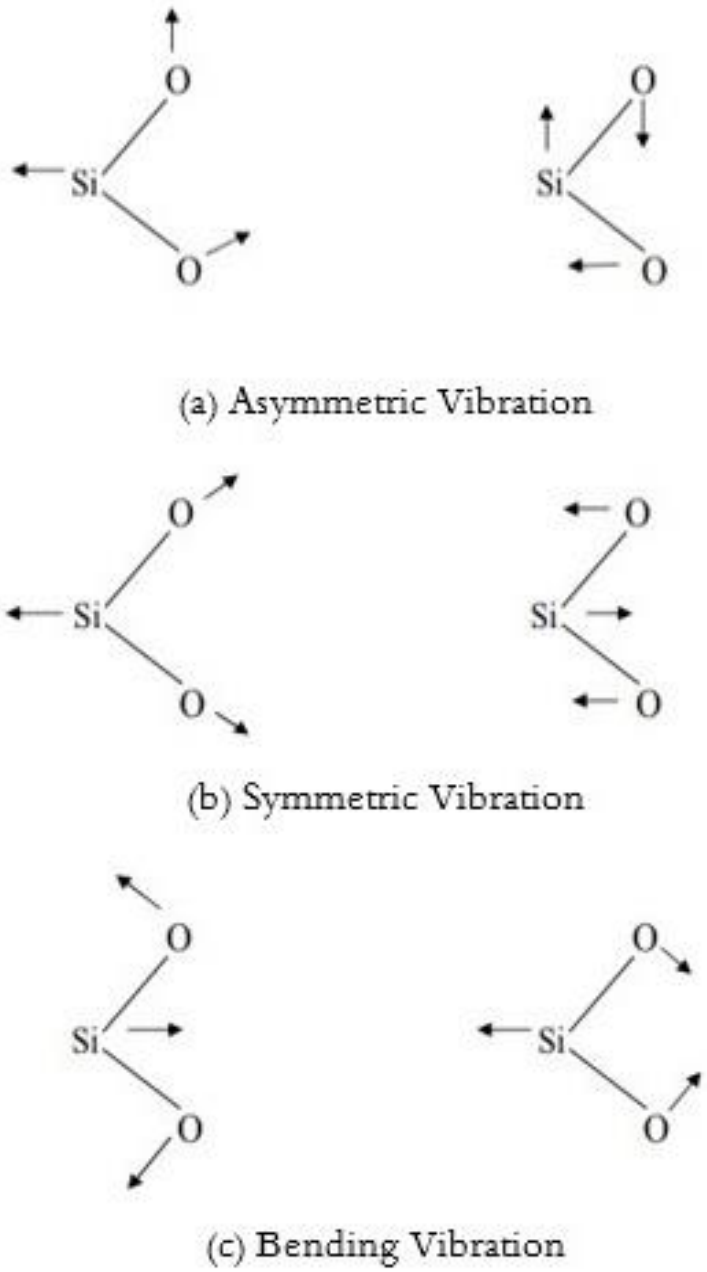

Figure IV.17 : The main vibrations of the SiO_2 molecule.

IV.6. Optical properties of thin layers

Studying the optical properties of any semiconductor material is important for understanding the nature of the material, and its properties, and the possibility of using it in various practical applications, and information about their properties can be obtained from their optical behavior, which is closely related to the composition of the energy levels, which in turn is related to the chemical and crystalline structure of the material.

IV.6.1. Optical transmittance

The optical properties of thin films were studied by obtaining transmittance spectra for various layers prepared in the presence of two external magnetic fields with the same direction. Based on the optical transmittance values, the transmittance relationship was drawn as a function of wavelength T=f(λ) within the wavelengths of the 200-900 nm range, which is characterized by its behavior being opposite to the absorbance values, as shown in the **figure (IV.18)**. It is clear from the figure that the permeability generally begins to appear at low wavelengths and increases at the wavelength that represents the dividing line between the absorbance and permeability of the membrane material, or what is called the cut-off wavelength ($\lambda_{cut.\ off}$), and it generally rises at lower-energy wavelengths of incident electromagnetic radiation.

These results showed that there is a clear increase in the permeability values with increasing wavelength. It was also noted that the permeability increases with increasing deposition temperature and for all temperatures as well. Can be noted that the membranes have a transmittance rate estimated at approximately (~88%) at a temperature of 150°C, and this value quickly increases with increasing temperature to reach a rate of (~97%) at a temperature of 300°C within the visible spectrum region and the near-infrared region with long wavelengths, this is due to a decrease in the absorption of visible light by electrons, that is, a decrease in the number of electronic transitions between the transport band and the valence band, as the optical energy is less than the absorption edge, and this leads to an increase in transmittance.

On the other hand, we note that there is little permeability of all membranes in the UV area to increase sharply at the value (380-400 nm), this area is called the basic absorption edge. The decrease at these short wavelengths is due to the high absorption of photons falling on the membrane in this area of the electromagnetic spectrum as well as a slight displacement at the

edge in the absorption, because the energy of the emitted photons is close to this edge, this indicates that the material is a semiconductor with a wide energy interval and that the energy of the photons in the high-permeability region does not suffer from high absorption.

It can also be said that the concentration of transporters, the size of the granules, and the smoothness of the membrane surface have a role in reducing dispersion[32].

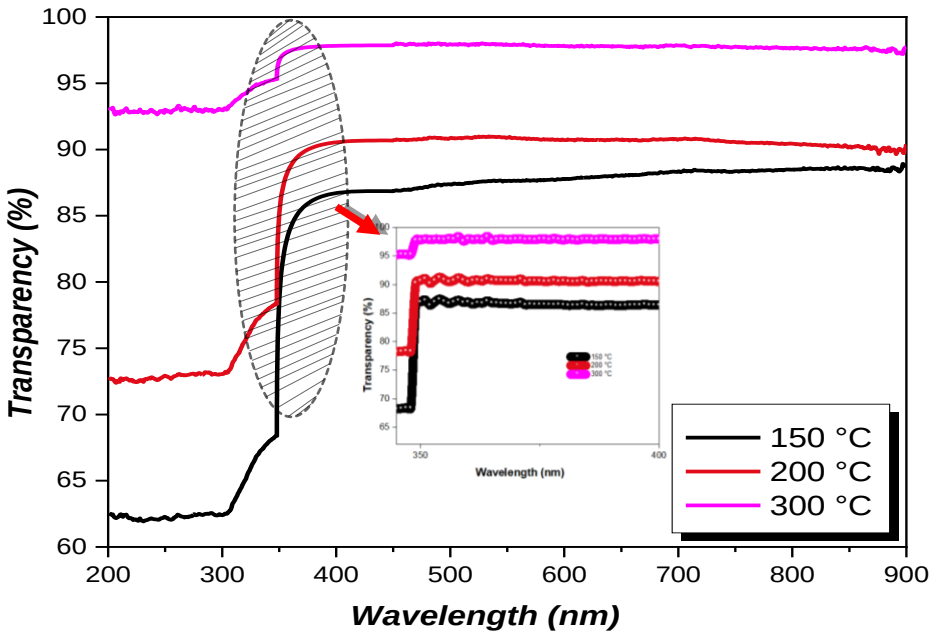

Figure IV.18 : Change of transmittance spectrum as a function of wavelength for films prepared at different deposition temperatures in the presence of two external magnetic fields with the same direction.

In the case of applying two external magnetic fields such that the external magnetic field has a direction opposite to the direction of the other field, we found that permeability increases significantly to rise to (~97 %) at 150 °C and (~98%) at 200 °C, there was also found to be a decrease in the value of permeability and an increase in the absorption of the membrane at 300 °C **figure (IV.19)**, this means that the deposition rate was affected by the magnetic field and at this degree (300 °C) led to an increase in the granular growth process, that is, an increase in the size of the granules and thereby absorbing photons and reducing permeability, this was confirmed by the results of the previous analysis (SEM), and these effects are consistent with the Beer-Lambert law, which links transmittance to thickness and wavelength with the following relationship[40][45]:

$$T \propto \exp[-\alpha(\lambda).t] \qquad \textbf{(IV.9)}$$

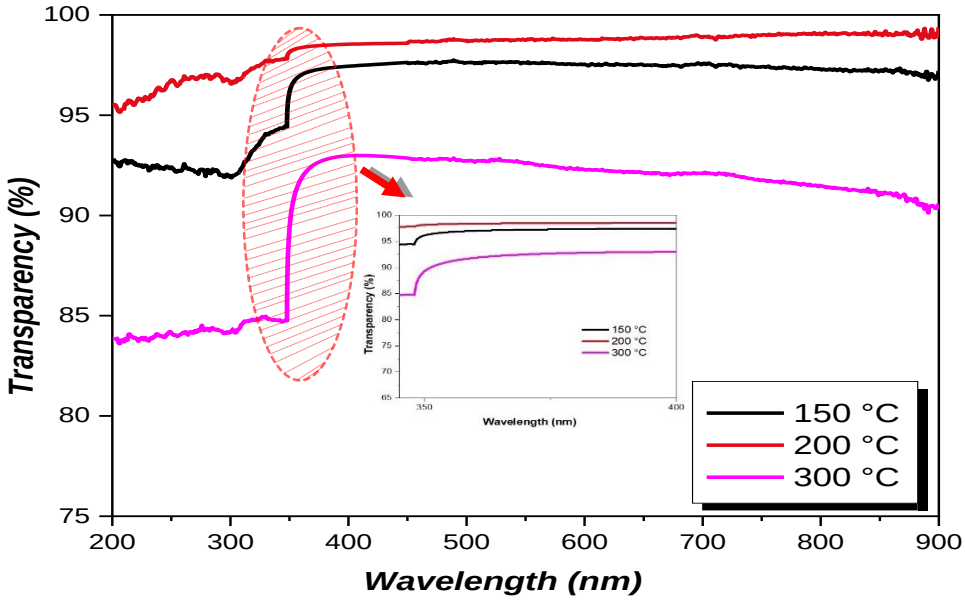

Figure IV.19 : Change of transmittance spectrum as a function of wavelength for films prepared at different deposition temperatures in the presence of two external magnetic fields such that the external magnetic field has an opposite direction to that of the other field.

The thickness was obtained using the weight method and through the relationship (**IV.10**) and relying on the values of the latter, **table (IV.8)**, and the permeability values, we notice that there is an inverse relationship between them and this is in accordance with the Beer-Lambert law.

$$t = \frac{\Delta w}{\tilde{n}.s} \qquad \textbf{(IV.10)}$$

For: (t) the thickness of the films, (ΔW) the difference between the film before and after the sedimentation, (ρ) the density of the film material, (s) the area of the sample.

Table (IV.8) : Thickness and transmittance values obtained at different temperatures.

	Deposition Temperature (°C)	Thickness (nm)	Transmittance (%)
In the presence of two external magnetic fields so that they have the same direction.	150	2872	88
	200	2673	89
	300	1780	97
In the presence of two external magnetic fields so that the external magnetic field is for it the opposite direction of the direction of the other field.	150	1938	97
	200	1849	98
	300	2062	90

IV.6.2. Optical absorption

Figures (IV.20), (IV.21) show the optical absorbance spectrum of magnesium oxide and silicon dioxide films at a change in deposition temperatures and at the strength of an applied magnetic field, in the presence of two external magnetic fields that have the same direction, we notice that the absorbance values decrease increasing the deposition temperature while displacing the absorption edge towards low wavelengths with high energies, this is due to the fact that with the increase in temperature and at this applied strength of the magnetic field, it led to the removal of levels of structural defects accompanying the preparation process and positional levels have been removed, it is also noted when applying two external magnetic fields so that the external magnetic field has the opposite direction to the direction of the other field there is the highest absorption value at 300°C temperature with the displacement of the absorption edge towards the high wavelengths with low energies, this is because the membranes at this thermal degree have created localized levels between the parity and conductivity packages

and act as auxiliary levels for the transport of photon-absorbing electrons with lower energies than the optical energy gap value of the prepared membranes.

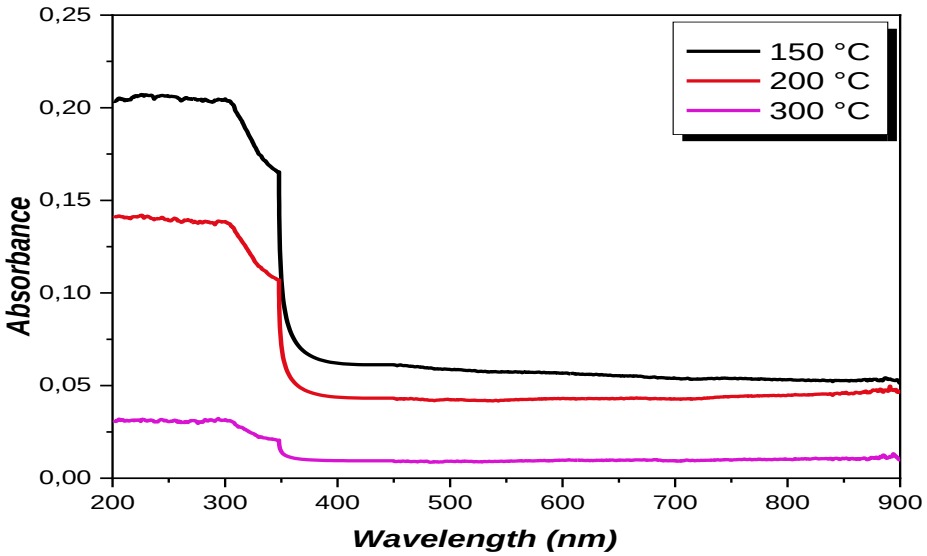

Figure IV.20 : The changing spectrum of optical absorption of prepared membranes appears at different deposition temperatures in the presence of two external magnetic fields so that they have the same direction.

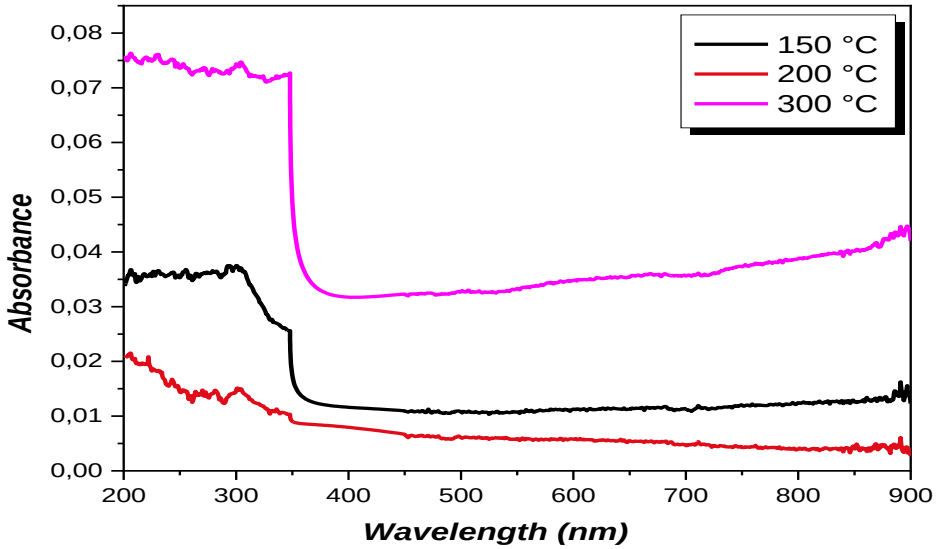

Figure IV.21 : The changing spectrum of optical absorption of prepared membranes appears at different deposition temperatures in the presence of two external magnetic fields such that the external magnetic field has an opposite direction to that of the other field.

IV.6.3. Absorption coefficient

The values of the absorption coefficient (α) were calculated through **equation** (**IV.11**) for the prepared membranes, and as shown in **figure (IV.22)**, which represents the change in the absorption coefficient as a function of the energy of the incident photon and different temperatures, it in turn depends on the properties of the semiconductor, which is represented by the type of electronic transfers that occur between the energy bands as well as the energy gap, and from which we note that the absorption coefficient generally starts with a small gradual increase with increased photon optic energy in the range of hν energies < 3.4 eV, followed by a rapid increase in range (3.4- 3.6 eV), and the results showed that increasing the deposition temperature led to a clear decrease in all absorption coefficient values, and this seems obvious at low energies, and however, it is noted from **figure (IV.23)** that the film deposited at a temperature of 300 °C and under the application of two magnetic fields in opposite directions increase in the value of the absorption coefficient, and in this case, this is due to a decrease in the energy gap, as the effect of localized levels in the energy gap appears at this temperature degree, a relative increase was also observed when two external magnetic fields were applied so that they had the same direction. We also note that the absorption coefficient in the high absorption region for all cases and at different temperatures has values $\alpha<10^4$ cm^{-1}, and that these values indicate the possibility of indirect electronic transfers occurring between the valence and conduction bands at those energies[33-36].

$$\alpha = - \ln (T) / t \qquad \textbf{(IV.11)}$$

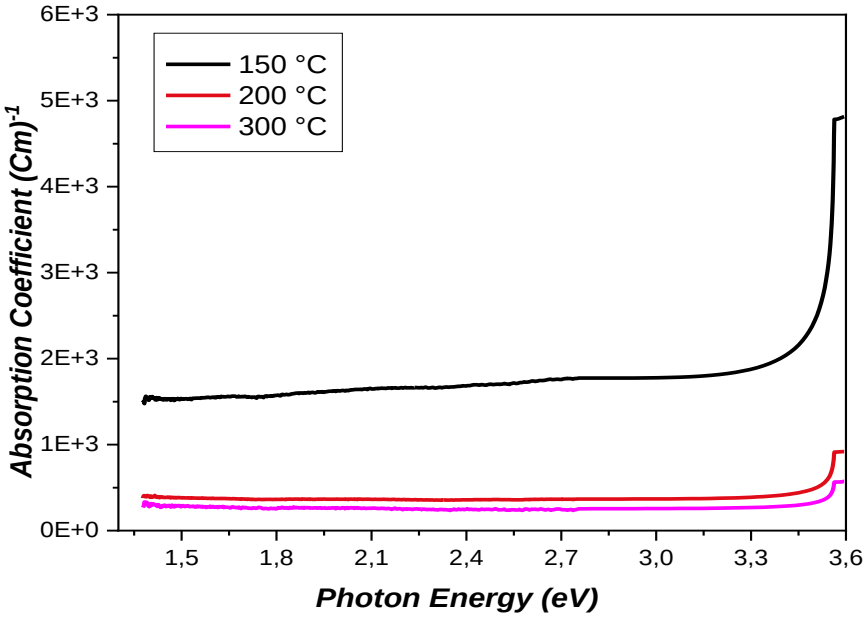

Figure IV.22 : Change of absorption coefficient as a function of photon energy for films prepared at different deposition temperatures and in the presence of two external magnetic fields so that they have the same direction.

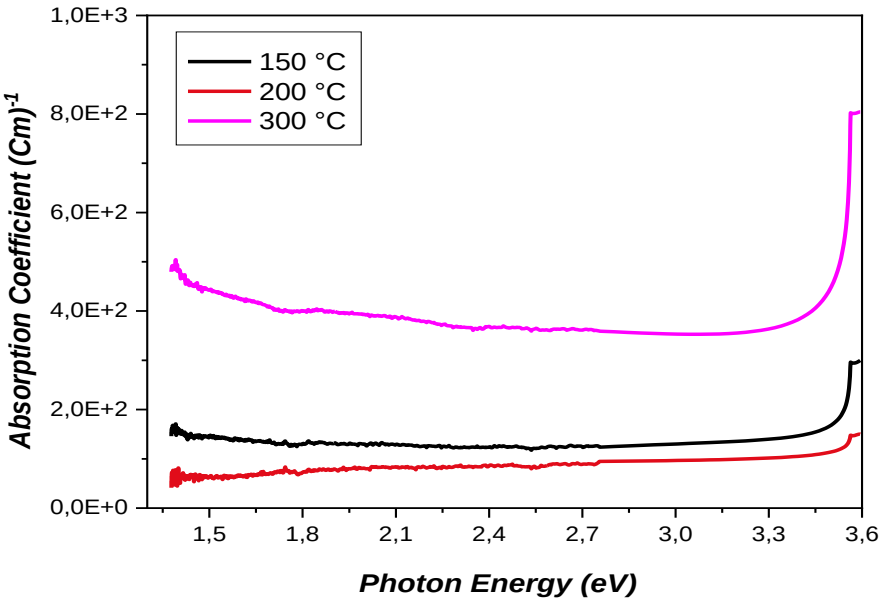

Figure IV.23 : Change of absorption coefficient as a function of photon energy for films prepared at different deposition temperatures and in the existence of two exterior magnetic fields so that the external magnetic field has a direction opposite to the direction of the other field.

IV.6.4. Energy Separation

The energy gap is considered one of the important constants that is relied upon in semiconductor physics and through which it is used in various applications such as optical cells, solar cells, etc, and thus, optical absorption is clearly recognized.

The current study shows the nature of electronic transfers and this is by calculating the absorption coefficient, when the values of the absorption coefficient are high ($\alpha>10^4$ cm^{-1}), direct electronic transitions can occur, in which the energy and momentum of the electron and photon are conserved, however, if its value is low ($\alpha<10^4$ cm^{-1}), it is likely that indirect electronic transfers will occur, in which the momentum of the electron and photon is conserved with the help of the phonon, and this type of transition occurs in different regions of (K) space, the results showed that the values of the absorption coefficient for magnesium oxide and silicon dioxide membranes when changing the deposition temperatures and the strength of the applied magnetic field are less than 10^4 cm^{-1}, and therefore indirect electronic transfers can occur, according to which the value of the energy gap can be calculated in both permissible and prohibited types as follows[37][38]:

First: The value of the optical energy gap for the permissible indirect electronic transitions was calculated, that is, the energy gap located between the top of the valence band and the bottom of the conduction band in different regions of K space using the following (Tauc) relationship[38][39]:

$$(\alpha h\nu)^{1/2} = B^{1/2} (h\nu - E_g \pm E_{ph}) \qquad \textbf{(IV.12)}$$

Where:

(E_{ph}) auxiliary phonon energy, (E_g) energy gap for indirect transmission, (B) constant of proportionality, (+) phonon absorption, (-) phonon emission.

By charting relationship between the energy of the incident photon ($h\nu$) and $(\alpha h\nu)^{1/2}$ and extending the straight part of the curve to intersect the photon energy axis at $(\alpha h\nu)^{1/2}= 0$, we obtain the value of the optical energy gap, where we note that the value of the optical energy gap increased as the deposition temperature increased and when two external magnetic fields are

applied such they have the same direction, as shown in **figure (IV.24)**, and this increase can be attributed to the effect of Burstein-Moss[40], as for the high value of the optical energy gap at 200 °C and when two external magnetic fields are applied so that the external magnetic field has a direction opposite to the direction of the other field, this is due to the possibility of forming nanoparticles and the presence of the quantum confinement effect. If the field is small, the movement of the electron and hole is restricted, so it appears limited to Increasing the energy required to stimulate the electron in the transport band[40][41], we also notice a decrease in the optical energy gap at 300 °C, **figure (IV.25)**, this is because the thermal treatment at this degree increased the granular volume rate by increasing the membrane thickness at this degree, which was confirmed by the results of the previous analysis (SEM).

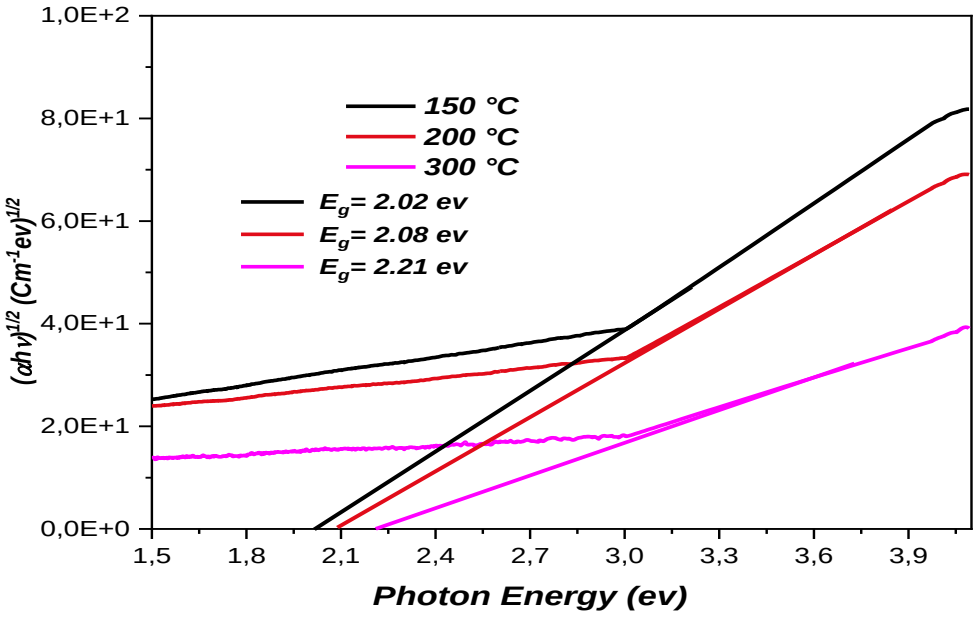

Figure IV.24 : Energy gap for indirect transmission permitted at different deposition temperatures and in the existence of two exterior magnetic fields so that they have the same direction.

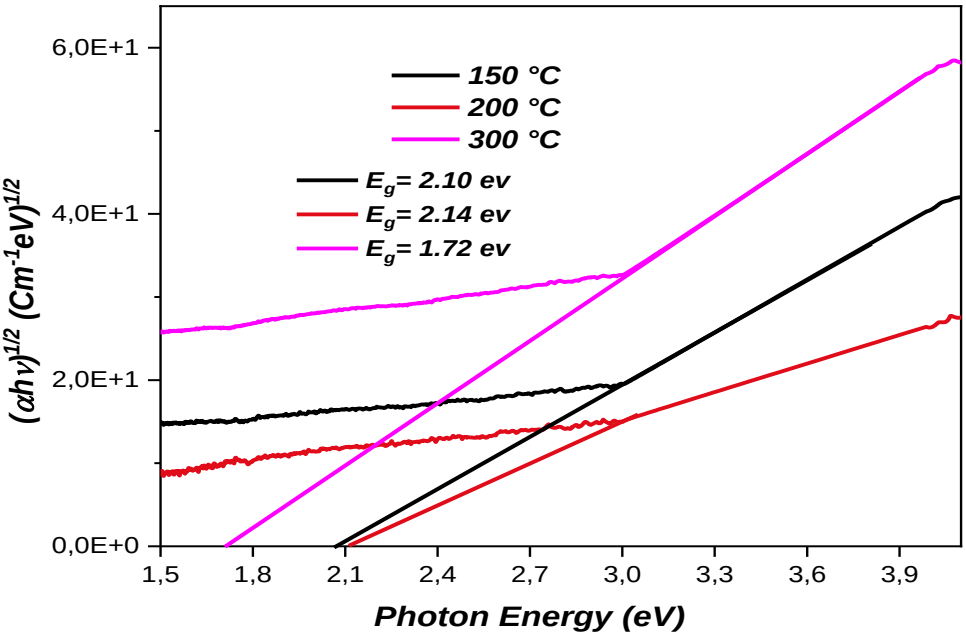

Figure IV.25 : Energy gap for indirect transmission permitted at different deposition temperatures and in the existence of two exterior magnetic fields so that the exterior magnetic field has an opposite orientation to the orientation of the other field.

Second: The value of the optical energy gap for prohibited indirect electronic transitions was calculated, that is, the energy gap between points adjacent to the highest point and the slowest in the valence band and the conduction band, using the following relationship[38][39]:

$$(\alpha h\nu)^{1/3} = B^{1/3} (h\nu - E_g \pm E_{ph}) \qquad \textbf{(IV.13)}$$

Figure (IV.26) shows the relationship between $(\alpha h\nu)^{1/3}$ and the photon energy ($h\nu$), and by extending the straight part of the high absorption region of the curve to intersect the photon energy axis at $(\alpha h\nu)^{1/3} = 0$, we obtain the value of the optical energy gap, and the **table (IV.9)**, and we note the same previous observations and for the same reason. It is also clear from **table (IV.9)** that the value of the energy gap for indirect electronic transfers increased when two magnetic fields were applied in opposite directions compared to when two external magnetic fields were applied in the same direction and at temperatures of 150 and 200 degrees Celsius, this is due to the possibility of forming nanoparticles and the presence of the quantum confinement effect. If the field is small, the movement of the electron and hole is restricted, so it

appears limited to Increasing the energy required to stimulate the electron in the transport band[40][41], it also means that if two external magnetic fields are applied, such that the external magnetic field has a direction opposite to the direction of the other field, and at these temperatures of 150 and 200 degrees Celsius, it affects the sedimentation and decrease in thickness with a decrease in the rate of grain size, which consequently led to an increase in the value of the energy gap for the transitions indirect electronic.

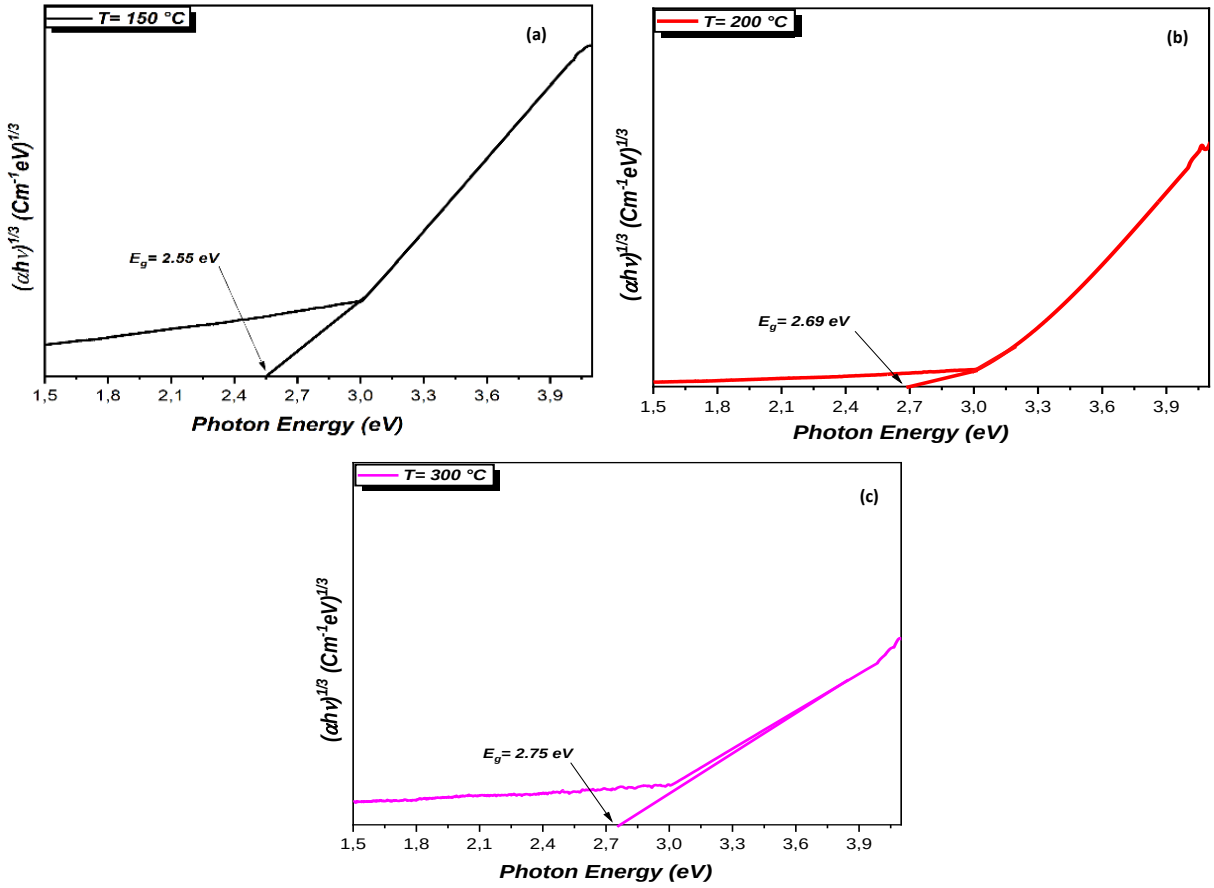

Figure IV.26 : The energy gap for the indirect prohibited transition at different deposition temperatures and in the presence of two external magnetic fields that have the same direction.

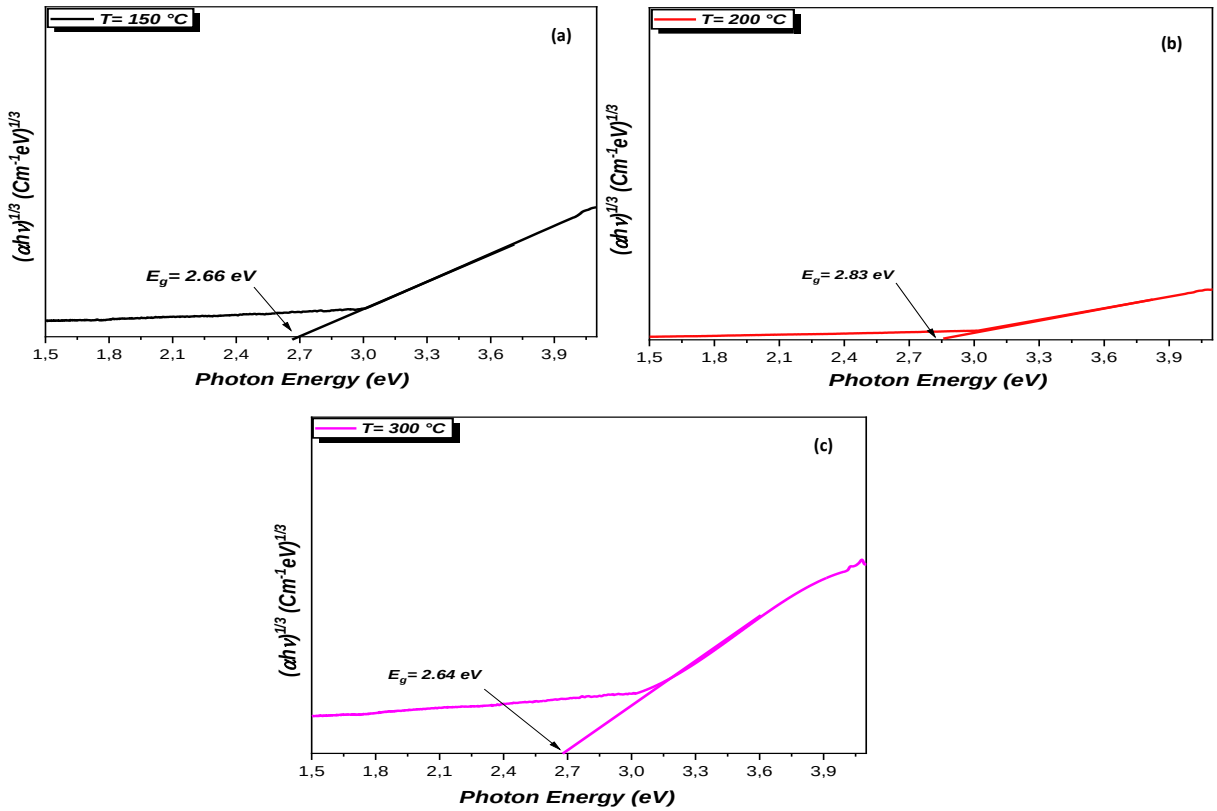

Figure IV.27 : The energy gap for the indirect prohibited transition at different deposition temperatures and in the existence of two exterior magnetic fields so that the exterior magnetic field has an opposite orientation to the orientation of the other field.

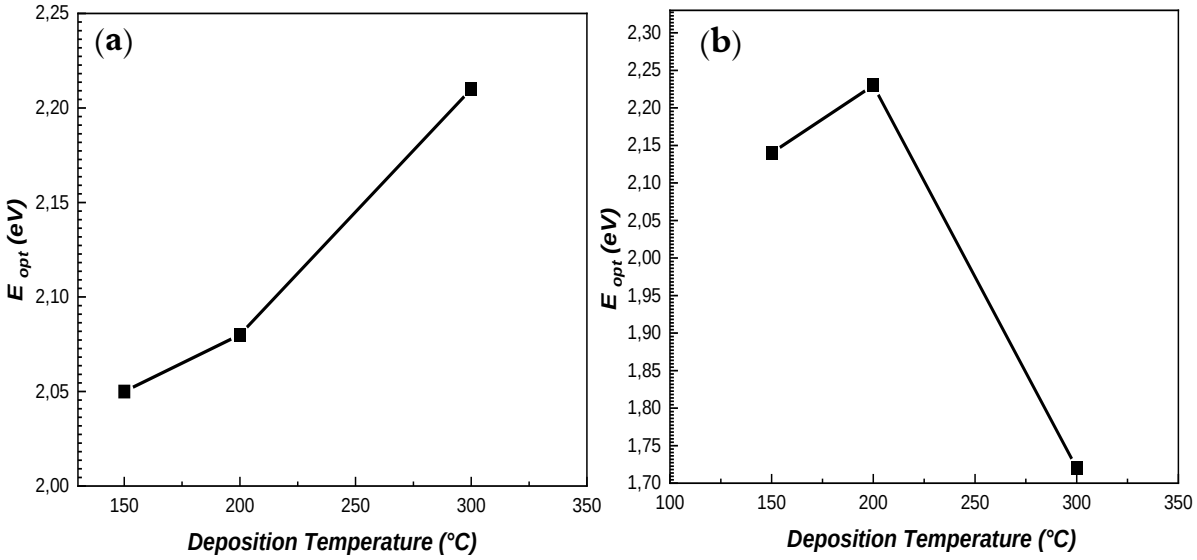

Figure IV.28 : The relationship between the allowed indirect transition energy gap and different deposition temperatures and at different coordinates: (a) in the existence of two exterior magnetic fields so that they have the same direction, (b) in the existence of two exterior magnetic fields so that the external magnetic field has a direction opposite to the direction of the other field.

Table (IV.9) summarizes the results of the energy gap values obtained for the permitted and prohibited indirect transmission at different temperatures and different strength of the applied magnetic field.

Table (IV.9) The energy gap values of the two indirect transitions allowed and forbidden by the change of sedimentation temperatures.

	sedimentation temperatures (°C)	***Indirect transition allowed***	***Indirect transitions is forbidding***
		E_g (eV)	E_g (eV)
In the presence of two external magnetic fields so that they have the same direction.	150	2.02	2.55
	200	2.08	2.69
	300	2.21	2.75
In the presence of two external magnetic fields so that the external magnetic field is for it the opposite direction of the direction of the other field.	150	2.10	2.66
	200	2.14	2.83
	300	1.72	2.64

IV.6. Conclusion

In this chapter we studied the experimental work done to prepare magnesium oxide and silicon dioxide membranes prepared at different deposition temperatures (150-200-300 °C) and in the presence of a change in the strength of the external magnetic field applied according to the hydrothermal technique, and this study included results presented by XRD, SEM, EDX, FT-IR, UV -Visible, respectively, and they were discussed and the impact of heat and magnetic field strength applied to the structural, morphological, optical properties of the prepared thin membranes was studied. We have been shown by X-ray diffraction results that membranes with a multi-crystallized composition of cubic phase MgO membranes with preferred growth direction [0 0 2] and hexagonal phase SiO_2 membranes within the preferred growth direction [0 1 1], and the results showed a high degree of crystallinity, and the average size of the crystals size was between (18-30 nm) for MgO and (13-115 nm) for SiO_2. Morphological studies using SEM also showed that the membranes have clear fullness surfaces and homogeneous, while EDX measurement proves the presence of both magnesium (Mg), silicon (Si) and oxygen (O) within the thin layers. Structural analyzes by FT-IR showed the presence of vibration patterns of Mg-O and Si-O confirming the presence of MgO-SiO_2 films. In addition, optical measurements reveal that transmittance values range between 88-98% in the visible area and were best when applying two external magnetic fields so that the external magnetic field has the opposite direction to the other field. This confirms the high transparency of these membranes in this area, and the energy interval decreases by decreasing temperature and has a value between 2.02 -2.21 eV for permitted indirect electronic transmission and 2.55-2.75 eV for prohibited indirect electronic transmission, while the thickness of the films ranged between 1780-2872 nanometers, the lowest value of the thickness was when two external magnetic fields were applied so that they had the same direction and at a temperature of 300 degrees celsius, the value of which was inversely proportional to the transmittance, and this is according to the (Beer-Lambert) law.

References

[1] A. Moses Ezhil Raj, L. C. Nehru, M. Jayachandran, and C. Sanjeeviraja, Spray pyrolysis deposition and characterization of highly (100) oriented magnesium oxide thin films, Cryst. Res. Technol. 42, No. 9, (2007), pp 867 – 875.

[2] Harun Güney, Demet İskenderoğlu, Synthesis of MgO thin films grown by SILAR technique, Ceramics International, (2018).

[3] A. Al-TABBAA, Reactive magnesia cement, University of Cambridge, UK, Woodhead Publishing Limited, 2013.

[4] OUALDINE Allal, Etude des propriétés structurales, électroniques, élastiques et optiques de l'Oxyde de Magnésium (MgO), Mémoire de magister, Université des Sciences et de la Technologie d'Oran- Mohamed Boudiaf, 2010.

[5] A. Moses Ezhil Raj, M. Jayachandran, C. Sanjeeviraja, Fabrication techniques and material properties of dielectric MgO thin films—A status review, CIRP Journal of Manufacturing Science and Technology, 2 (2010), pp 92–113.

[6] Didier Roux, Le verre : un matériau éternel, Académie des Sciences et Académie des Technologies, Paris.

[7] Brandon S. McKeon, Characterization of Silicon Dioxide Thin Film Deposition, A senior thesis submitted to the faculty of Brigham Young University, 2015.

[8] ATTALLAH MOURAD, Elaboration et caractérisation des couches minces d'oxyde de silicium, obtenues par voie sol-gel, Mémoire de magister, UNIVERSITE MENTOURI-CONSTANTINE, 2010.

[9] X. He, J. Wu, X. Li, X. Gao, L. Zhao, and L. Wu, "Synthesis and properties of silicon dioxide films prepared by pulsed laser deposition using ceramic SiO_2 target," Applied Surface Science, vol. 256, no. 1, 2009, pp. 231–234.

[10] X-RAY DIFFRACTION STUDY OF A SUSPECTED METEORITE**,** https://www.rigaku.com/es/node/548.

[11] A. Mhamdi et al., "Study of vanadium doping effects on structural, opto-thermal and optical properties of sprayed ZnO semiconductor layers," Optik, vol. 124, no. 18, 2013, pp. 3764–3770.

[12] A. Purohit, S. Chander, A. Sharma, S. P. Nehra, and M. S. Dhaka, "Impact of low temperature annealing on structural, optical, electrical and morphological properties of ZnO thin films grown by RF sputtering for photovoltaic applications", Optical Materials 49,pp 51–58, 2015.

[13] SANA HARIECH, Elaboration et caractérisation des couches minces de sulfure de cadmium (CdS) préparées par bain chimique (CBD), MEMOIRE MAGISTER, UNIVERSITE MENTOURI-CONSTANTINE ALGERIENNE, 2009.

[14] cherrer, P. Nachrichten von der Gesellschaft der Wissenschaften zu Göttingen, Mathematisch-Physikalische Klasse, vol. 2, (1918), pp 98-100.

[15] G. Balakrishnan, R. Velavan, Khalid Mujasam Batoo, Emad H. Raslan, Microstructure, optical and photocatalytic properties of MgO nanoparticles, Results in Physics, 16, (2020).

[16] Chyuan-Haur Kao, Chia Lung Chang, Wei Ming Su, Yu Tzu Chen, Chien Cheng Lu, Yu Shan Lee, Chen Hao Hong, Chan-Yu Lin & Hsiang Chen, Magnesium Oxide (MgO) pH sensitive Sensing Membrane in Electrolyte-Insulator Semiconductor Structures with CF4 Plasma Treatment, Scientific REPOrTS, (2017).

[17] Mukes Kapilashrami, Jun Xu, K V Rao, Lyuba Belova, Elin Carlegrim and Mats Fahlman, "Experimental evidence for ferromagnetism at room temperature in MgO thin film," J. Phys. Condens, MATTER 22, (2010).

[18] Dr.Ali H.Ataiwi & Dr.Alaa A. Abdul-Hamead, Study Some of the Structure Properties of ZrO2 Ceramic Coats Prepared by Spray Pyrolysis Method, Eng. & Tech. Journal, Vol.27, No.16, 2009.

[19] Chaojun Wang," Multiscale Modeling and Simulation of Nano crystalline Zirconium Oxide" Ph.D Thesis, engineering mechanics dissertations, university of nebraska, (2009).

[20] Ali Kadhim Tak, "Study of thickness effect on some structural and optical properties of (CdO) thin films prepared by vacuum thermal evaporation method", vol. 20, no. 3, 2017, pp. 178–184.

[21] S. Gnanasaravanan and P. Rajkumar, "Characterization of minerals in natural and manufactured sand in Cauvery River belt, Tamilnadu, India", Infrared Physics and Technology, vol. 58,2013, pp. 21–31.

[22] F. Bosch Reig, J.V. Gimeno Adelantado, M.C.M. Moya Moreno, FTIR quantitative analysis of calcium carbonate (calcite) and silica (quartz) mixtures using the constant ratio method. Application to geological samples, Talanta vol. 58, 2002, pp. 811-821.

[23] Ali Sdiri, Teruo Higashi, Tamao Hatta, Fakher Jamoussi, Norio Tase, Mineralogical and spectroscopic characterization, and potential environmental use of limestone from the Abiod formation, Tunisia, Environ Earth Sci 61, 2010, pp 1275–1287.

[24] DAVE K. VERMA, DIANE M. JOHNSON and KAREN DES TOMBE, A Method for Determining Crystalline Silica in Bulk Samples by Fourier Transform Infrared Spectrophotometry, Ann. occup. Hyg, Vol. 46, No. 7, 2002, pp 609–615.

[25] N.V. Vagenas, A. Gatsouli, C.G. Kontoyannis, Quantitative analysis of synthetic calcium carbonate polymorphs using FT-IR spectroscopy, Talanta 59, (2003), pp 831-836.

[26] Chiew Wee Wong, Yen San Chan, Jaison Jeevanandam, Kaushik Pal, Mikhael Bechelany, M. Abd Elkodous, Gharieb S. El-Sayyad, Response Surface Methodology Optimization of Mono-dispersed MgO Nanoparticles Fabricated by Ultrasonic-Assisted Sol–Gel Method for Outstanding Antimicrobial and Antibiofilm Activities, Journal of Cluster Science, 2019.

[27] J. Ji, Y. Ge, W. Balsam, J. E. Damuth, and J. Chen, "Rapid identification of dolomite using a Fourier Transform Infrared Spectrophotometer (FTIR): A fast method for identifying Heinrich events in IODP Site U1308," Mar. Geol., vol. 258, no. 1–4, 2009, pp. 60–68.

[28] A. Sdiri, T. Higashi, T. Hatta, F. Jamoussi, and N. Tase, "Mineralogical and spectroscopic characterization, and potential environmental use of limestone from the Abiod formation, Tunisia," Environ. Earth Sci., vol. 61, no. 6, 2010, pp. 1275–1287.

[29] F. B. Reig, J. V. G. Adelantado, and M. C. M. Moya Moreno, "FTIR quantitative analysis of calcium carbonate (calcite) and silica (quartz) mixtures using the constant ratio method. Application to geological samples", Talanta, vol. 58, no. 4, 2002, pp. 811–821.

[30] F. A. Andersen and L. Brečević, "Infrared spectra of amorphous and crystalline calcium carbonate," Acta Chemica Scandinavica, vol. 45, 1991, pp 1018–1024.

[31] N.V. Vagenas, A. Gatsouli, C.G. Kontoyannis, Quantitative analysis of synthetic calcium carbonate polymorphs using FT-IR spectroscopy, Talanta, 59, (2003), pp 831-836.

[32] Kanchan Joshi, Mukesh Rawat, Subodh K. Gautam, R.G. Singh, R.C. Ramola, Band gap widening and narrowing in Cu-doped ZnO thin films, Journal of Alloys and Compounds, 2016.

[33] Y. Mohammed, "Effect of Deposition Temperature on the Physical Performance of n-ZnO/p-Si Heterojunction," J. Educ. Sci., vol. 29, no. 2, 2020, pp 118–132.

[34] Hussein Ali Noor, Dakhil Abbas AbdZaid, study the structural and optical properties of pure and lithium doped CdS thin films by chemical bath deposition method, University of Qadisiyah, College of Education, Physics Department, Iraq, 2017.

[35] Mekhaiel Manssor, Studying the Structural and Optical Properties of ZnO: Cu Prepared by APCVD Technique, Jordan Journal of Physics, Vol 5, no 2, 2012, pp 89-103.

[36] K. The, "Polycrystalline Lead Tin Chalcogenide Thin Film Grown by Spray Pyrolysis", pp. 71–75, 2000.

[37] M. Soylu and O. Savas, "Electrical and optical properties of ZnO/Si heterojunctions as a function of the Mg dopant content", Materials Science in Semiconductor Processing, 2013, pp 1–7.

[38] Muhammad Hamid Abdullah, Obeida Amer Abdel-Hussein Widad Hanu Abbas, Energy gap study of polystyrene (PS) doped with iron dichloride ($FeCl_2$), Al-Mustansiriya Science Journal, vol. 21, no 6, 2010, pp. 2–6.

[39] Charles Kittel, Introduction to solid state physics, vol. 6, no. 1, 1957.

[40] S.O. Kasap, Solutions to Principles of Electronic Materials and Devices, University of Saskatchewan, (2001).

[41] H. Chen, J. Ding, W. Guo, F. Shi, and Y. Li, "Violet-blue-green emission and shift in Mg-doped ZnO films with different ratios of oxygen to argon gas flow," Appl. Surf. Sci, vol. 258, no. 24, (2012), pp 9913–9917.

General conclusion

General conclusion

In this work we studied the thin layers of magnesium oxide, silicon dioxide (MgO-SiO_2) prepared from natural resources at different deposition temperatures (150-200-300 °C), and a change in the strength of the external magnetic field applied using the hydrothermal technique deposited on glass. Through the results we obtained using XRD, SEM, EDX, FT-IR, and UV-Visible analysis techniques to study the structural, morphological, molecular structure, and optical properties respectively, and demonstrate the possibility of depositing MgO-SiO_2 membranes using rocks, hydrothermal method and successfully, we have also been able to study the impact of both the deposition temperature and the strength of the applied magnetic field and to conclude the extent to which these properties have improved, and we can reflect the most important findings and conclusions as follows:

1. Impact of deposition temperature on prepared thin films
   - The study of structural properties showed that magnesium oxide and silicon dioxide membranes have a polycrystalline structure, so that MgO membranes are cubic phase with preferred growth direction [0 0 2] and SiO_2 membranes with hexagonal structure within the preferred growth direction [0 1 1], we noticed that the difference in deposition temperature did not change the nature of the crystal structure, but rather changed the constants of the crystal structure, if the increase in temperature leads to a decrease in the average size of its grains (G.S) and a decrease in the values of the network constants (a_0, c_0), and this is due to more recrystallization, and as well as the increase in the number of crystals, the density of dislocations, which may lead to the possibility of stress and compression occurring, with the exception of membranes prepared at 200 °C, formed crystal grains of larger size, that is, at this temperature, it led to the cancellation of some grain boundaries when the grains coalesce, as well as the cancellation of defects that existed after the growth process occurred, rearranging the crystalline grains, and improving the crystallinity of the material.

- Through the results of the diagnosis of using SEM, it was shown that the formation of the topographic surface of the membrane depends primarily on the deposition temperature, it affects the dimensions of the granules and thus affects the geometric shape, with the exception of films deposited at a temperature of 200°C when two external magnetic fields are applied in the same direction and 300°C when two magnetic fields are applied in opposite directions, EDX analysis confirms the presence of magnesium, oxygen, and silicon within the layers, and FT-IR analysis results confirm the presence of vibration patterns for Mg-O and Si-O in all prepared membranes.
- The study of optical properties revealed an increase in the values of optical transmittance and a decrease in the values of absorbance and absorption coefficient. The energy gap (Eg) also increased with increasing temperature with the occurrence of indirect electronic transitions, with the exception of films deposited at 300°C when two magnetic fields in opposite directions are applied, this is due to the formation of positional levels and increased thickness, and this is confirmed by the results of SEM analysis, while the thickness of the films ranged between 1780-2872 nm according to the changing magnetic field strength and deposition temperature.

2. Impact of the applied external magnetic field strength on the deposition of the prepared thin films.
    - Through studying the structural properties when two magnetic fields were applied in opposite directions, it was revealed that there was an increase in the values of the average grain size (G.S.) compared to the films prepared when two external magnetic fields were applied in the same direction, thus, we notice an increase in the peak intensity of the prominent peaks in the X-ray diffraction scheme, especially at a temperature of 200 degrees Celsius, they are considered ideal conditions for the arrangement of atoms with minimal defects and maximum packing density, thus increasing the crystalline order and degree of crystallization of the membrane material upon preparation.
    - Showed through SEM images of the surface of the membranes when two magnetic fields in opposite directions are applied, that there is a marked homogenization and intensification of physical distribution, this appears in the sample surface at 200 °C where the granular particles become small in size with

high density while increasing their growth and crystallization, likewise, at a temperature of 300 °C, the surface of the membrane becomes more homogeneous in distribution and free of islands and voids with the granules gradually coalescing.

- Optical transmittance spectra showed a noticeable increase in their values when two magnetic fields in opposite directions were applied, consequently, there is a decrease in absorbance values and absorption coefficient, it was also observed that an increase in the energy gap values was observed at the temperatures of 150 and 200 degrees Celsius, and this is due to the possibility of the formation of nanoparticles and the presence of the quantum confinement effect, with the exception of the films deposited at a temperature of 300 degrees Celsius, which witnessed an increase in thickness, this is demonstrated by the results of the scanning electron microscope analysis, this means that the deposition rate and distribution of the membrane material was affected by the applied external magnetic field due to the arrangement of particles and atoms in these membranes, as it showed an improvement in the characteristics when two opposite magnet fields were shed in the direction.

Future prospects

- Preparing thin layers of $MgO\text{-}SiO_2$ by the chemical bath method, studying their structural, electrical and optical properties and comparing them to the results of the current study.

- Study the impact of thickness and annealing of $MgO\text{-}SiO_2$ membranes on their synthetic, electrical and visual properties prepared in a Sol-gel method.

- Study more properties of thin membranes in different preparation methods.

- Prepare thin membranes for other oxides and publish them in international journals.

- The possibility of using $MgO\text{-}SiO_2$ membranes in various applications such as gas sensors, ultra-storage condensers, Spintronics applications and photovoltaic uses.

العنوان: تركيب مواد نانوية جديدة للتطبيق في تكنولوجيا الـ Spintronics

الملخص

في هذه الدراسة، قمنا بترسيب أغشية رقيقة نانوية لأوكسيد المغنيسيوم (MgO) وثاني أوكسيد السيليكون (SiO_2) من خلال معادن تم استخراجها من موارد طبيعية (الصخور) والمنتجة بواسطة الطريقة الحرارية المائية عند درجات حرارة ترسيب مختلفة وفي وجود تغيير في قوة المجال المغناطيسي الخارجي المطبق، وذلك بهدف الحصول على مادة جديدة يمكن استغلالها ضمن تطبيقات تكنولوجيا اللف المغزلي الالكتروني Spintronics. تم تحليل الأغشية التي تم انتاجها بتقنيات مختلفة: مطيافية انعراج الأشعة السينية (XRD)، الماسح المجهري الالكتروني (SEM)، التحليل الطيفي لطاقة الأشعة السينية المشتتة (EDX)، مطيافية امتصاص الأشعة تحت الحمراء بتحويل فوري (FTIR)، مطياف الأشعة فوق البنفسجية المرئية (UV-Visible).

تظهر الدراسة البنيوية باستعمال مطيافية انعراج الأشعة السينية (XRD) أن الأغشية المحضرة ذات تركيب متعدد التبلور بحيث أن MgO ذات طور مكعب مع الاتجاه المفضل للنمو [2 0 0] وأغشية SiO_2 ذات بنية سداسية ضمن الاتجاه المفضل للنمو[1 1 0]، كما اتضح أن الاختلاف في درجة حرارة الترسيب لم تغير من طبيعة التركيب البلوري بل عملت على تغيير طفيف في قيم ثوابت الشبكة، حيث أن الزيادة في درجة حرارة الترسيب تؤدي الى انخفاض حجم الحبيبات البلورية وكذلك في ثوابت الشبكة (a_0,c_0) باستثناء الأغشية المرسبة عند 200°C وفي كلا الحالتين والتي أدت الى التحسن بلورية المادة وذلك بإلغاء الحدود الحبيبية والتحامها. كما تبين أن عند تسليط حقلين متعاكسين في الاتجاه يؤدي الى ارتفاع في قيم متوسط حجم الحبيبي (G.S) وكانت أعلى درجة من تبلور عند الأغشية المحضرة في 200°C عند تطبيق حقلين متعاكسين في الاتجاه. أثبت المجهر الالكتروني الماسح أن الشكل التضاريسي للغشاء يعتمد بالدرجة الأساسية على درجة حرارة الترسيب فهي تؤثر على أبعاد الحبيبات وبالتالي تؤثر على الشكل الهندسي لها، حيث انخفض الحجم وكثافة الحبيبات بزيادة درجة حرارة الترسيب باستثناء الأغشية المرسبة في 200°C عند تسليط حقلين لهما نفس الاتجاه و 300°Cعند تسليط حقلين متعاكسين في الاتجاه، كما تبين أن عند تسليط حقلين متعاكسين في الاتجاه يعمل على تجانس وتكاثف أكثر للتوزيع المادي مع التحام للحبيبات تدريجيا. أكد كل من تحليل EDX وFTIR وجود المغنيسيوم والاكسجين والسيليكون داخل الطبقات الرقيقة. أظهرت الأشعة الفوق البنفسجية المرئية أن النفاذية والفاصل الطاقي يزداد مع الزيادة في درجة حرارة الترسيب وأن قيمها تسجل اعلى ارتفاع عند تطبيق حقلين متعاكسين في الاتجاه باستثناء الأغشية المرسبة عند 300°C عند تطبيق حقلين متعاكسين في الاتجاه، ويرجع ذلك لزيادة السمك مما يعي أن معدل الترسيب وتوزيع مادة الغشاء تأثر بالمجال المغناطيسي الخارجي المطبق وهذا راجع الى ترتيب الجزيئات والذرات الموجودة في هذه الأغشية.

الكلمات المفتاحية: المواد النانوية، اللف المغزلي الالكتروني، الطريقة الحرارة المائية، الأغشية الرقيقة.

Titre : Elaboration des nouveaux nanomatériaux à l'application dans la Spintronics

Résumé

Dans cette étude, nous avons déposé des films nano-minces d'oxyde de magnésium (MgO) et de dioxyde de silicium (SiO_2) à travers des minéraux extraits de ressources naturelles (roches) et produits par la méthode hydrothermale à différentes températures de dépôt et en présence d'un changement de la force du champ magnétique externe appliqué, ceci dans le but d'obtenir un nouveau matériau pouvant être exploité dans des applications de la technologie Spintronics. les membranes produites ont été analysées avec différentes techniques : spectroscopie de diffraction des rayons X (DRX), microscopie électronique à balayage (MEB), spectroscopie de rayons X à dispersion d'énergie (EDX), spectroscopie d'absorption infrarouge à transformée de Fourier (FTIR), spectroscopie ultraviolette-visible (UV-Visible).

L'étude structurelle utilisant la spectroscopie de diffraction des rayons X (DRX) montre que les films préparés ont une structure polycrystalline telle que MgO a une phase cubique avec la direction détaillée de croissance [0 0 2] et les films SiO_2 ont une structure hexagonale dans la direction détaillée de croissance [0 1 1], il s'avère également que la différence dans la température de dépôt n'a pas changé la nature de la structure cristalline mais a plutôt changé les valeurs des constantes du réseau, l'augmentation de la température de dépôt entraîne une diminution de la taille des grains cristallins, ainsi que des constantes de réseau (a_0, c_0), à l'exception des films déposés à 200°C, et dans les deux cas, ce qui conduit à ont amélioré la cristallisation de la substance par suppression des joints de grains et de leur coalescence. Il a également été montré que l'application de deux champs opposés dans la direction entraîne une augmentation des valeurs de la taille moyenne des grains (G.S), et que le degré de cristallinité le plus élevé se trouvait dans les films préparés à 200°C lorsque deux champs opposés étaient appliqué dans la direction. Le microscope électronique à balayage a prouvé que la forme topographique de la membrane dépend principalement de la température de dépôt, car elle affecte les dimensions des grains et donc leur forme géométrique. La taille et la densité des grains diminue avec l'augmentation de la température de dépôt, à l'exception des films déposés à 200°C lorsque deux champs dans la même direction sont appliqués et à 300°C lorsque deux champs dans des directions opposées sont appliqués, il a également été montré que lorsque deux champs sont dirigés dans des directions opposées, la répartition physique devient plus homogène et plus dense, les grains fusionnant progressivement. Les analyses EDX et FTIR ont confirmé la présence de magnésium, d'oxygène et de silicium dans les couches minces. Le rayonnement ultraviolet-visible a montré que la transmittance et gap d'énergie augmentent avec l'augmentation de la température de dépôt et que leurs valeurs enregistrent la plus forte augmentation lors de l'application de deux champs opposés dans la direction, à l'exception des membranes déposés à 300°C lorsque deux champs opposés sont appliqués dans la direction, cela est dû à l'augmentation de l'épaisseur, ce qui signifie que la vitesse de dépôt et la répartition du matériau de la membrane sont affectées par le champ magnétique externe appliqué, et cela est dû à la disposition des molécules et des atomes présents dans ces membranes.

Mots Clés : nanomatériaux, spintronique, hydrothermale, couches minces.

Title: Elaboration of New Nanomaterials for Spintronic Applications

Abstract

In this study, we deposited nano-thin films of magnesium oxide (MgO) and silicon dioxide (SiO_2) through minerals extracted from natural resources (rocks) and produced by the hydrothermal method at different deposition temperatures and in the presence of a change in the force of the applied external magnetic field, this with the aim of obtaining a new material that can be exploited in applications of Spintronics technology. The membranes produced were analyzed with different techniques: X-ray diffraction spectroscopy (XRD), scanning electron microscopy (SEM), energy dispersive X-ray spectroscopy (EDX), Fourier transform infrared absorption spectroscopy (FTIR), and ultraviolet-visible spectroscopy (UV -Visible).

The structural study using X-ray diffraction (XRD) spectroscopy shows that the prepared films have a polycrystalline structure such that MgO has a cubic phase with the detailed direction of growth [0 0 2] and the SiO_2 films have a hexagonal structure in the detailed direction of growth [0 1 1], it also turns out that the difference in the deposition temperature did not change the nature of the crystalline structure, but rather changed the values of the network constants, the increase in deposition temperature leads to a decrease in the size of the crystalline grains, as well as network constants (a_0, c_0), with the exception of films deposited at 200°C, and in both cases, which leads to improved crystallization of the substance by removing grain boundaries and their coalescence. It has also been shown that the application of two fields opposite in direction results in an increase in the average grain size (G.S) values, and that the highest degree of crystallinity was in prepared films at 200°C when two opposite fields were applied in the direction. The scanning electron microscope proved that the topographic shape of the membrane depends mainly on the deposition temperature, because it affects the dimensions of the grains and therefore their geometric shape. Grain size and density decreases with increasing deposition temperature, with the exception of films deposited at 200°C when two fields in the same direction are applied and at 300°C when two fields in opposite directions are applied, it has also been shown that when two fields are directed in opposite directions, the physical distribution becomes more homogeneous and denser, the grains gradually fusing. EDX and FTIR analyses confirmed the presence of magnesium, oxygen and silicon in thin films, ultraviolet-visible radiation showed that the transmittance and energy gap increase with increasing deposition temperature and that their values register the highest increase when applying two opposite fields in the direction, with the exception of membranes deposited at 300°C when two opposite fields are applied in the direction, this is due to the increase in thickness, which means that the deposition rate and distribution of membrane material are affected by the applied external magnetic field, and this is due to the arrangement of molecules and atoms present in these membranes.

Keywords: nano-materials, spintronics, hydrothermal, thin films.